INVESTIGATING THE DOWNSTREAM SIGNALLING OF THE RHO GTPASE RHOJ

by

MONA SALEM

A thesis submitted to the University of Birmingham for the Degree of

MASTER BY RESEARCH

Molecular Angiogenesis Group

School of Immunity and Infection

College of Medical and Dental Sciences

The University of Birmingham

May 2023

Abstract

RhoJ is an endothelial expressed Rho GTPase which regulates cell migration, protein trafficking and angiogenesis. Previous studies demonstrated that GTP-bound RhoJ activated MAP kinases, interacted with the GIT-PIX complex, caused a retarded electromobility shift of GIT2 and promoted focal adhesion disassembly. The aims of this study were to further characterise how RhoJ regulates MAP kinases and the GIT-PIX complex. The activity of RhoJ was manipulated in human umbilical vein endothelial cells (HUVECs) by either lentiviral transduction of constitutively active mutant form of RhoJ (daRhoJ) or transfection with RhoJ-specific si-RNA duplexes, to activate and inhibit it, respectively. Expression of daRhoJ resulted in a small increase in ERK1/2, but not JNK, phosphorylation in HUVECs cultured in complete media. In a time-course experiment, si-RNA-mediated RhoJ knockdown significantly reduced levels of phospho-ERK1/2, this was particularly evident after 15 min stimulation with VEGFA, FGF2 or complete growth media. Other groups had shown that the GIT-PIX complex interacted with and regulated the activity of MEK1 and ERK1/2, and that ERK1/2 localised to focal adhesions; we therefore aimed to test how RhoJ affected this. Experiments demonstrated that very low levels of GIT1 co-precipitated with either MEK1 or ERK1/2, and there was no evident co-localisation of ERK1/2 with vinculin, a focal adhesion protein. This low level of co-precipitation combined with some technical difficulties hindered the assessment of how RhoJ affected this interaction. This, combined with the lack of focal adhesion localisation of ERK1/2 led to our hypothesising that the GIT-PIX complex was not involved in RhoJ's regulation of ERK1/2 in endothelial cells. One potential alternative mechanism is via p21-activated kinases (PAK), kinases known to be both downstream of RhoJ and able to regulate RAF1. The role of PAKs in the daRhoJ-mediated change in the electrophoretic mobility of GIT2 was assessed. Two PAK inhibitors were tested, and PF-3758309, but not IPA-3, abrogated GIT2's mobility shift in daRhoJ expressing

endothelial cells. This suggests that the electromobility shift of GIT2 is due to serine and threonine phosphorylation and the differential effect of the inhibitors suggests that PAK4 acts downstream of RhoJ to affect phosphorylation of GIT2. Data in this thesis further delineates the molecular pathways downstream of RhoJ and offers insight into the mechanisms by which RhoJ regulates its endothelial functions.

KEY WORDS: RhoJ, ERK, GIT, PAK, Angiogenesis.

Acknowledgments

I would like to express my sincere gratitude to my supervisor, Dr Victoria Heath, for her guidance and support throughout this research project. I am grateful for her patience, help in writing, making corrections, dedication in reviewing the thesis, giving fruitful feedback and suggestions.

I would also like to thank the following people:

Prof Roy Bicknell for his suggestions and advice.

Dr Sarah Jenkinson, with whom I shared the RhoJ's journey, for her collaboration with Dr Heath in teaching me the different lab techniques and skills. Both were continually supporting and offering a help whenever my laboratory hours were limiting me, and were always willing to discuss my results, answer my endless questions and giving advice.

All other members of Bicknell team and other groups that join our weekly lab meetings for their suggestions, advice and for offering help. In particular, Dr Peter Hewett for allowing me to use his reagents to try an alternative technique or when I need to modify a protocol, for Rebecca Gascoyne, Dr Alessandro Di Maio and Jenefa Begum for giving tips in picture acquisition at the microscopy facility, and for all other past and present lab colleagues for providing genuine help whenever needed.

Finally, I would like to deeply thank my husband for his help and contributions in sponsoring this project, my kids and friends for their love and support during this process. Their words of encouragement helped me to stay motivated and complete this thesis. My warm thanks go to my parents for their financial and emotional support. I miss them so much and hoped that they were here to witness this moment.

Table of contents

List of Figures

Chapter1

Chapter 3

Chapter 4

Chapter 5

List of Tables

Chapter2

List of abbreviations

aa	Amino acid
AID	Autoinhibitory domain
$\alpha_v\beta_1$	Alpha5 beta 1
Ang II	Angiotensin II
Ank	Ankyrin repeats
ARF	ADP-ribosylation factor
BBE	Bovine brain extract
BCA assay	Bicinchoninic acid assay
BM	Basement membrane
BSA	Bovine serum albumin
C-terminus or terminal	Carboxyl-terminus or terminal
CAAX	C-cysteine, A-aliphatic amino acid, X-any
CC	Coiled coiled
cM199	Complete M199
co-IP	Co-immunoprecipitation
CO2	Carbon dioxide
CRIB	CDC42 and Rac-interactive binding
CSF	Cytoskeletal fraction
DAPI	4',6-diamidino-2-phenylindole
daRhoJ	Dominant active RhoJ
dH_2O	Deionized water
DMEM	Dulbecco's Modified Eagle's Medium
DMSO	Dimethyl sulfoxide
DTT	Dithiothreitol
E	Embryonic day
ECL	Enhanced chemiluminescence
ECM	Extracellular matrix
EC(s)	Endothelial cell (s) or inter-endothelial cell (s)
EDTA	Ethylenediamine tetra acetic acid
EGF	Epidermal growth factor
EGFR	Epidermal growth factor receptor
EndMT	Endothelial to mesenchymal transition
eNOS	Endothelial nitric oxide synthase
ERK	Extracellular receptor kinase or total ERK

ETS	Erythroblast transformation-specific
ETV2	ETS variant 2
FA(s)	Focal adhesion(s)
FAK	Focal adhesion kinase
FAT	Focal adhesion targeting domain
FCS	Fetal calf serum
FGF2	Fibroblast growth factor 2
FGFR2	Fibroblast growth factor receptor 2
FMNL3	Formin Like 3
g	Gravity
GAPs	GTPase-activating proteins
GDP	Guanosine diphosphate
GEF(s)	Guanine exchange factor(s)
GFP	Green fluorescent protein
GF(s)	Growth factor(s)
GIT	G protein coupled receptor kinase interacting target
GPCR	G protein coupled receptor
GRB2	Growth factor receptor-bound protein 2
GTPase	Guanosine triphosphatase
GTP	Guanosine triphosphate
H3K4	Histone H3 lysine 4 methyltransferase
hBMEC	Human brain microvascular endothelial cell
HEK293T	Human embryonic kidney 293T cells
HRP	Horseradish peroxidase
HUVECs	Human umbilical vein endothelial cells
IF	Immunofluorescence
Ig	Immunoglobulin
IP	Immunoprecipitation
ITSN1	Intersectin1
intersegmental vessels	ISV
MAP	Mitogen activated protein
MEK	Mitogen-activated protein kinase kinase
MicroRNAs	miRNA;miR
Minute(s)	Min(s)
MLCK	Myosin light chain kinase

MMPs	Matrix metalloproteinases
N-terminus	Amino terminus/terminal
NO	Nitric oxide
p value	Probability value
PAK	p21 activated kinase
PBD	p21-binding domain
PBS	Phosphate buffered saline
PEI	Polyethyleneimine
pERK	Phospho-ERK
PIX, α or β	PAK interacting exchange factor α or β
pJNK	Phospho-JNK
PVDF	Polyvinylidene difluoride
ROCK	Rho kinase
Robo4	Roundabout Guidance Receptor
RT	Room temperature
RTK(s)	Receptor tyrosine kinase(s)
RSK	p90 ribosomal S6
SDS-PAGE	Sodium dodecyl sulphate-polyacrylamide gel electrophoresis
Sema3E	Semaphorin 3E
SH2 or SH3	Src homology 2 or 3
SHD	Spa or Spa2 homology domain
SOS	Son of Sevenless
TBST	Tris-buffered saline Tween-20
TEMED	Tetramethylethylenediamine
VE	Vascular endothelial
VEGF	Vascular endothelial growth factor
VEGFR	Vascular endothelial growth factor receptor
VWF	Von Willebrand factor
WCL	Whole cell lysate

CHAPTER 1

Introduction

1.1 Angiogenesis

1.1.1 Vascular development

1.1.1.1 overview

The human vascular system is composed of a network of blood and lymphatic vessels. They function to ensure the stability of various physiological mechanisms inside the body such as the supply of oxygen and nutrients to tissues/organs and removal of waste materials (Adams and Alitalo, 2007). Vascular dysfunction can lead to serious pathological consequences that alter blood pressure and tissue perfusion (Carmeliet, 2003; Alitalo *et al.*, 2005).

Endothelial cells (ECs) form the inner lining of the vascular wall. They are responsible for mediating angiogenesis (Risau, 1997), and have a number of other critical functions as outlined below. ECs function as a barrier that separates blood from the adjacent tissues allowing the selective trans-endothelial transport of gases and molecules (Cines *et al.*, 1998). They have a secretory function producing vascular constricting/relaxing agents and Von Willebrand factor (VWF), involved in controlling blood pressure and haemostasis, respectively, during vascular injury (Dong *et al.*, 2002). ECs also regulate the trafficking of leukocytes from blood into tissues at sites of inflammation via the cell surface expression of cell adhesion molecules (Gonlugur and Efeoglu, 2004).

1.1.1.2 Vasculogenesis

The emergence of blood vessels starts at the very early stages of embryonic development by a process called vasculogenesis. During this process certain mesodermal precursor cells called angioblasts are recruited to the sites of initial blood vessel formation and these develop into ECs. These ECs then fuse and branch forming a primary vascular network (Carmeliet, 2003; Risau and

Flamme, 1995). Further growth and development of the vascular system is carried out by a second process called angiogenesis (Flamme *et al.*, 1997).

1.1.1.3 Angiogenesis

Angiogenesis is a dynamic process in which new blood vessels are generated from the existing vasculature. It consists of series of events that are mediated mainly by the angiogenic factors, one of the most potent is vascular endothelial growth factor (VEGF) A (Blanco and Gerhardt, 2013).

1.1.1.3.1 Mechanisms of angiogenesis

Tipping the equilibrium of the angiogenic switch such that vascular promoting agents are in excess of repressive agents results in angiogenesis. A key driver of this is tissue hypoxia, which causes the expression of VEGFA and other angiogenic factors, and together these mediate new vessel formation by ECs (Adams and Alitalo, 2007; Carmeliet, 2003; Ferrara *et al.*, 2003; Karamysheva, 2008). The angiogenic response is critical during embryogenesis and also occurs physiologically during tissue repair and in female menstruation (Carmeliet, 2003; Pandya *et al.*, 2006). Angiogenesis can also occur aberrantly in ischemic ocular pathologies, chronic inflammatory conditions and in cancer (Crawford *et al.*, 2009; Papetti and Herman, 2002).

1.1.1.3.2 Types of angiogenesis

A) intussusceptive/splitting angiogenesis

Intussusceptive angiogenesis occurs when there is intraluminal invagination and migration of the endothelium towards the centre, where cells from opposite sides meet and fuse forming a septum that divides each vessel into a pair of tubes. It is a rapid and an efficient form of angiogenesis that

occurs mainly during development when the local blood supply is insufficient for fast-growing tissues or high energy metabolic processes. It also occurs during vascular remodelling to prune regressing malfunctioning vessels (Caduff *et al.*, 1986; Mentzer and Konerding, 2014).

B) Sprouting angiogenesis

Sprouting angiogenesis is the emergence of new capillaries from preformed vasculature (Hillen and Griffioen, 2007). In the initial stages of sprouting angiogenesis (Figure 1.1) the mural cells (pericytes) start to detach from the ECs and the inter-endothelial junctions loosen. This is followed by focal degradation of the basement membrane (BM) as well as the deposition of extracellular matrix (ECM) molecules to support endothelial sprout formation. Some ECs are selected as tip cells, these have filopodial processes which facilitate the growth of the sprout towards an increased concentration gradient of the chemoattractant/angiogenic factors. Cells behind the tip cells are specified as stalk cells. These are highly proliferative cells that divide rapidly to form columns behind the tip, and these subsequently form lumens. Elongating sprouts emerging from adjacent vessels meet and fuse, establishing blood flow, relieving the hypoxia, and reducing levels of pro-angiogenic factors. The newly formed vessels are stabilised through the production of a BM and the reattachment of the pericytes (Carmeliet, 2003). Tip and stalk cell selection is regulated primarily through Delta-Notch signalling which causes a differential response to VEGFA by these two endothelial subtypes; this results in vascular endothelial growth factor receptor (VEGFR) 2 rich filopodia in tip cells facilitating their directional migration towards VEGFA. Conversely, tip cell-mediated Notch signalling in stalk cells reduces filopodia formation and enhances the proliferation and extension of these cells (Blanco and Gerhardt, 2013).

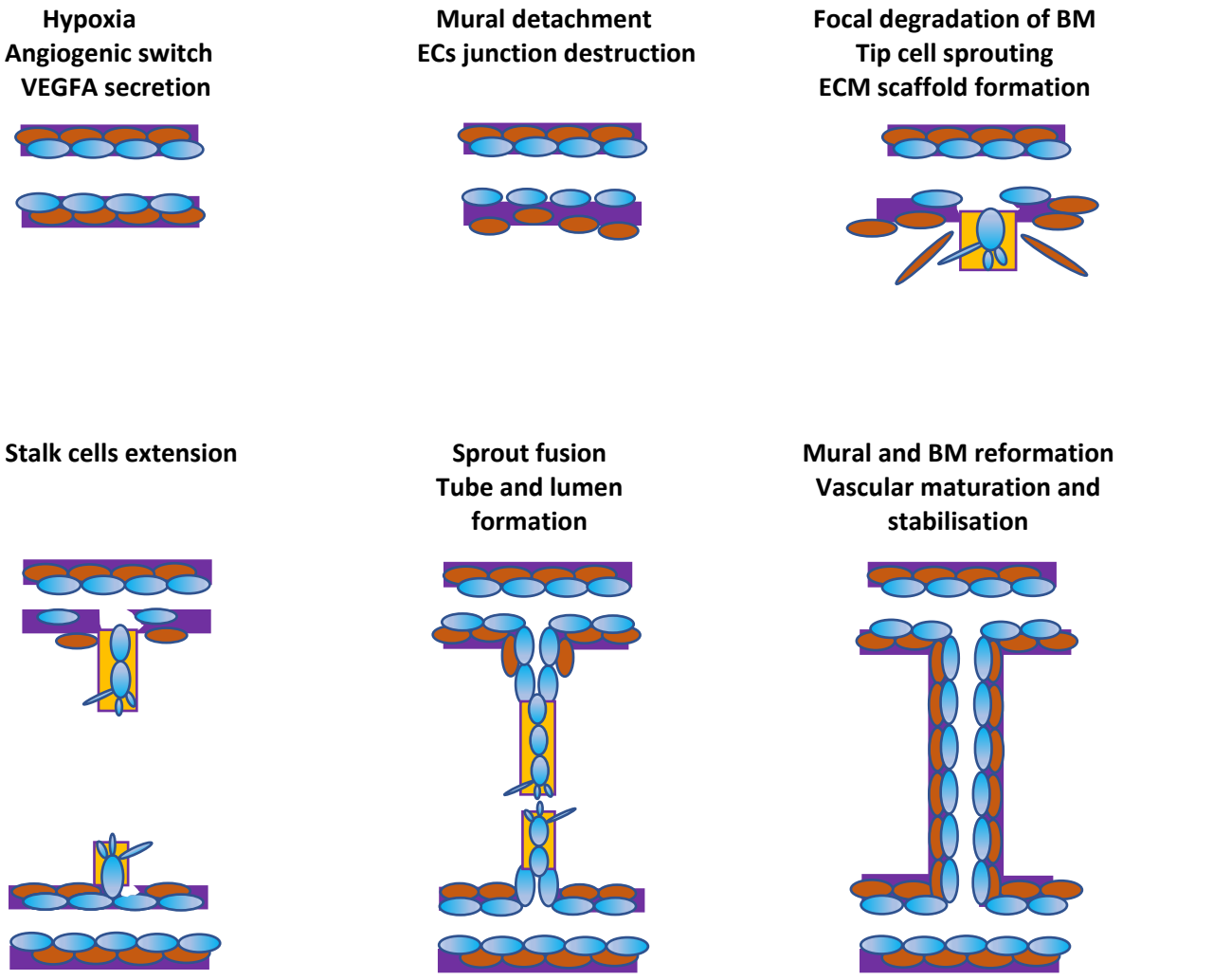

Figure 1.1. Sprouting angiogenesis.
Tissue ischemia switches the angiogeneic response. Mural cells (pericytes) detach, and the inter-endothelial (ECs) junctions break followed by focal destruction of the BM. Tip cells are selected and migrate on a scaffold of ECM towards a gradient of angiogeneic factors (VEGFA). Stalk cells are dividing and elongating forming tubes that canalise and fuse with the adjacent vessels forming lumens. Final vascular stability and maturation are reached by the reformation of the BM and reattachment of the pericytes.

1.1.1.3.3 Stimulators and repressors of angiogenesis

Most angiogenic promotors are growth factors (GFs) either secreted from ECs themselves or from the neighbouring cells and are sometimes formed or stored in BM or ECM and released upon matrix disintegration causing ECs activation (Kalluri, 2003).

As previously mentioned, VEGFA is the main driver of angiogenesis (Roy *et al.*, 2006). VEGFA signalling is mediated by receptor tyrosine kinases (RTKs), VEGFR 1/2 and neuropilin, a cofactor bound to the endothelial membrane. During hypoxia VEGFA-VEGFR2 signalling predominates, promoting the angiogenic cascade listed above (Shweiki *et al.*, 1992; Distler *et al.*, 2003; Staton *et al.*, 2007). VEGFA signal transduction was found to be essential for vessel formation during embryogenesis, the absence of VEGFA resulting in embryonic lethality (Breier and Risau, 1996; Carmeliet *et al.*, 1996). Fibroblast growth factor2 (FGF2) was among the first characterised angiogenic promoting agents. It acts through fibroblast growth factor receptor2 (FGFR2) which is an RTK present on the ECs and stimulates ECM degradation, endothelial proliferation, specialization and maturation, motility and promotes the secretion of matrix metalloproteinases (MMPs) and plasminogen activator (Schott and Morrow, 1993; Barkefors *et al.*, 2008).

There are many more regulators of angiogenesis which include Angiopoietin I and II, integrins (including $\alpha_v\beta_3$ and $\alpha_v\beta_5$), cytokines such as IL-8 and derivatives of clotting factors which typically have an inhibitory role (Lamalice *et al.*, 2007; Karamysheva, 2008; Beck Jr and D'Amore, 1997; Papetti and Herman, 2002; Neufeld and Kessler, 2006; Rüegg *et al.*, 2004). These different factors act in concert in a variety of physiological and pathological contexts to mediate the angiogenic process.

1.2 RhoJ/TCL GTPase

1.2.1 RhoJ overview

RhoJ is a member of the Rho family of small guanosine triphosphatases (GTPases). Rho GTPases play a role in multiple cellular functions including regulating actin and focal adhesion (FA) dynamics, protein trafficking and gene expression. In addition, they play a number of roles in angiogenesis including ECM degradation, endothelial proliferation and motility and tubulo/ lumengenesis (Bryan and D'amore, 2007). RhoJ (TCL) was first cloned in 2000 and belongs to the CDC42 subfamily of Rho GTPases (Figure 1.2A) (Chiang *et al.*, 2002; Heasman and Ridley, 2008; Vignal *et al.*, 2000). Most Rho GTPases act as molecular switches that cycle between active guanosine triphosphate (GTP)-bound and inactive guanosine diphosphate (GDP)-bound forms. Nevertheless, some atypical members as Rnd 1-3 and RhoH are not regulated by this switch mechanism; they are persistently found in an active GTP-bound state (Heasman and Ridley, 2008). Guanine nucleotide exchange factors (GEFs) mediate exchange of GDP for GTP and GTPase-activating proteins (GAPs) promote Rho GTPases' intrinsic GTP hydrolysis activity (Figure 1.2B) (Burridge and Wennerberg, 2004; Schmidt and Hall, 2002).

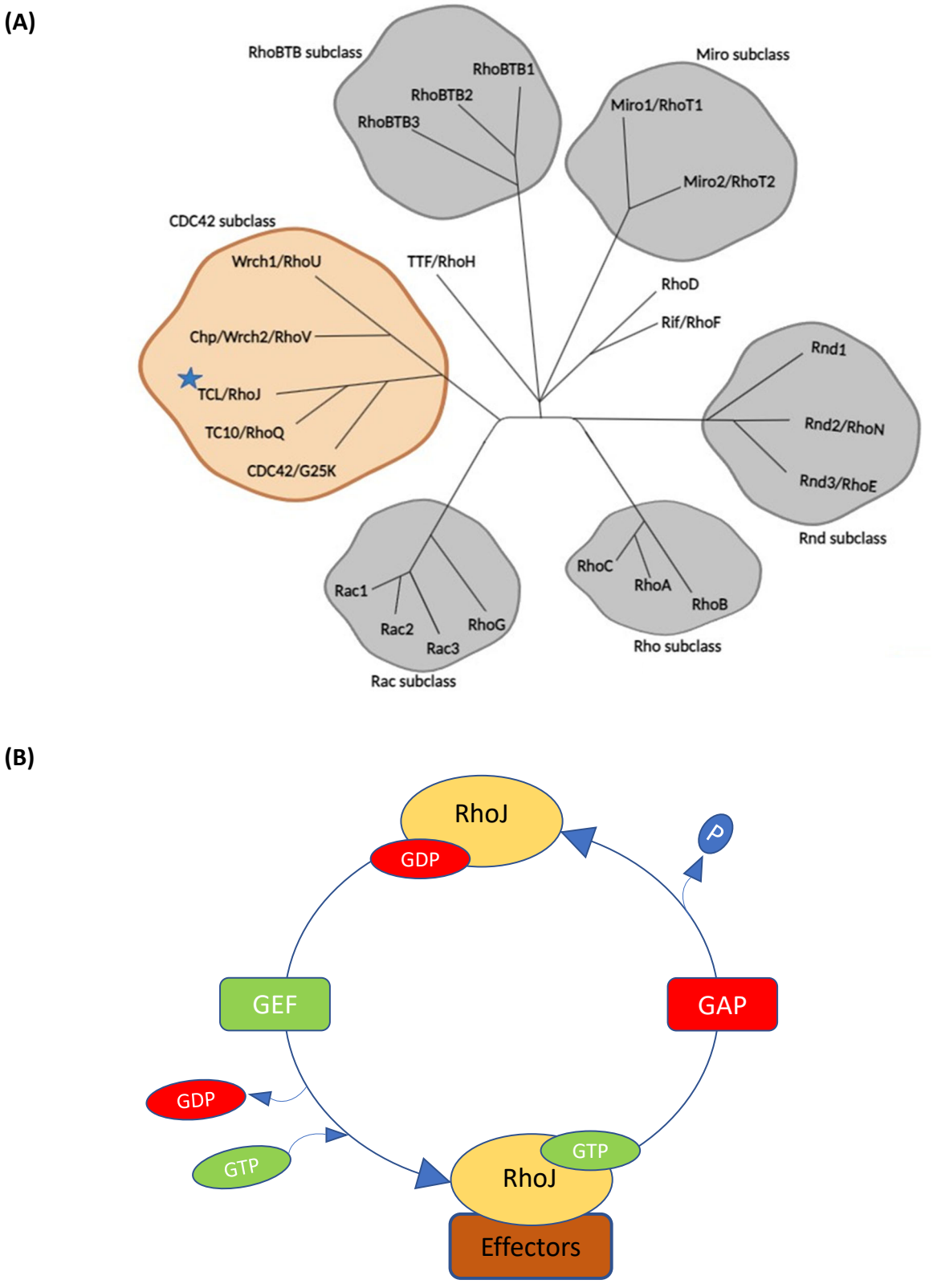

Figure 1.2. Rho GTPase family subclassification and GDP/GTP switch mechanism for RhoJ activation.

(A) A dendrogram showing the 23 small Rho GTPase members. They are further classified into eight subclasses on the basis of their amino acid sequence and domain similarities. RhoJ (blue star) belongs to CDC42 group of GTPases (orange). (B) RhoJ switches between active GTP-bound RhoJ and inactive GDP-bound RhoJ forms. The activation is mediated by GEF proteins which promote the exchange of GDP for GTP. Active RhoJ binds effector proteins to mediate downstream functions. GAPs enhance the hydrolysis of GTP to become GDP causing RhoJ inactivation. *The dendrogram is adapted from Grise et al. (2009).*

1.2.2 RhoJ structure and functions

All Rho GTPases have a similar structure consisting of a Rho-like insert domain, an effector motif and some contain a carboxyl (C)-terminal CAAX region (C- cysteine, A- aliphatic amino acid, X- any amino acid) (Madaule and Axel, 1985; Jaffe and Hall, 2005). The CAAX sequence is subjected to isoprenylation, proteolysis of AAX and methylation of C (Foster *et al.*, 1996; Liang *et al.*, 2002) resulting in attachment to cellular membranes, in the case of RhoJ this motif is farnesylated *in vitro* and *in vivo* (Roberts *et al.*, 2008). Proximal to the CAAX region, there is a hypervariable domain which contains a polybasic motif, predominantly consisting of arginine and lysine amino acid (aa) residues and the configuration of these residues within this motif determines subcellular localisation (Jack *et al.*, 2008) (Figure 1.3). The amino (N)-terminal region of Rho GTPases, consisting of p-loop and switch I and II regions, mediates binding of GDP and GTP, and this is stabilised by Mg^{+2} which prevents the spontaneous GDP/GTP switching (Paduch *et al.*, 2001). During Rho GTPase activation, the GEF binds to the p-loop, GDP detaches, the γ-phosphate of GTP binds the switch area and then the GEF dissociates (Cherfils and Chardin, 1999). The conformational change in the switch regions induced by GTP binding results in binding to effector proteins, and RhoJ, like CDC42 and Rac, binds effector proteins containing CDC42 and Rac-interactive binding (CRIB) domain (Vignal *et al.*, 2000; Leszczynska *et al.*, 2011). Signalling is switched off when GTP is hydrolysed to GDP, and this intrinsic activity of Rho GTPases is promoted by GAPs (Cherfils and Zeghouf, 2013).

Ackermann *et al*. (2016) determined that aa residues 17-20 (Asp-17, Glu-18, Lys-19 and Lys-20) are involved in directing localisation of RhoJ to the plasma membrane, and that this N-terminal region in concert with 121-129 aa residues are involved in the regulation of nucleotide exchange (Ackermann *et al.*, 2016). As well as RhoJ's aforementioned farnesylation, RhoJ contains two

putative palmitoylation sites at the C-terminus (Aicart-Ramos *et al.*, 2011) (Figure 1.3) and indeed recently glutamine synthetase has been demonstrated to be involved in promoting and sustaining palmitoylation of RhoJ. This post-translation promotes membrane localisation and activation of RhoJ, which in turn positively regulates angiogenesis and cell migration (Eelen *et al.*, 2018).

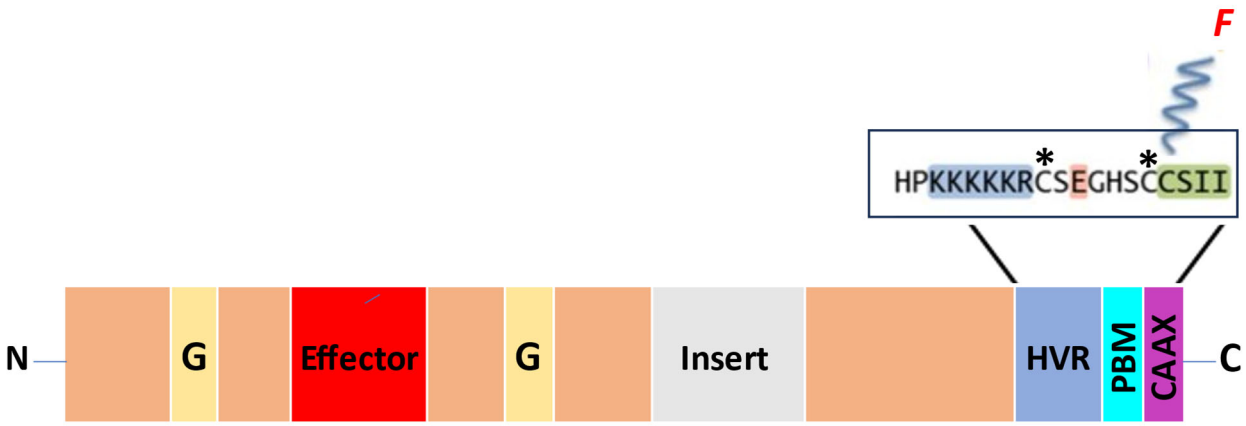

Figure 1.3. Main structural domains of RhoJ GTPase.
RhoJ protein has GTP/GDP binding domains (G), an effector motif, a Rho-insert region, and a C-terminus hypervariable domain (HVR) with its polybasic motif (PBM) and a distal CAAX region that is farnesylated (*F*), promoting RhoJ membrane anchorage. Top box shows the carboxylic aa sequence with the potential palmitoylation sites (*) proximal to farnesylated cystine of RhoJ CAAX motif sequence (highlighted in green). Positively and negatively charged aa residues are highlighted in blue and red, respectively.

1.2.3 RhoJ plays a key role in endothelial biology and angiogenesis

1.2.3.1 Endothelial expression of RhoJ

When first characterised, RhoJ was identified as being involved in adipocyte differentiation, endocytic trafficking and actin organisation (Nishizuka *et al.*, 2003; Vignal *et al.*, 2000; Abe *et al.*, 2003; de Toledo *et al.*, 2003; Chiang *et al.*, 2002). However, several subsequent studies by multiple groups have demonstrated that RhoJ is highly expressed in the endothelium of both normal and tumour vessels (Kaur *et al.*, 2011; Takase *et al.*, 2012) and its expression is regulated by ETS transcription factor ERG (Yuan *et al.*, 2011). *In vivo*, endothelial expression of RhoJ was observed in the intersegmental vessels (ISV) (the first angiogenic vessels) of mouse embryos at embryonic day (E) 9.5 (Kaur *et al.*, 2011) as well as in the developing retinal vasculature of new-born mouse (Fukushima *et al.*, 2020).

Recent studies also showed that overexpression of transcription factor ETV2 (ETS variant 2) resulted in enhanced expression of RhoJ in embryoid bodies and mouse embryonic fibroblasts, and using chromatin precipitation this transcription factor was found associated with the RhoJ promoter (Singh *et al.*, 2020). This group showed that mouse endothelial progenitors at E7.75 and E8.75 expressed RhoJ, and its expression was also found in human hemogenic ECs as well as haematopoietic progenitor cells (Angelos *et al.*, 2018). Another study looking at gene expression during human embryonic stem cell differentiation *in vitro* found that while RhoJ was not expressed in stem cells, it was strongly upregulated upon differentiation (Kim *et al.*, 2014b). While RhoJ is clearly expressed during the development of the vasculature, it was also found in a primary tumour angiogenesis signature determined by analyses of 121 primary breast, renal clear cell and head and neck squamous cell carcinomas (Masiero *et al.*, 2013).

1.2.3.2 Role of RhoJ in angiogenesis

As well as its endothelial expression pattern, there is considerable evidence indicating a functional role for RhoJ in modulating angiogenesis *in vivo.* RhoJ knockdown prevented tubule formation in mice treated with RhoJ si-RNA–Matrigel plugs (Yuan *et al.*, 2011).

Genetically modified mice have given considerable insight into the function of RhoJ in vessel formation and stability. Global RhoJ gene deletion does not affect viability indicating that RhoJ is not essential for vessel development, however subcutaneously implanted tumours grew more slowly in RhoJ knockout mice and showed reduced vascular density compared to tumours in control mice (Wilson *et al.*, 2014). This was also observed in a different tumour model, where tumour vessel integrity was impaired in mice lacking RhoJ; there was vascular wall distortion, intra-tumour haemorrhage and reduced expression of vascular endothelial (VE)-cadherin. The reduction in vessel integrity was associated with reduced metastasis (Kim *et al.*, 2014a).

A number of studies have also investigated how RhoJ affects the retinal vasculature in neonatal mice; conditional deletion of RhoJ negatively affected the number and radial arborisation of these vessels and this was more pronounced in small frontal/peripheral blood vessels. This was associated with marked regression in isolectin B4-expressing ECs causing an increase in the BM empty sleeves (Takase *et al.*, 2012). Investigation of the embryonic vasculature in RhoJ knockout mice has uncovered defects in additional vascular beds including abnormalities in the intersegmental and cephalic vasculature (Fukushima *et al.*, 2020). These data all indicate that RhoJ plays a role in vessel formation and stabilisation *in vivo.*

1.2.4 Molecular functions of RhoJ

Roles for RhoJ have been identified in regulating cytoskeletal dynamics, cell polarisation and protein trafficking and the integration of directional cues in endothelial migration (Fukushima *et al.*, 2020; Yuan *et al.*, 2011; Vignal *et al.*, 2000; Aspenström *et al.*, 2004).

1.2.4.1 RhoJ regulates the cytoskeleton

A number of studies have indicated that RhoJ plays a role in regulating the actin cytoskeleton. Manipulating RhoJ activity has been shown to affect actin stress fibres, dorsal ruffles, lamellipodia and podosomes (Vignal *et al.*, 2000; Aspenström *et al.*, 2004; Billottet *et al.*, 2008; Monypenny *et al.*, 2009) all this is indicative of a role for RhoJ in regulating cell shape. Our group observed that RhoJ knockdown resulted in reduced endothelial motility, increased actomyosin contractility and FA numbers, whereas expression of dominant active RhoJ (daRhoJ) had the converse effect (Kaur *et al.*, 2011). Additionally, daRhoJ expression enhanced the FA instability and reduced disassembly time. Active RhoJ co-immunoprecipitated with PAK interacting exchange factor (β-PIX) and with G protein coupled receptor kinase interacting target proteins (GIT1 and GIT2), and also co-localised with these proteins at FAs in ECs (Wilson *et al.*, 2014). The GIT-PIX complex has been identified as having a role in regulating FA turnover and this complex is discussed in more detail in section 1.3.2 below (Feng *et al.*, 2010; Zhao *et al.*, 2000; Kuo *et al.*, 2011; Nayal *et al.*, 2006). Active RhoJ interacted with the Spa homology domain (SHD) of GIT1 and together these findings suggest that RhoJ is recruited to FAs via its binding to GIT proteins and is involved in regulating FA disassembly (Wilson *et al.*, 2014), a model for RhoJ interacting with the GIT-PIX complex at FAs is shown in Figure 1.4.

RhoJ's regulation of FAs has been shown to impact neutrophil transmigration. Reducing RhoJ's expression augmented basal FA formation, which caused significant reduction in the basolateral mobility of transmigrated neutrophils, whereas the rate and velocity of apical migration were not impacted (Arts *et al.*, 2021).

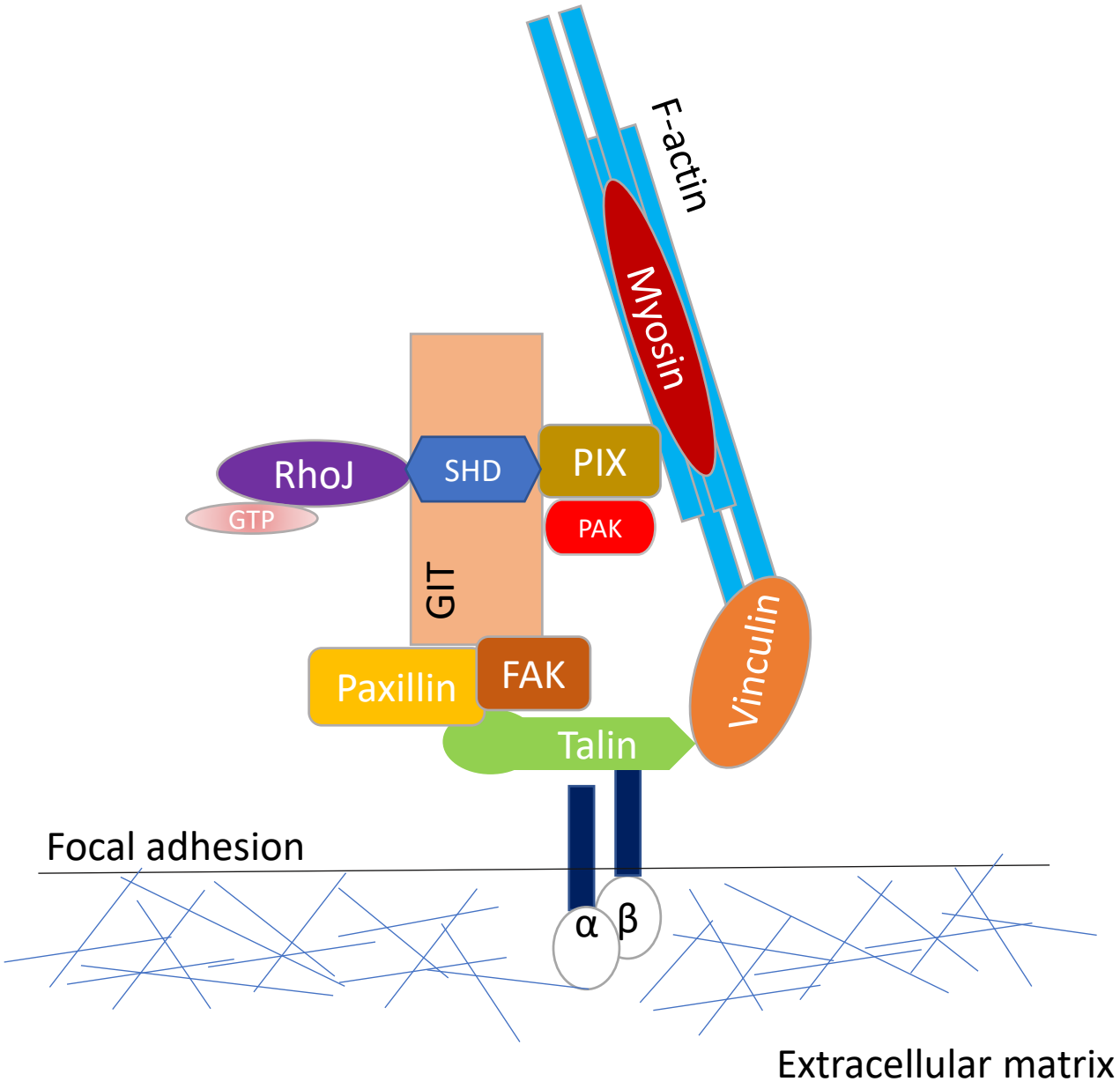

Figure 1.4. A cartoon of RhoJ-GIT-PIX interaction at FA.
GTP-RhoJ binds GIT-PIX through SHD of GIT protein. GIT associates with β-PIX (a GEF for Rac and CDC42) and paxillin. This enhances the recruitment of Rac and CDC42 to FAs via PAK and their subsequent activation by β-PIX causing FA dissociation and enhancement of cell migration. This is concomitant with reduction of RhoA activity and inhibition of actomyosin contractility.

1.2.4.2 RhoJ is involved in lumen formation and cell polarisation

Early studies indicated a role for RhoJ in endocytic trafficking (de Toledo *et al.*, 2003), and in an endothelial context RhoJ has been shown to play a role in lumen formation and cell polarisation. RhoJ was found to be involved CDC42/Rac1-mediated activation of PAK proteins 2 and 4 which were required for luminogenesis, with knockdown of RhoJ significantly inhibiting Rac1/CDC42 activity and preventing lumen formation (Yuan *et al.*, 2011). RhoJ was also involved in EC polarisation, specifically it localised with FMNL3 (Formin Like 3) at the early apical surface, mediating the assembly of actin filaments to facilitate the recruitment of podocalyxin to this cell location. Podocalyxin is a glycoprotein which is a major component of the glycocalyx, its localisation to the apical membrane is an initial key step in lumen formation (Richards *et al.*, 2015).

RhoJ also regulates trafficking of alpha5 beta1 ($\alpha_v\beta_1$) integrin which in turn negatively affects the assembly of fibrillar fibronectin. Specifically, RhoJ knockdown increased both levels of cell surface active $\alpha_v\beta_1$ and deposition of fibrillar fibronectin. An increase of fibronectin formation was also observed *in vivo* in the developing retina of the knockout mice, negatively impacting angiogenesis. This activity of RhoJ was mediated by the effector protein PAK3 (Sundararaman *et al.*, 2020).

1.2.4.3 RhoJ integrates endothelial response to migratory signals

RhoJ is involved in regulating the endothelial response to the attractive VEGFA and repulsive Semaphorin 3E (Sema3E) signals. VEGFA and Sema3E act through the VEGFR2 and PlexinD1 receptors, respectively, and these receptors form a complex at the cell surface (Bellon *et al.*, 2010). RhoJ was found to regulate the composition of this receptor complex and so enabled cells to differentially respond to different ratios of VEGFA and Sema3E. At high VEGFA levels, RhoJ was

required for stabilising a complex of VEGFR2, Neuropilin-1 and PlexinD1, resulting in sustained VEGFR2 phosphorylation, activation of downstream signalling proteins including ERK1 and driving forward migration. High Sema3E levels caused RhoJ release from PlexinD1, an altered VEGR2 complex, cell contraction and reverse migration (Fukushima *et al.*, 2020). Consistent with a role for RhoJ in migration, is its recently identified function in the endothelial to mesenchymal transition (EndMT). Silencing RhoJ in ECs cultured under hypoxic conditions reduced upregulation of TWIST and SNAIL, transcription factors involved in promoting mesenchymal gene expression; there was also less inhibition of VE-cadherin expression. Mechanistically, it was determined that RhoJ was involved in the upregulating WDR5, a core subunit of the histone H3 lysine 4 (H3K4) methyltransferase (Liu *et al.*, 2018). As well as its role in regulating endothelial motility, a large number of studies have identified a role for RhoJ in promoting migration and invasion of a number of different carcinoma types, this is discussed in section 1.2.6.

1.2.5 Regulation of RhoJ activity

RhoJ is a typical Rho GTPases that cycles between GTP-bound active and GDP-bound inactive forms and this is mediated by GEFs and GAPs, currently GEFs and GAPs of RhoJ are unknown. β-PIX has shown direct GEF activity for CDC42 (Feng *et al.*, 2006). Our group showed that β-PIX knockdown caused modest reduction for GTP-RhoJ levels in HUVECs stimulated for 30 minutes (mins) with VEGFA in comparison to the control level (Wilson, 2014, pp. 174-176), suggesting that it may be a GEF for RhoJ. Color-Aparicio *et al.* (2020) determined that the GEF Intersectin (ITSN) 1 when co-expressed with RhoJ in the Human embryonic kidney cell line (HEK293T) increased levels of active GTP-bound RhoJ; they additionally demonstrated that an active membrane-anchored mutant of ITSN1 was retained in endosomal compartments when co-expressed with a dominant negative form

of RhoJ, indicating an interaction between these proteins (Color-Aparicio *et al.*, 2020). Although these data are suggestive of ITSN1 being a GEF for RhoJ, it is unclear whether endogenous ITSN1 plays a key role as GEF for RhoJ in ECs.

VEGFA has both been shown to both stimulate and reduce RhoJ activation, and it is likely that VEGF's action on RhoJ is context dependent. Low levels of activated RhoJ were detected after short treatment (2 mins) of HUVECs with a high dose of VEGFA (Fukushima *et al.*, 2011; Kusuhara *et al.*, 2012). By contrast RhoJ was shown to be activated by VEGFA and FGF2 for a more prolonged stimulation (Kaur *et al.*, 2011).

1.2.6 Role of RhoJ in human pathology

In addition to RhoJ's physiological roles in endothelial biology and angiogenesis, there is increasing evidence for non-endothelial expression of RhoJ contributing to various pathologies including cancer and cardiovascular disease.

RhoJ in cancer

Expression of RhoJ has been reported in tumour cells in a number of types of cancer, including melanoma, glioblastoma, gastric cancer, breast cancer and sarcoma (Ruiz *et al.*, 2017; Wang *et al.*, 2022; Kim *et al.*, 2016; Chen *et al.*, 2020; Mills *et al.*, 2011) and its presence is typically associated with poor prognosis (Kim *et al.*, 2016; Bai *et al.*, 2020; Wang *et al.*, 2020). As with its role in promoting endothelial migration, it has been associated with promoting migration and invasion of tumour cells. In some cancer types its mechanism of action has been explored and this has shown interactions and functions of RhoJ which may also be relevant to its role in EC biology. In melanoma,

glioblastoma and breast cancer, RhoJ was found to depend on PAK1 for promoting a more aggressive cancer cell phenotype (the interaction between RhoJ and PAK is discussed in section 1.5.4). This included a role in mediating cytoskeletal rearrangement and enhanced motility (Ho *et al.*, 2013) and also in altering responses to DNA damage and the induction of apoptosis (Ho *et al.*, 2012). In relation to melanoma, RhoJ was upregulated in melanocyte precursor cells treated with ultraviolet radiation, its upregulation was associated with increased motility of these cells, and it has been hypothesised that RhoJ is a regulator of melanogenesis (Goldstein *et al.*, 2021). In contrast to the multiple reports of RhoJ expression being associated with poor prognosis, the converse has been reported in non-small cell lung carcinoma where low RhoJ expression was associated poor prognosis. *In vitro* experiments suggested that RhoJ was acting to suppress TGF-β-mediated epithelial to mesenchymal transition (Nozaki and Nishizuka, 2021).

It is not clear why RhoJ expression is upregulated in tumours, but at least two different transcription factors, EVI1 and c-jun have been implicated in promoting RhoJ expression in cancer cells (Wang *et al.*, 2017; Wang *et al.*, 2022). The large number of reports of RhoJ involved in cancer cells highlight a non-endothelial pathological role for this Rho GTPase. Its expression status within tumours may also help in treatment stratification, for example its expression levels relative to that of another gene CUGBP2 determined the level of cytotoxicity of sarcoma cells in response to histone deacetylase and DNA-methyltransferase inhibitor treatment (Mills *et al.*, 2011).

RhoJ in cardiovascular disease

A number of transcriptomics analyses suggest that RhoJ expression is altered in various cardiac pathologies. Studies of human heart samples indicated altered levels of RhoJ expression in dilated cardiac myopathy, but not ischaemic cardiac myopathy (Molina-Navarro *et al.*, 2014), and RhoJ was also found to be part of gene signature associated with a mouse model of progressive cardiomyopathy (Auerbach *et al.*, 2010). Investigating gene expression in leukocytes from patients with non-valvular atrial fibrillation also demonstrated differences in RhoJ expression, but it is not clear what, if any, impact this might have on leukocyte biology in this pathology (Duzen *et al.*, 2019). Analyses of MicroRNAs (miRNA; miR) in exosomes in plasma from patients with coronary artery disease, showed an increase in miR-146a-5p and miR-146b-5p compared with levels in plasma from control patients, this miRNA was found to target a number of genes encoding pro-angiogenic proteins, including the 3' untranslated region of RhoJ. Consistent with this, expression of miR-146a-5p or miR-146b-5p reduced migration and tubulogenesis in endothelial progenitor cells, but the patho-physiological consequence of this is unclear (Chang *et al.*, 2017).

1.3 GIT proteins

1.3.1 GIT overview

GIT1 and GIT2 (GIT1/GIT2) are adaptor proteins that have multiple domains and cellular functions (Figure 1.5). They are signal coordinators, cytoskeletal and protein trafficking regulators, have a GAP activity for ADP-ribosylation factor (ARF), and are scaffolds for many signalling molecules (Hoefen and Berk, 2006). Although there is a high degree of sequence homology between GIT1 and 2 (more than 80%), they are subject to different levels of RNA splicing (Premont *et al.*, 2000; Lee *et al.*, 2019)

as well as having different expression profiles. Using beta-galactosidase reporter mice GIT2 was found to be more ubiquitously expressed, whereas GIT1 was expressed in a more limited range of cell types including ECs and cells lining bronchi and bile ducts (Schmalzigaug *et al.*, 2007).

GIT proteins have been shown to play vital roles in cell migration through their interactions with RhoJ (Wilson *et al.*, 2014), PIX (Premont *et al.*, 2004; Zhao *et al.*, 2000), Mitogen-activated protein kinase kinase (MEK) 1 and ERK proteins (Yin *et al.*, 2004; Yin *et al.*, 2005) (Figure 1.5).

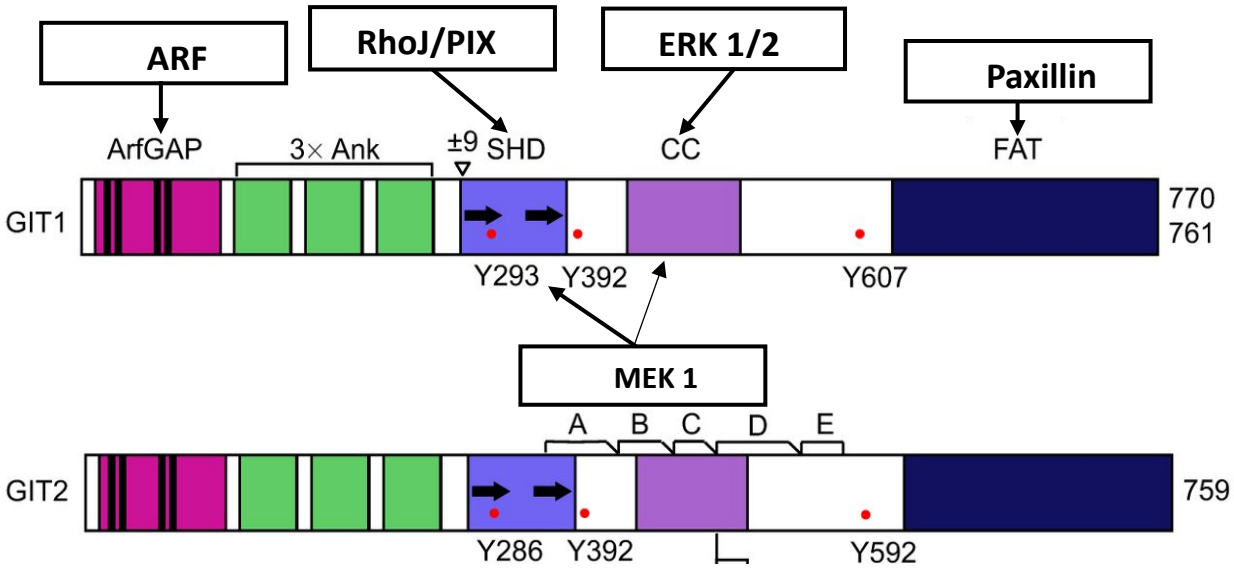

Figure 1.5. The domain structure of GIT1 and GIT2.
These schematics indicate the domain structure and show the ArfGAP domain, 3 ankyrin repeats (Ank), the Spa2 homology domain (SHD), a coiled-coil (CC) domain and focal adhesion targeting domain (FAT). The arrows show the interaction of GIT1 domains to different proteins. RhoJ and PIX bind the SHD domain, while MEK1 mainly interacts with the SHD (thick arrow) with a smaller involvement of the CC (thin arrow), ERK binds the CC domain, paxillin interacts with the FAT domain and ARF binds ArfGAP domains. A-E are the sites of GIT2 gene splicing. *Adapted from Zhou et al. (2016).*

1.3.2 The GIT-PIX complex

The GIT-PIX complex is a scaffold for various cellular macromolecules and a regulator for a vast range of signalling pathways (Frank and Hansen, 2008). There are two PIX genes, which encode α-PIX and β-PIX protein isoforms (Premont *et al.*, 2004; Ohara *et al.*, 1997; Bagrodia *et al.*, 1998). Like the GIT proteins, both α-PIX and β-PIX (GEFs for Rac/CDC42) have many domains and are involved in many protein-protein interactions (Zhou *et al.*, 2016). PIX proteins bind the SHD of GIT1/2 (Premont *et al.*, 2004; Zhao *et al.*, 2000) and this complex is found to play positive roles in cell migration by enhancing the FA formation and disassembly cycles (Feng *et al.*, 2010; Zhao *et al.*, 2000; Kuo *et al.*, 2011; Nayal *et al.*, 2006). PAK is recruited to FA, by binding the proline containing src homology (SH) 3 sequence of β-PIX protein (Manser *et al.*, 1998) which was shown to promote cell protrusion and mobility (Manabe *et al.*, 2002; Zhao *et al.*, 2000; West *et al.*, 2001). PAK also phosphorylates paxillin and enhances its binding to GIT proteins stabilising the GIT-PIX complex at adhesion sites (Nayal *et al.*, 2006).

Additionally, GIT1-β-PIX-PAK1 play roles in regulating microtubule synthesis (Oakley and Oakley, 1989; Cernohorska *et al.*, 2017). The function of PAK is considered in more detail in section 1.5. Several studies showed the GIT-PIX complex is involved in endothelial permeability and vascular homeostasis. PIX and GIT1 genetic alterations caused intracranial bleeding in zebrafish (Liu *et al.*, 2012). The GIT-β-PIX oligomer was an essential mediator for the PAK-MEK-ERK dependant hyperpermeability response in the mouse lung endothelium during inflammation (Stockton *et al.*, 2007). Conversely the interaction of GIT-β-PIX with SCRIB (an endothelial polarising and atheroprotective protein) intensified the endothelial junction integrity and restricted vascular permeability. Absence of SCRIB or β-PIX promoted endothelial hyperpermeability and inflammatory

responses both *in vitro* and *in vivo* (Donners and Biessen, 2019; Schürmann *et al.*, 2019). Moreover, GIT proteins were specifically implicated in the regulation of endothelial barrier functions and vascular tone. Although it was demonstrated that GIT1 promoted endothelial hyperpermeability responses in HUVECs following growth factor stimulation in one study (Stockton *et al.*, 2007), several other studies showed that GIT1 sustained vascular integrity. GIT1 depletion was associated with increased permeability response in thrombin treated HUVECs (van Nieuw Amerongen *et al.*, 2004) and GIT1/2 were found to be involved in cytoskeletal changes observed in sphingosine 1-phophate-mediated enhancement of pulmonary endothelial monolayer integrity (Shikata *et al.*, 2003). Roundabout Guidance Receptor (Robo4) acts via GIT1 to modulate endothelial protrusion and enhances vascular stabilisation (Jones *et al.*, 2009).

In other vascular beds, GIT1 was found to be involved in the regulation Endothelial nitric oxide synthase (eNOS) activation and nitric oxide production (NO), a key vascular tone regulator. Liu *et al.* (2014) observed that GIT1 expression and tyrosine phosphorylation were essential for GIT1-eNOS interaction, which facilitated Src-AKT-mediated eNOS stimulation and NO production in the endothelium of hepatic sinusoids (Liu *et al.*, 2014). It was also demonstrated that β-PIX was highly expressed in these sinusoids and interacted with eNOS-associated GIT1. The SHD of GIT1 was identified as a region essential for trimer formation and eNOS stimulation. Depletion of GIT1 or β-PIX altered the eNOS activity (Liu *et al.*, 2022).

1.4 Extracellular regulated kinase 1 and 2 (ERK1/2) mitogen activated protein (MAP) kinases

1.4.1 ERK overview

ERK1 and ERK2 are MAP kinases that are stimulated by a variety of agonists, and are involved in regulating cell division, growth, survival, and differentiation (Buscà *et al.*, 2016). There is accumulating evidence that ERK is also involved in cell migration and angiogenesis (Song and Finley, 2018; Mavria *et al.*, 2006; Lavoie *et al.*, 2020). ERK is stimulated downstream of many signalling pathways including those mediated by RTK (Figure 1.6) and GPCR. ERK is activated by MEK1 and MEK2, which mediates consecutive phosphorylation of tyrosine 187 followed by threonine 185 (Chang and Karin, 2001). ERK phosphorylates a variety of effector proteins including RSK (p90 ribosomal S6) (Pearson *et al.*, 2001) and these proteins mediate a variety of responses resulting in the activation of various structural and regulatory proteins (Tanimura and Takeda, 2017).

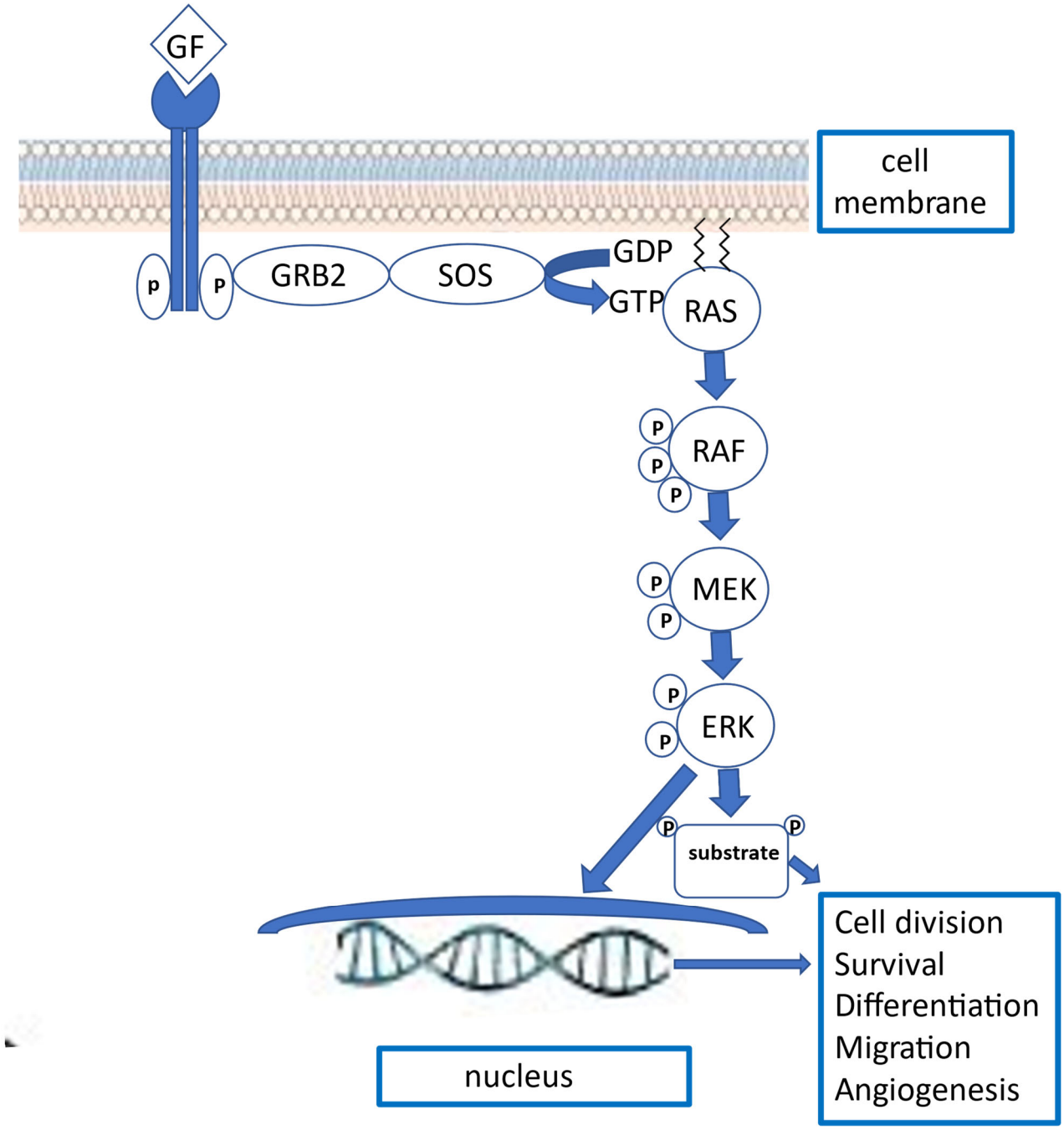

Figure 1.6. The MAP/ERK kinase signalling cascade.
The interaction between RTKs and their cognate GFs cause their dimerisation and subsequent phosphorylation (P) of the partner receptor's cytoplasmic tail. RTK phospho-tyrosine residues serve as docking sites for binding SH2 containing GRB2 (growth factor receptor-bound protein 2). This in turn enhances GRB2-SOS (Son of Sevenless) interaction. SOS is a GEF for RAS GTPase. Active RAS promotes the consecutive activation of RAF, MEK, ERK MAP kinases. Activated ERK enhances the gene expression and phosphorylation of various cytoplasmic substrates that are involved in vital cellular functions.

1.4.2 Role of ERK in regulation of endothelial motility and angiogenesis

Multiple studies observed ERK's functions during angiogenesis in various species. In mice, endothelial specific deletion of ERK1 and ERK2 severely limited angiogenesis and was embryonically lethal (Srinivasan *et al.*, 2009). Moreover, ERK was shown to be a VEGF target for inducing angiogenesis during zebrafish vascular development. ERK was selectively upregulated and activated in the sprouting ISV, but not in the terminally differentiated vasculature. Additionally, VEGF-ERK signal activation was found to be critically involved the angiogenic cascade promoting vessel growth in zebrafish embryos. Expression of VEGFA or C promoted ERK activation in zebrafish ISV and activated ERK promoted VEGFR3 expression. Consistent with these observations, blockade of ERK activity inhibited ISV elongation, endothelial proliferation and sprout formation, VEGFR3, Delta4 and Notch1b expression in these vessels (Shin *et al.*, 2016).

Recently, Fukushima *et al.* (2020), showed that RhoJ activity in mammalian ECs sustained VEGFR2 phosphorylation in response to high VEGFA levels, which caused activation of downstream signalling molecules including ERK1 promoting EC forward migration (Fukushima *et al.*, 2020). In tumour vessels, ERK was found to be involved in promoting angiogenic behaviour via negative regulation of Rho kinase (ROCK) (Mavria *et al.*, 2006). Likewise, Kaur *et al.* (2011) demonstrated that RhoJ activity reduced actomyosin contractility, and this was associated with enhanced EC sprouting and migration (Kaur *et al.*, 2011).

1.4.3 RhoJ and MAP kinase signalling functions in ECs

Crosstalk between RhoJ-PAK and MAP kinase signalling pathway during angiogenesis and in cancer have been reported in various studies. Yun *et al.* (2011) observed the involvement of RhoJ in Rac1

and CDC42 mediated-PAK2 and PAK4 activations in lumen formation. It was also reported that activation of CDC42 is essential for YES/Src-mediated PAK2 and PAK4 phosphorylation in RAF-ERK activation during luminogenesis. Absence of ERG or RhoJ inhibited the activity of CDC42, Rac1, PAK2 and PAK4 and B-RAF proteins and caused suppression of lumen formation (Koh *et al.*, 2008; Yuan *et al.*, 2011).

1.4.4 GIT-MEK1-ERK

In addition to the roles of the GIT-PIX complex described above in ECs, active GIT1 also scaffolds MEK1 during Angiotensin (Ang) II/EGF signalling in vascular smooth and in HEK293 cells causing ERK activation. The GIT1-MEK1 interaction was mediated by the SHD and to a lesser extent by the CC2 domain of GIT1 (Figure 1.5). This interaction was found to be constitutive and not affected by exogenous agonist stimulation and was essential for ERK activation. MEK1 and ERK phosphorylation were significantly increased in cells expressing wild type GIT1 compared to cells expressing GIT1 with mutant SHD (Yin *et al.*, 2004). Subsequent studies showed that GIT1 was also needed for ERK recruitment and activation at FAs in response to growth signal stimulation. This interaction was found to be mediated through the CC2 domain of GIT1 (Figure 1.5). ERK is involved in the phosphorylation of FA proteins, and hence ERK may play role in promoting cell motility through FA disassembly (Yin *et al.*, 2005). GIT1 acted as an essential pro-angiogenic mediator, with GIT1 knockdown resulting in reduced VEGFA stimulated ERK1/2 phosphorylation and GIT1 knockout mice showing defective alveovascular development (Pang *et al.*, 2009).

1.5 p21-activated kinases (PAKs)

1.5.1 PAK overview

PAKs are serine/threonine kinases (Martin *et al.*, 1995) involved in numerous vital cellular functions, including regulation of cell division, shape, migration, survival, angiogenesis, and gene expression (Yao *et al.*, 2020). PAKs are divided into 2 main subgroups: Group I (PAK 1, 2 and 3) and Group II (PAK 4, 5 and 6) and this classification is based on domain structure (Hofmann *et al.*, 2004) (Figure 1.7). PAKs possess an N-terminal regulatory domain, proline-rich motifs and a C-terminal catalytic site. In Group I PAKs, the regulatory region consists of 2 overlapping domains: the p21-binding domain (PBD) (which harbours the CRIB region) and an autoinhibitory domain (AID). The N-terminus also has a basic motif for interaction with cell membrane phospholipids. Proline rich motifs bind the SH3 domains of NCK, GRB2 and β-PIX. The proline region for β-PIX binding has a unique sequence (PxxxPR) which specifically potentiates PAK-PIX interaction and was found to be essential for PAK's recruitment to FAs (Strochlic *et al.*, 2010; Manser *et al.*, 1998). The catalytic region is highly conserved, and its activation loop contains one phosphorylation site at threonine 423 (Lei *et al.*, 2000; Zhao and Manser, 2012).

In Group II PAKs, the regulatory region either consists of the conserved AID/PBD overlapping domains as in PAK5 or PBD and an atypical pseudosubstrate domain (PSD) as occurs in PAK4 and PAK6. The latter domain is located at the proline rich region of the N-terminus (Figure 1.7A). Group II PAKs preferentially bind CDC42 Rho GTPases and were found to be more catalytically active than Group I PAKs under basal conditions (Abo *et al.*, 1998; Shao *et al.*, 2016; Ha *et al.*, 2015).

1.5.2 Regulation of PAK activity

In the inhibited state of AID-containing PAKs, the molecules dimerise. These dimers are configured in an antiparallel orientation such that the AID of one monomer locks the ATP loading cleft (activation site) of the other, forming a closed conformation that halts PAK's activation. When a cognate Rho GTPase becomes activated, it binds the PBD/CRIB domain, and causes structural alterations promoting the release of AID from the kinase region. This enables the phosphorylation of the threonine 423 which is followed by autophosphorylation of PAK at multiple residues, allowing for the closed dimer to open into single monomeric structure with subsequent full activation and substrate phosphorylation (Buchwald *et al.*, 2001; Eswaran *et al.*, 2008; Kumar *et al.*, 2017) (Figure 1.7B). Other studies challenged this mechanism for regulating Group I PAK activity by showing that this group of proteins were consistently exist in a monomeric conformation regardless of their activation status. It was also demonstrated that their activation follows a 2-step mechanism consisting of a GTPase binding which induces *cis*/self-autophosphorylation of the kinase domain. This is followed by a brief intermolecular interaction promoting *trans*-phosphorylation and amplification of PAK's activity (Sorrell *et al.,* 2019; Wang *et al.,* 2011).

In contrast, PSD-containing PAKs are not regulated by phosphorylation as described above, instead they are persistently phosphorylated and their activity is autoinhibited by binding of PSD to the activation loop (while PAK is in a single monomeric conformation), which blocks the substrate's access to the kinase domain. Upon GTPase binding, PSD-containing PAKs are recruited to their targeted sites of action within the cell, where SH3-mediated signalling promotes the detachment of the PSD allowing PAK's activation and subsequent substrate(s) phosphorylation (Zhang *et al.*, 2009; Ha *et al.*, 2012; Ha *et al.*, 2015; Won *et al.*, 2019).

Proteolytic digestion of the N-terminus, Akt or RAS-mediated PAK phosphorylation were other reported mechanisms for PAK activation (Walter *et al.*, 1998; King *et al.*, 2000; Menard and Mattingly, 2004).

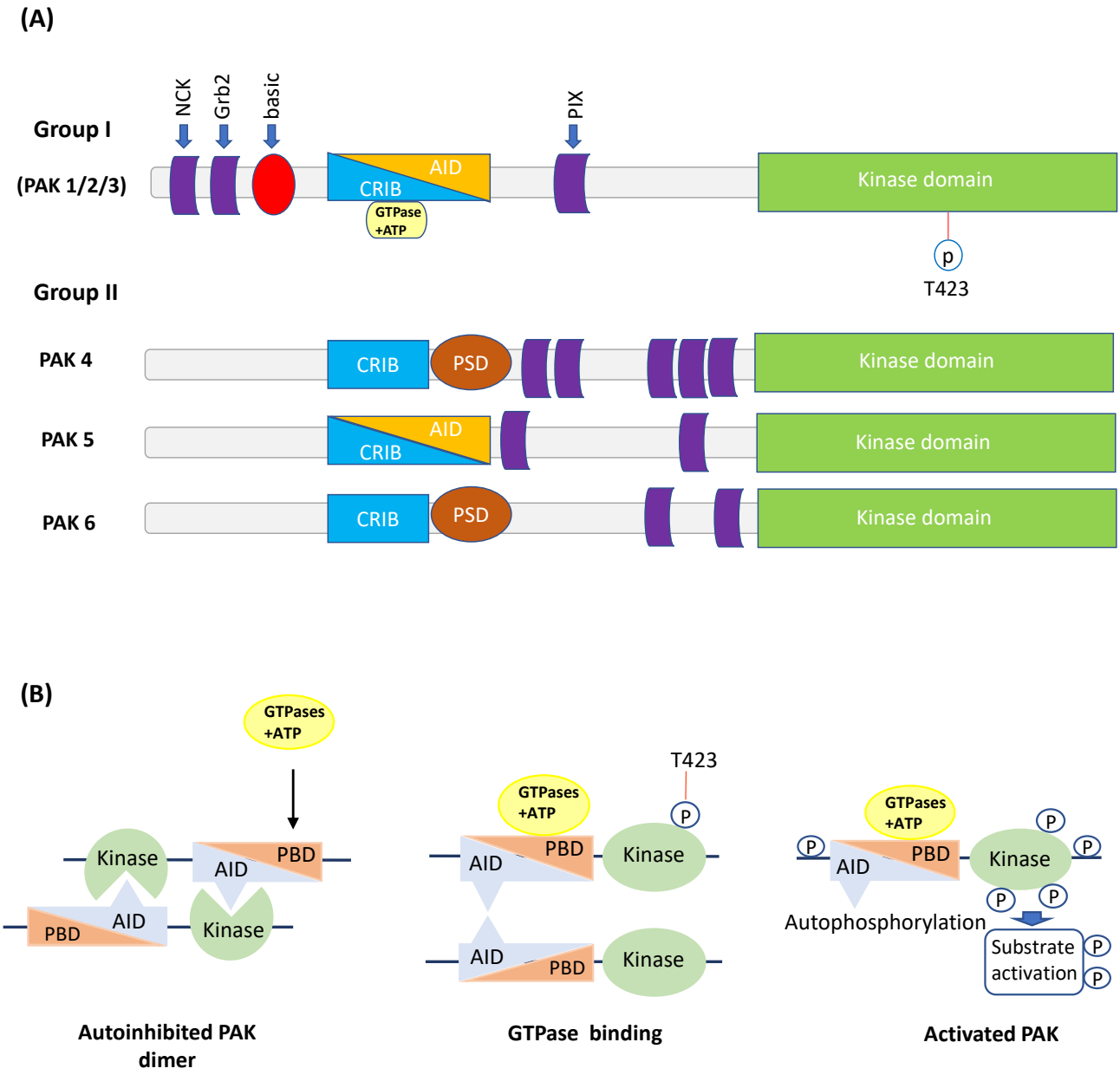

Figure 1.7. Domain structure of Group I and II PAKs and a schematic representation of the autoinhibition mechanism and GTPase-mediated activation.
(A) Group I and II PAKs consist of an N-terminal regulatory region and a conserved C-terminal kinase domain. A basic motif (red) for phospholipid dependent PAK stimulation, is also commonly found in the N-terminus of Group I PAKs and the proline rich motifs (purple) of this group bind SH3 residues of NCK, GRB2 and β-PIX (purple). The autoregulatory region of Group I PAKs and PAK 5 consists of PBD/CRIB that overlaps with AID, the former domain serves as a binding site for activated Rho GTPases. Instead of an AID, PAK4 and 6 possess a PSD domain at their N-terminus which binds the kinase domain abrogating substrate interaction and activation. (B) An illustration of the mechanism of AID autoinhibition; PAKs forms a homodimer where AID of one subunit blocks the kinase domain's active site of the other monomer. GTP-bound Rho GTPase-CRIB binding promotes the dissociation of the AID from the catalytic region allowing for monomer separation, T423 phosphorylation followed by autophosphorylation of kinase domain at multiple sites and full PAK's activation. When PAK becomes activated, it phosphorylates its substrates enabling them to perform various cellular functions.

1.5.3 The function of PAKs in EC biology and angiogenesis

Much evidence has shown various roles for PAK in EC biology, including in the regulation of angiogenesis and in vascular integrity. In the latter case PAKs are involved in the complex reorganisation of both junctional proteins and the cytoskeleton that are necessary for endothelial layers to modulate their permeability in response to a variety of environmental stimuli (Radu *et al.*, 2014).

PAKs are also involved in vascular development, depletion of PAK2 or PAK4 in mice during embryogenesis caused marked retardation in the vascular development and was associated with high lethality (Qu *et al.*, 2003; Hofmann *et al.*, 2004). PAK2 was reported to be the most highly expressed PAK in ECs, and specific endothelial deletion of PAK2 was associated with global cardiovascular defects at E9.5 in mouse (Radu *et al.*, 2015), this is a stage when the vasculature is developing and angiogenesis actively occurring (Walls *et al.*, 2008). Global PAK1 deletion did not significantly affect new vessel formation or tissue repair in mice subjected to limb vascular ischemia; however, there was a concomitant increase in PAK2 expression and activity, which enhanced ERK2 phosphorylation. Additionally, treatment of aortic explants from both PAK1 knockout and wild type mice with the PAK inhibitor IPA-3 resulted in dramatic reduction of tubule sprouting; thus, PAK2 could have been candidate target kinase for IPA-3 inhibitory effect in these experiments (Elsherif *et al.*, 2014).

In zebrafish, both β-PIX and PAK2a were shown to have essential roles in the development of brain vasculature, with reduced expression of any of these genes resulting in impairment of vascular integrity causing severe intracranial bleeding and hydrocephalus (Liu *et al.*, 2007).

1.5.4 Role of RhoJ-PAK in regulation of endothelial and non-endothelial functions

Our laboratory and other research groups have shown RhoJ interacts with CRIB-containing proteins such as PAKs (Vignal *et al.*, 2000; Leszczynska *et al.*, 2011). Yuan *et al.* (2011) determined that si-RNA-mediated knockdown of RhoJ markedly reduced levels of both active GTP-bound CDC42 and Rac1 as well as the activated phosphorylated forms of PAK2 and PAK4 (Yuan *et al.*, 2011). From these studies, however, it was not possible to discern whether RhoJ might be directly influencing PAK2 and PAK4 activations, or whether it was working via CDC42 and Rac1. In another study, CDC42 and RhoJ were found to play opposing roles in regulating ECs' formation of fibronectin fibrils, with CDC42 promoting and RhoJ inhibiting this process. This was found to be mediated by PAK3, an effector protein bound by both these Rho GTPases, and it was hypothesised that these GTPases which exhibit different localisation patterns both compete for limited pools of PAK3 to differentially modulate fibrillogenesis at different stages of angiogenesis (Sundararaman *et al.*, 2020). There is thus a complex interaction between RhoJ and PAKs in ECs which is yet to be fully elucidated.

As noted earlier in Section 1.2.6 RhoJ's expression in tumour cells plays a role in the pathogenesis of cancer, these studies have also highlighted connections between RhoJ and PAKs. In melanoma, RhoJ-PAK1 signalling modulated cytoskeletal dynamics and DNA damage responses which enhanced tumour invasiveness and resistance to therapy (Ho *et al.*, 2012; Ho *et al.*, 2013). Also, in this cancer type inhibition of PAK1 interfered with RhoJ's ability to promote an anti-apoptotic phenotype (Ruiz *et al.*, 2017). In glioblastoma, RhoJ-PAK (2 and 4)-ERK signalling downstream of JNK (c Jun N terminal kinase) MAP kinase was found to be essential tumour neovascularisation and progression (Wang *et al.*, 2022).

1.5.5 PAK inhibitors

1.5.5.1 PAK inhibitors and their mechanism of action

PAKs have been targeted with a range of small molecule inhibitors which typically fall into two main categories, ATP, and non-ATP competitive (allosteric) blockers. ATP-competitive inhibitors are a group of compounds that interact with the purine binding pocket, preventing ATP access to the activation loop of PAK's kinase domain (Semenova and Chernoff, 2017). An example of such an inhibitor is PF-3758309, a pyrrolopyrazole PAK inhibitor. It was initially formulated to target PAK4 (IC_{50} 1.3 nM - 4.7nM), however later studies demonstrated that it targets all PAK subtypes as well as showing some nonspecific inhibitory effects for other kinases (Murray *et al.*, 2010). It has been shown to have a variety of effects on EC function including abrogation of *in vitro* tube formation (Gopal *et al.*, 2016) and the potentiation of TNFα- release of inflammatory secretory bodies in HUVECs (Zhang *et al.*, 2020).

Allosteric inhibitors are small molecule inhibitors that interact with a site distinct from the active site. An example of an allosteric inhibitor of PAK kinases is IPA-3 (also called 2,2'-dihydroxy-1,1'-dinaphthyldisulfide), this is an allosteric inhibitor for Group I PAKs that showed specific potency against PAK 1. It modifies the regulatory region by forming chemical bonds with AID region to disable GTPase binding (Deacon *et al.*, 2008; Viaud and Peterson, 2009). It has been demonstrated in a number of experimental systems to affect angiogenesis and endothelial barrier function (Yan *et al.*, 2013; Jagadeeshan *et al.*, 2017; Hao *et al.*, 2019). However, IPA-3 (IC_{50} 2.5 µM) has been generally identified as a short acting inhibitor, showing less efficacy against GTPase pre-stimulated PAK1, and exerting its anti-PAK1 activity only at high doses (30 µM) in Platelet-derived growth factor (PDGF) pre-treated murine fibroblasts. This is possibly due to the rapid reduction of its disulphide bonds in

the cell's cytosol or in the presence of Dithiothreitol (DTT) rendering it structurally and functionally unstable (Deacon *et al.*, 2008).

1.6 Hypothesis and aims

The work described in this thesis aimed to investigate the molecular mechanisms of RhoJ function in ECs and to address the following hypothesis:

RhoJ positively regulates signalling pathways involved in EC motility, and specifically via its interaction with the GIT-PIX complex.

The three overarching aims of this thesis are outlined below.

Aim 1 – Investigate how RhoJ activity modulates activity of kinases in ECs.

Previous data from kinase arrays suggested that daRhoJ expressed in ECs resulted in the activation of a number of kinases including JNK, EGFR (epidermal growth factor receptor), AMPKα2, STAT5ab, Hck, MSK1/2, and PRAS40 kinases (Wilson, 2014, pp. 182-190). This formed the basis for the first aim which was to explore how RhoJ regulates the levels of active ERK and JNK MAP kinases in ECs. RhoJ activity was modulated by either transducing HUVECs to express daRhoJ or transfecting them with RhoJ specific si-RNA duplexes to reduce its expression and activation of ERK and JNK was assessed.

Aim 2 – Investigate how RhoJ regulates GIT2.

Previous work has demonstrated that the expression of daRhoJ caused an upward electrophoretic mobility shift of GIT2, potentially due to its increased phosphorylation (Wilson *et al.*, 2014). Preliminary data produced in the lab also identified serine and threonine residues that were

differentially phosphorylated in ECs expressing daRhoJ. This second aim used kinase inhibitors to investigate which kinase(s) were involved in this process.

Aim 3 – Determine if RhoJ regulates interactions between MEK1, ERK1/2 and the GIT-PIX complex and the recruitment of ERK1/2 to FAs.

Previously it was reported that GIT1 interacted with MEK1 and ERK1/2 in non-endothelial cells (Yin *et al.*, 2004) and that ERK1/2 was localised to FAs (Yin *et al.*, 2005; Zhang *et al.*, 2009). Our group had also reported an interaction between GIT1/2 and RhoJ and had observed that RhoJ affected the recruitment of the GIT1/2 and β-PIX to FAs (Wilson *et al.*, 2014). The aim of this work was to determine using co-IP if RhoJ regulated the interaction between MEK1 and ERK1/2. Fluorescence microscopy was also used to determine if RhoJ affected the localisation of ERK1/2 to FAs.

CHAPTER 2

Materials and methods

2.1 Buffers and reagents

The different buffers/reagents used in this study including their composition, if applicable, are detailed in Table 2.1 below. All reagents listed below were purchased from Sigma (UK) unless otherwise stated. The details of their usage are described in the relevant sections in this chapter. Tables 2.2.1 and 2.2.2 list the primary and secondary antibodies used in this study, respectively.

Table 2.1 Standard buffers

Buffer/Reagent	Ingredients
NP40 lysis buffer	-20 mM Tris-HCl pH 7.5, 150 mM NaCl, 1% (v/v) nonidet P40 (NP40), 1 mM EDTA, 0.02% (w/v) Sodium azide -Mammalian protease inhibitor (Sigma) and phosSTOP (Roche) were used according to manufacturer's instructions
2X SDS-PAGE sample buffer (Laemmli sample buffer)	100 mM Tris-HCl pH 6.8, 20% (v/v) glycerol, 20% (v/v) 2-mercaptoethanol, 4% (w/v) SDS, 0.2% (w/v) bromophenol blue
Tris-buffered saline (TBS)	150 mM NaCl, 20 mM Tris-HCl pH 7.5
Tris-buffered saline Tween-20 (TBST)	150 mM NaCl, 20 mM Tris-HCl pH 7.5, 0.1% (v/v) Tween-20
4X Stacking gel buffer	125 mM Tris-HCl pH 6.8, 0.1% (w/v) SDS
4X Resolving gel buffer	375 mM Tris-HCl pH 8.8, 0.1% (w/v) SDS
SDS-PAGE running buffer	250 mM glycine, 25 mM Tris-base, 0.1% (w/v) SDS, pH 8.3

Western blotting transfer buffer	47.6 mM glycine, 6 mM Tris-base, 20% (v/v) methanol, pH 8.3
Western blotting blocking buffer	5% (w/v) dried skimmed milk in TBST
Protogel	30% (w/v) Acrylamide: 0.8% (w/v) Bis-acrylamide in a proportion of (37.5:1)
Western Blotting stripping buffer	62.5 mM Tris-HCl pH 6.8, 2% (w/v) SDS, 100 µM 2-mercaptoethanol
1%(v/v) Triton X100 lysis buffer	1%(v/v) Triton X 100, 150 mM NaCl, 10 mM Tris HCl pH 7.5, 1 mM EDTA, 0.01% (w/v) NaN3
Immunofluorescence (IF) blocking buffer	10% (v/v) foetal bovine serum, 3% (w/v) bovine serum albumin, 0.1% (v/v) Tween20, 0.01% (w/v) NaN3
TEEND buffer	25 mM Tris-HCl, 2 mM EDTA, 5 Mm DTT, 10 mM Nacl
NaCl/sucrose buffer	150 mM NaCl, 2 mM EDTA, 10 mM sodium azide, 20 mM Tris base (pH 7.4), 0.25 M sucrose
RIPA buffer	-150 mM Sodium chloride, 50 mM Tris-base (pH 8.0), 0.5% Sodium deoxycholate, 0.1% SDS, 1 mM EDTA -Mammalian protease inhibitor (Sigma) and phosSTOP (Roche) were used according to manufacturer's instructions

2.2 Antibodies

Table 2.2.1 Primary antibodies

Antibody	Clone number/ product code	Working concentration / dilution	Manufacturer/Supplier
Mouse monoclonal anti-GFP	3E1	1: 1000	CRUK central services
Rabbit polyclonal anti-human phospho JNK (pJNK) (Thr183/Tyr185)	Code 9251S	1: 1000	Cell Signalling Technology, UK
Rabbit polyclonal anti-human JNK	Code 9252S	1: 1000	Cell Signalling Technology, UK
Rabbit monoclonal anti-human phospho-p44/42 MAPK (pERK1Thr202/Tyr20) (pERK2Thr185/Tyr187)	D13.14.4E Code 4370P	1: 1000	Cell Signalling Technology, UK
Rabbit monoclonal anti-human p44/42 MAPK (ERK or total ERK 1/2)	137F5 Code 4695S	1: 1000 (WB) 1: 200 (IP) 1: 400 (IF)	Cell Signalling Technology, UK
Rabbit monoclonal anti-human GIT2	D11B8, Code 8072S	1: 1000	Cell Signalling Technology, UK
Rabbit polyclonal anti-human α-Tubulin	Code 2144S	1: 1000	Cell Signalling Technology, UK

Mouse monoclonal anti-human RhoJ	1E4 Code H00057381	1: 1000 (0.5 µg/ml)	Abnova
Mouse monoclonal anti-human MEK1	25/MEK1 (RUO)	1:1000 (WB) (0.25 µg/ml) 1µg/ml (IP)	BD Transduction Laboratories
Mouse monoclonal anti-human vinculin	hVIN-1	1:400 (IF)	Sigma
control IgG		1 µg/ml	Sigma-Aldrich/Merck

Table 2.2.2 Secondary antibodies

Antibody	**Working concentration /dilution**	**Manufacturer/Supplier**
Goat anti-mouse IgG HRP linked	1: 1000	Caymen Chemical
Goat anti-rabbit IgG HRP linked	1: 1000	Cell Signalling Technology, UK
Donkey polyclonal anti-rabbit conjugated to Alexa Fluor488	4 µg/ml (IF)	Invitrogen

2.3 si-RNA duplexes

These consist of 2 RNA strands that have 19 complimentary base-pairs. Each strand has twoThymidine (dTdT) nucleotides overhangs at the 3' end . RhoJ and negative control si-RNAs were supplied by Eurogentec. The negative control is a si-RNA duplex that is not complimentary to any mRNA sequence.

Table 2.3 si-RNA duplexes

si-RNA duplex	Gene of interest	Sequence
RhoJ si-RNA 1	Human RhoJ (bases155- 174)	5`-ccacuguguuugaccacuau-3`
RhoJ si-RNA 2	Human RhoJ (bases 455-474)	5`-agaaaccucucacuuacgag-3`
Negative control (si-Control)	Non-specific to any known human gene sequences	Undisclosed by Eurogentec

2.4 Plasmids

The plasmids listed in Table 2.4 used in this study had either been previously constructed in the laboratory or provided by other scientists.

Table 2.4 Plasmids

Plasmid	Source
pWPXL-GFP-daRhoJ	Dr.Katarzyna Lesczczynska (Leszczynska Katarzyna, 2011)

pWPXL-GFP	Addgene deposited by Prof. Didier Trono Swiss Institute of Technology (EPSL)
psPAX2	
pMD2G	

2.5 Standard tissue culture techniques

There were two sources of HUVECs: these were either isolated from umbilical cords obtained from University of Birmingham Human Biomaterials Resource Centre (project 16-266E1) and used in lentivirus transduction (see section 2.8.1) or procured commercially from Promocell. Commercially sourced HUVECs (Promocell) were from pooled donors. HUVECs were approximately used between passage 2 and 6 and experiments repeated with HUVECs at similar passage numbers.

HUVECs isolated in our laboratory were cultured in complete M199 (cM199): Medium 199 (Sigma) supplemented with 10% (v/v) foetal calf serum (FCS) (Gibco), 2 mM L-glutamine (Thermo Fisher Scientific), 90 µg/ml heparin (Sigma) and 10.1% (v/v) bovine brain extract (BBE) purified as previously described (Maciag *et al.,* 1979). For commercially sourced HUVECs, cM199 was prepared by supplementing basal M199 with 10% (v/v) FCS and 1% (v/v) L-glutamine, as above and Endothelial Cell Growth Medium 2 Supplement Mix (Promocell) according to the manufacturer's instructions. Antibiotics consisting of I00 I.U of penicillin and 100 µg Streptomycin/ml (Invitrogen) were added when needed. Under complete aseptic conditions, cM199 was sterilized using 0.22 µm pore size filters, kept at 4 ^{0}C and pre-warmed in water bath at 37 ^{0}C just prior use in cell culture. Plates for HUVECs culture were pre-coated with 0.1% gelatin (w/v) (Sigma- Aldrich) in phosphate-buffered saline (PBS) (Sigma). 2 ml or 4 ml were added to 6 or 10 cm dishes, respectively, and incubated for 20 mins at room temperature (RT), then aspirated.

SV40 large T-antigen-transformed HEK293T cells (Lebkowski *et al.*, 1985) were grown in complete growth media using Dulbecco's Modified Eagle's Medium (DMEM) (Sigma) with added 10% (v/v) FCS and 2 mM L-glutamine (cDMEM). Cells were incubated at 37 ^{0}C in a humidified incubator (Sanyo)

with 5% carbon dioxide (CO_2). A Leica DM IL inverted phase contrast microscope (Leica Microsystems, Houston, USA) was used to regularly check cell culture conditions.

2.5.1 Cell Passage

HUVECs were passaged approximately every 5 days (1:3 split) with cell feeding 2-3 days after passaging; HEK293T cells were passaged approximately every 2-3 days (1:10 split). Cells from a 10 cm dish were harvested as follows: first, adherent cells were washed with sterile PBS to remove all FCS-containing medium. Next, 3 ml (0.1% (v/v) of trypsin-EDTA (Ethylenediamine tetra acetic acid) diluted in PBS (Thermo Fisher Scientific), was added to detach the cell monolayer. Cells were incubated with trypsin for few mins at RT and then promptly neutralised with cM199 or cDMEM to deactivate trypsin. Cells were then collected and centrifuged for 5 mins at 195 g (Biofuge Primo Heraeus centrifuge, Thermo Electron Corporation) at RT. The cell pellet was then resuspended in the appropriate media and either passaged further or used in experiments.

2.5.2 Cell Counting

Cells were counted using a haemocytometer slide (Neubauer, Paul Marienfeld GmbH & CO), adding a 10 µl of cell suspension under the cover slip. The number of cells in haemocytometer grids were counted, averaged and the number of cells needed for seeding was then calculated.

2.5.3 Cryopreservation and thawing cells

Cells were harvested and passaged as mentioned in section 2.5.1. The cell pellet was resuspended in a freezing solution consisting of volumes of dimethyl sulfoxide (DMSO) (Sigma) and FCS (Thermo Fisher Scientific) mixed at a ratio of 1: 9. Aliquots of the cell suspension were placed in cryovials,

frozen gradually using a Mr Frosty freezing container (NalgeneTM, Thermo Fisher Scientific) and placed at -80 ^{0}C for short term storage, while for longer term storage, cells were placed in liquid nitrogen storage facilities. Whenever needed, cells were thawed by briefly placing the cryovial in a warm water bath (37 ^{0}C) then washed with 10 ml growth media prior to plating.

2.6 Protein analysis

2.6.1 Preparation of whole cell lysate (WCL)

Prior to protein extraction, cells were washed once with PBS and then detached in a small volume of PBS using a cell scraper then transferred to a 1.5 ml tube. The cell suspension was then spun at 2,500 g at RT for 2 mins to pellet the cells (Heraeus™ Pico™ 17 Microcentrifuge, Thermo Eectron LED Gmbh LR56495 D-37520, Osterode Germany). The supernatant was discarded, and the pellet was then resuspended in ice cold NP40 lysis or RIPA buffer containing protease and phosphatase inhibitors (Table 2.1). Samples were centrifuged at 16,602 g at 4 ^{0}C for 15 mins (Refrigerated Microfuge Sigma 1-14k, Sigma Laborzentrifugen GmbH, Germany). The supernatant (cell lysate) was then collected and if necessary, a small volume (5-10 µl) was used for protein quantification. The lysate was used either in immunoprecipitation (IP) assays or for analysis by western blotting. In the latter case, lysate was mixed with an equal volume of 2X Laemmli sample buffer (containing 5% (v/v) 2-mercaptoethanol, Sigma) (Table 2.1). All samples were stored at -20 ^{0}C until further processing.

2.6.2 Bicinchoninic acid assay (BCA assay) for protein quantification

The protein concentration in samples was measured using a BCA assay (ThermoFisher scientific) according to the manufacturer's protocol for measuring protein in a 96 well plate. A standard curve was prepared using bovine serum albumin (BSA) (VWR chemicals) diluted in NP40 lysis buffer (Table

2.1) at the following concentrations: 0, 0.25, 0.5, 1 and 2 mg/ml. NP40 lysis buffer served as blank (0 mg/ml) concentration. Lysates of unknown protein concentrations were either diluted 1: 2 or 1: 5 in NP40 lysis buffer (Table 2.1). In a 96 well plate, 10 µl of blank, BCA standards and samples of lysate were added in duplicate. BCA reagents were mixed and 200 µl were then added to the proteins in each well. The samples were incubated at 37 ^{0}C for half an hour to allow the purple coloration to develop. Absorbance intensity (which correlates with protein concentration) was measured using a Versamax microplate reader spectrophotometer (Molecular Devices, LLC, Silicon Valley, CA, United States) at a wavelength of 562 nm. Absorbance readings were then exported to Microsoft Excel software to enable generation of a standard curve and subsequent calculation the unknown protein concentrations.

2.6.3 Sodium dodecyl sulphate-polyacrylamide gel electrophoresis (SDS-PAGE)

2.6.3.1 SDS-PAGE gel preparation:

For SDS gel preparation, the resolving gel mix was first prepared, using the recipe listed in Table 2.5. The reagents were well-mixed in a tube then 6ml was added promptly to the gel cassette (Thermo Scientific). The resolving gel was then overlayed with a small amount of ethanol (VWR chemicals) to exclude air. The gel was allowed to polymerise at RT for about 20 mins. The ethanol was then discarded, and the top of the resolving gel was rinsed with deionized water (dH_2O). Then the stacking gel mix was prepared as indicated in Table 2.5, then and approximately 2 ml was added on top of the resolving gel. 10 or 12 well-combs were quickly inserted to form the gel's lanes. The stacking gel was left to polymerise for another 15 mins at RT. Gels were either used immediately or stored in humidified environment at 4 ^{0}C for 24 hours.

Table 2.5 SDS-PAGE running gel ingredients and their suppliers

Ingredients	**6% resolving gel**	**10% resolving gel**	**12% resolving gel**	**Stacking gel**
dH_2O	5.2 ml	4 ml	3.2 ml	2.1 ml
Protogel (30%) (National Diagnostics)	2 ml	3.3 ml	4 ml	500 µl
4X Resolving buffer (Table 2.1)	2.6 ml	2.6 ml	2.6 ml	_
4X Stacking buffer (Table 2.1)	_	_	_	380 µl
10% (w/v) ammonium persulphate (Sigma)	100 µl	100 µl	100 µl	30 µl
Tetramethylethylenediamine (TEMED) (Sigma)	10 µl	10 µl	10 µl	3 µl

2.6.3.2 SDS-PAGE

Prior to gel loading, samples in Laemmli sample buffer were heated at 95 ^{0}C for 5 mins and briefly centrifuged. The gel cassette was then inserted into the X cell II™ Mini cell and X cell sure lock™ system (Invitrogen) and 1X running buffer (Table 2.1) was added. Equal amounts of protein were loaded in each lane (2-10 µg) in volumes ranging from 10-30 µl. 4 µl protein ladder (Page Ruler Plus Prestained Protein Ladder, Thermoscientific) was used with each gel. Electrophoresis was carried out at 100 V until the samples entered the resolving gel and then at 130 V.

2.6.4 Western blotting

2.6.4.1 Protein Transfer

Following gel electrophoresis, proteins were transferred to polyvinylidine difluoride (PVDF) membrane (ImmobilonTP, Millipore) using an X Cell II Blot Module (Invitrogen). Before carrying out protein transfer, the PVDF blotting membrane was incubated in 100% methanol for 30 seconds. The membrane was then washed with dH_2O and immersed in transfer buffer (Table 2.1) together with, filter papers (Whatman) and transfer sponges. Gels were equilibrated in transfer buffer for 10-15 mins before setting up the transfer procedure. This wet protein transfer was carried out at 30 V (4 ^{0}C) for 2 hours. Protein transfer was checked by Ponceau S (Sigma) stain prior to immunoblotting.

2.6.4.2 Immunoblotting, protein detection and analysis

After confirming successful transfer using Ponceau S staining as described above, the membrane was incubated in a blocking solution (5% (w/v)) non-fat milk powder (Marvel) or BSA in TBST (Table 2.1) for 1 hour at RT with rocking. For immunoblotting, the primary antibody was first diluted in a solution consisting of 3% (w/v) BSA and 0.01% (w/v) sodium azide in TBST at concentrations listed in Table 2.1. Blots were incubated in primary antibody at 4 ^{0}C at concentrations/dilutions listed in Table 2.2.1 overnight. The membrane was then washed with TBST (6 washes, 5 mins each) and incubated with horseradish peroxidase (HRP) conjugated secondary antibody (Table 2.2.2) diluted in 5% (w/v) non-fat milk powder in TBST for 1 hour at RT. The membrane was washed again as above and covered evenly with freshly prepared Enhanced chemiluminescence (ECL) solution (GE Healthcare life sciences) for 1 min. The ECL solution was prepared by mixing equal volumes of reagents prior adding it to the membrane. The excess solution was then discarded, and the membrane was gently placed between 2 transparent sheets. Further chemiluminescence detection

and imaging were carried out in the dark room after exposing the blot to Hyperfilm ECL (GE Healthcare life sciences). Where indicated, imaging and protein band quantification were carried out using an Odyssey® Fc Imaging System (LI-COR Biosciences-U.S.) and image Studio Lite software 5.2.

2.6.4.3 Membranes stripping and re-probing

When indicated, membranes were stripped and re-probed with an alternative antibody. The membrane was heated at 60 ^{0}C in 50 ml stripping buffer (Table 2.1) for half an hour with rocking. 350 µl 2-mercaptoethanol was added to the buffer immediately before stripping. Afterwards, the membrane was washed and blocked as normal and then probed with the desired antibodies.

2.7 Transfection

2.7.1 RNAiMAX transfection

To knockdown RhoJ expression in HUVECs, a Lipofectanmine (Lipofectamine RNAiMAX; Invitrogen) based transfection technique was used to deliver RhoJ specific or negative control si-RNA duplexes. The required volumes for each cell density per dish size are defined below in Table 2.6. The protocol for transfecting cells in 6 cm dishes is described in detail here, for this dish size 360,000 HUVECs were seeded into gelatin pre-coated dishes one day before transfection. Cells were transfected with a Lipofectamine RNAiMAX at a final concentration of 0.3% (v/v) and duplexes at a concentration of 20 nM. This was performed as follows: initially for each 6 cm plate, two mixes were set up. The first contained 1.44 µl si-RNA duplexes (at a stock concentration of 20 µM) in 243.5 µl OptiMEM (Thermo Fisher Scientific) and the second contained 4.3 µl Lipofectamine RNAiMAX in 38.7 µl OptiMEM. Both mixtures were flicked and incubated at RT for 10 mins, after which point the two mixes were combined, mixed by flicking and incubated for a further 10 mins at RT. Meanwhile, cells were washed

once with 5 ml PBS and then 1152 µl OptiMEM was added to each 6 cm plate. Once the incubation was complete, the transfection mixture was added dropwise to the dish and gently mixed by tilting in north-south-east-west directions. The plates were incubated at 37 ^{0}C in 5% CO_2 incubator for 4 hours after which point the transfection mix was replaced cM199. HUVECs were used in assays 48 hours after si-RNA transfection.

Table 2.6. OptiMEM and lipofectamine volumes needed for transfecting different HUVECs densities

Dish size	Cell density	Duplex - OptiMEM Mixture Volumes	Lipofectamine volume	Optimem volume/ dish
6 well	2X10^5	170 µl (1 µl +169 µl OptiMEM)	3 µl + 27 µl OptiMEM	800 µl
6 cm	3.6X10^6	245 µl (1.44 µl +243.5 µl OptiMEM)	4.3 µl + 38.7 µl OptiMEM	1152 µl
10 cm	1X10^6	680 µl (4 µl +6.76 µl OptiMEM)	12 µl+108 µl OptiMEM	3200 µl

2.7.2 Polyethylenimine (PEI) transfection for production of lentivirus

To introduce plasmids DNA into HEK293T cells for lentivirus production, PEI transfections were carried out. 10^6 HEK293T were seeded into 6 cm dishes 24 hours before transfection using cDMEM without antibiotics. The next day, cells were transfected with 3 µg lentivirus plasmid DNA as follows; 1.09 µg packaging plasmid (PsPAX2), 0.44 µg envelop plasmid (PMD2G) and 1.46 µg transfer plasmid

(pWPXL GFP/ pWPXL GFP-daRhoJ) were added to a 1.5 ml microcentrifuge tube containing 300 µl OptiMEM (Thermo Fisher, scientific). 12 µl PEI (made up to 1 mg/ml) (Sigma) was then added and the tubes were gently vortexed. The mixture was incubated at RT for 10 mins to allow the PEI-plasmid complexes formation. Prior to adding the transfection mix, the media was replaced with fresh cDMEM without antibiotics. The transfection mix was then added drop by drop to HEK293T cells then the dishes were tilted in north, south, east, and west directions to disperse the mix evenly throughout the plate. The cells were placed in a humidified 5% Co_2 incubator at 37 ^{0}C for 2 days during which time lentiviral particles were produced.

2.8 Gene transduction

2.8.1 Viral transduction

2.8.1.1 HUVECs transduction with lentivirus

To transduce HUVECs with lentivirus particles generated by HEK293T cells after PEI transfection (see section 2.7.2 above) the following steps were used. The day prior to transduction, 350,000 HUVECs were plated in sterile gelatin pre-coated 6cm dishes. The next day, the conditioned media from the transfected HEK293T cells from each 6 cm dish containing virus particles was collected and filtered using 0.45 µm^2 pore sized filters. This filtered media was added to a mixture of 400 µl cM199 medium, 75 µl endothelial supplement mix 2 (Promocell) and 24 µl polybrene (1 mg/ml) (Sigma). The HUVECs growth media was then replaced by the virus and supplement mixture solution and incubated in CO_2 incubator at 37 ^{0}C. After 24 hours, the virus containing media was discarded, HUVECs were then passaged and expanded into 10 cm dishes as in section 2.5.1. Three days later, HUVECs were harvested and checked for successful transduction of GFP (green fluorescent protein)-tagged genes by flow cytometry using CyAn™ADP Analyzer (Beckman Coulter, Fullerton, CA) and

Summit 4.3 acquisitions software. Further cytometric data analysis was carried out by Flowing 2.5.1 software. Finally, the remaining cells were either plated for further experiments or were cryopreserved as per section 2.5.3.

2.9 HUVECs treatment with VEGFA/FGF2 or cM199 media

To investigate ERK1/2 activation dynamics in unmanipulated HUVECs treated with VEGFA /FGF2 or with cM199, 300,000 cells were seeded under normal culture conditions. After 24 hours, cells were starved for one hour using serum-free media with M199, then either harvested directly form culture (0 mins) or stimulated with 50 ng/ml of VEGFA (Pepro Tech EC Ltd) or 50 ng/ml FGF2 (Life Technologies Ltd) or with cM199 (control stimulant) over a range of time periods. The pro-angiogenic agonist's stock concentrations (100 µg/ml) were diluted in basal M199 media. 90 µg/ml heparin (LKT laboratories) was added to the diluted FGF2 solution, to enhance agonist receptor binding. Where this procedure was combined with si-RNA-mediated knockdown of RhoJ, 250,000 cells were seeded under normal culture conditions. The next day, cells were either RhoJ or negative control-si-RNAs transfected using the method described in section 2.7.1 and after 48 hours cells were starved and stimulated as describe above. For each stimulation condition, cell lysates were prepared as described above (in section 2.6.1) using RIPA lysis buffer.

2.10 Treatment of HUVECs with PAK inhibitors

To block PAK's activity, cells were treated with either vehicle control [0.1 % (v/v) DMSO (Sigma)] or with 2, 4 or 10 µM of PF-3758309 (Biotechne/Tocris) or with 20 µM of IPA-3 (Biotechne/Tocris) small molecule PAK Inhibitors. All inhibitors were prepared by diluting a stock concentration of 20 mM in

cM199. The treated cells were incubated at 37 ^{0}C in 5% CO_2 incubator for 24 hours before preparing cell extracts with RIPA lysis buffer as per section 2.6.1.

2.11 Co-immunoprecipitation (co-IP)

To determine the biochemical interaction between MEK1 or ERK with GIT1/2, co-IP experiments were carried out using protein A Sepharose beads (Sigma), protein A was selected because of the species and isotypes of the IP antibodies. Prior to co-IP, beads were briefly vortexed, 12-15 µl of the bead slurry 50 % (v/v) were added to microcentrifuge tubes, washed 3 times in NP40 lysis buffer and kept on ice. Between each wash, the beads were pelleted by centrifugation at 2,500 g at RT for 30 seconds. Meanwhile, cell lysates were freshly prepared with RIPA lysis buffer (see section 2.6.1), 20 µl of the WCL was then added to equal volume of 2X sample buffer as a loading control. The remaining lysate was added to the washed beads together with 1 µg of control IgG or anti-MEK1 or anti-ERK antibodies. The samples were allowed to rotate for 1-2 hours at 4 ^{0}C. Afterwards, beads were washed again 3 times with NP40 lysis buffer [supplemented with protease and phosphatase inhibitors (Table 2.1)]. To ensure that all excess wash buffer was removed after all the washing steps, the beads were re-centrifuged after removal of the third wash, and the small volume of remaining wash buffer was then aspirated with a thin gel loading tip. The beads were then denatured in 20-30 µl 2X sample buffer. The IP and WCL samples were either processed immediately for gel electrophoresis and western blotting or stored at -20 ^{0}C until further processing.

2.12 Preparation of cellular cytoskeletal fraction (CSF)

To isolate CSFs from HUVECs or HEK293T cells in order to interrogate interactions between ERK and the GIT-PIX complex, the following steps were performed. First, plated cells (either unmanipulated or treated with si-RNA transfection) were PBS-washed, collected, pelleted, and homogenised in 1ml TEEND buffer (Table 2.1) supplemented with protease and phosphatase inhibitors. The homogenate was then centrifuged (6000 g) (Refrigerated Microfuge Sigma 1-14k, Sigma Laborzentrifugen GmbH, Germany) for 10 mins at 4 ^{0}C, the supernatant was aspirated, homogenised and re-centrifuged at the same speed and duration. The supernatant was then transferred to an ultracentrifuge tube (Beckman Coulter Tube, Thick wall, Polyallomer, 1.0 mL, 11 x 34 mm, Thermo Fisher, scientific) and ultracentrifuged (100,000 g) for 1 hour at 4 ^{0}C (Beckman Optima MAX 130K Ultracentrifuge). After centrifugation, the supernatant (CSF) was removed, and the pellet was resuspended into 20 µl NaCl/sucrose buffer (Table 2.1) supplemented with protease and phosphatase inhibitors. Samples were incubated for 60 mins at 4 ^{0}C and then spun (2700 g) for 20 mins at 4 ^{0}C. The supernatant (membranes fraction) was discarded and the pellet containing the cytoskeletal proteins were resuspended into 30 µl RIPA buffer supplemented with protease and phosphatase inhibitors (Table 2.1). 10 µl of the fraction was resuspended into an equal volume of 2X sample buffer to serve as input sample and for the IP the remaining volume was used for co-precipitation.

2.13 Immunofluorescence (IF)

To investigate ERK localisation in FAs, HUVECs were plated on 13 mm coverslips (VWR Canlab, Canada), fixed, stained, and finally visualised with epifluorescence microscopy. Prior to usage, coverslips were incubated in 1 M HCl for 10 mins, washed 5 times in water and stored in 70% (v/v) ethanol. Before plating HUVECs and under complete aseptic conditions, the coverslips were placed

on 6 well plates, washed 6 times with PBS and gelatin coated as in section 2.5. For better visualisation of FAs, cells were plated at low density (50,000 cells/ well) and incubated at 37 ^{0}C for 24 hours. Cells were then washed 3 times in PBS and fixed in 4% (w/v) paraformaldehyde (Thermofisher) in PBS for 10 mins. Cells were washed again 3 times with PBS and then neutralised with 50mM ammonium chloride (NH_4Cl) in PBS for another 10 mins to remove the fixative's free aldehyde groups which might interfered with the staining. All subsequent steps were performed on parafilm (Heathrow Scientific) at RT. For permeabilization, coverslips were removed from the well, placed (cells facing downwards) on a 100 µl droplet of 0.1% (v/v) Triton X100 (Table 2.1) in PBS for 4 mins. Next, coverslips were rinsed 3 times in PBS and incubated with IF blocking buffer (Table 2.1) for 1 hour. Coverslips were then carefully removed, rinsed in PBS, and incubated with primary antibody (Table 2.2.1) diluted in IF blocking buffer for 1 hour. Afterwards, Coverslips were gently removed, rinsed again in PBS 3 times, and incubated with Alexa fluor- conjugated secondary antibodies (Table 2.2.2) diluted in IF blocking buffer for an hour. Coverslips were washed as per primary antibody incubation. For nuclear staining, coverslips were incubated with 2 µg/ml of 4',6-diamidino-2-phenylindole (DAPI) (Invitrogen) for 10 mins. They were then rinsed 3 times in PBS followed by 2 more rinses in d H_20 to remove the excess salt before mounting. For mounting, the excess liquid was briefly and gently drained from the coverslips on a piece of tissue. Coverslips with cells facing down were then slowly mounted on a clean glass slide containing a small drop of Hydromount medium (National diagnostics). The mounted coverslips were left to dry for 15-30 mins RT and then the edges of the coverslips were sealed with clear nail varnish, wrapped in a piece of foil and stored at -20 ^{0}C. Imaging was performed with Zeiss AxioObserver.Z1 widefield with Apotome epifluorescence microscopy.

CHAPTER 3

Role of RhoJ in the regulation of MAP kinase activation

3.1 Introduction

The involvement of RhoJ in MAP kinase regulation in ECs was previously reported in a number of studies. For example, Yuan *et al.* (2011) showed that the absence of ERG or RhoJ Inhibited B-RAF activation (Koh *et al.*, 2008; Yuan *et al.*, 2011) and Fukushima *et al.* (2020) also showed that RhoJ activation was essential for sustaining VEGFR2-ERK1 signalling which enhanced endothelial migration (Fukushima *et al.*, 2020).

In addition, our laboratory had previously generated kinase array data which suggested that active RhoJ may cause increased downstream signalling by affecting the phosphorylation of several kinases. Wilson (2014) found that overexpression of daRhoJ in HUVECs caused a significant increase in the phosphorylation of JNK MAP kinase and EGFR (Wilson, 2014, pp. 187), the latter being a key receptor in RAS-ERK MAP kinase signal activation (Klapper *et al.*, 2000). The purpose of this work was to follow up these findings and investigate how MAP kinase signalling cascades were regulated in HUVECs both expressing daRhoJ and with si-RNA-mediated reduced expression of RhoJ in response to various agonists.

3.1.1 Lentiviral-mediated RhoJ hyperactivation

To assess the effect of expressing an active mutant of RhoJ, HUVECs were transduced with lentivirus to express either GFP only or GFP fused with constitutively active RhoJ (Q79L; GFP-daRhoJ). To establish the level of transduction, flow cytometry was used to determine the proportion of ECs expressing either GFP or GFP-daRhoJ. Transduction efficiencies were over 99 and 97 % for GFP and GFP-daRhoJ, respectively, and representative examples are shown in Figure 3.1A. In addition, expression of the transduced proteins was confirmed by western blot (Figure 3.1B). As in previous

work, an upward shift of GIT2 was detected in cells transduced with GFP-daRhoJ compared with those transduced with GFP (Figure 3.1B). This electrophoretic shift may be due to phosphorylation of GIT2 mediated by kinases activated by daRhoJ, the increased molecular weight of GIT2 retarding its electrophoretic mobility.

3.1.2 DaRhoJ did not alter levels of phospho-JNK

One of the kinases previously identified in the kinase array to be activated in HUVECs expressing daRhoJ was JNK. To investigate this further, the genetically manipulated HUVECs expressing GFP or GFP-daRhoJ were harvested directly from culture at confluency. Lysates were prepared and subjected to western blotting for phospho-JNK and as a loading control, blots were stripped and re-probed to assay for total JNK levels. The blots showed that levels of phospho-JNK in HUVECs both expressing GFP and GFP-daRhoJ samples were low as shown Figure 3.2. These data indicated that in both samples there were low levels of phospho-JNK and that there was little change in the cells transduced with GFP-daRhoJ. This was not pursued further, but it was decided instead to look at another MAP kinase, ERK.

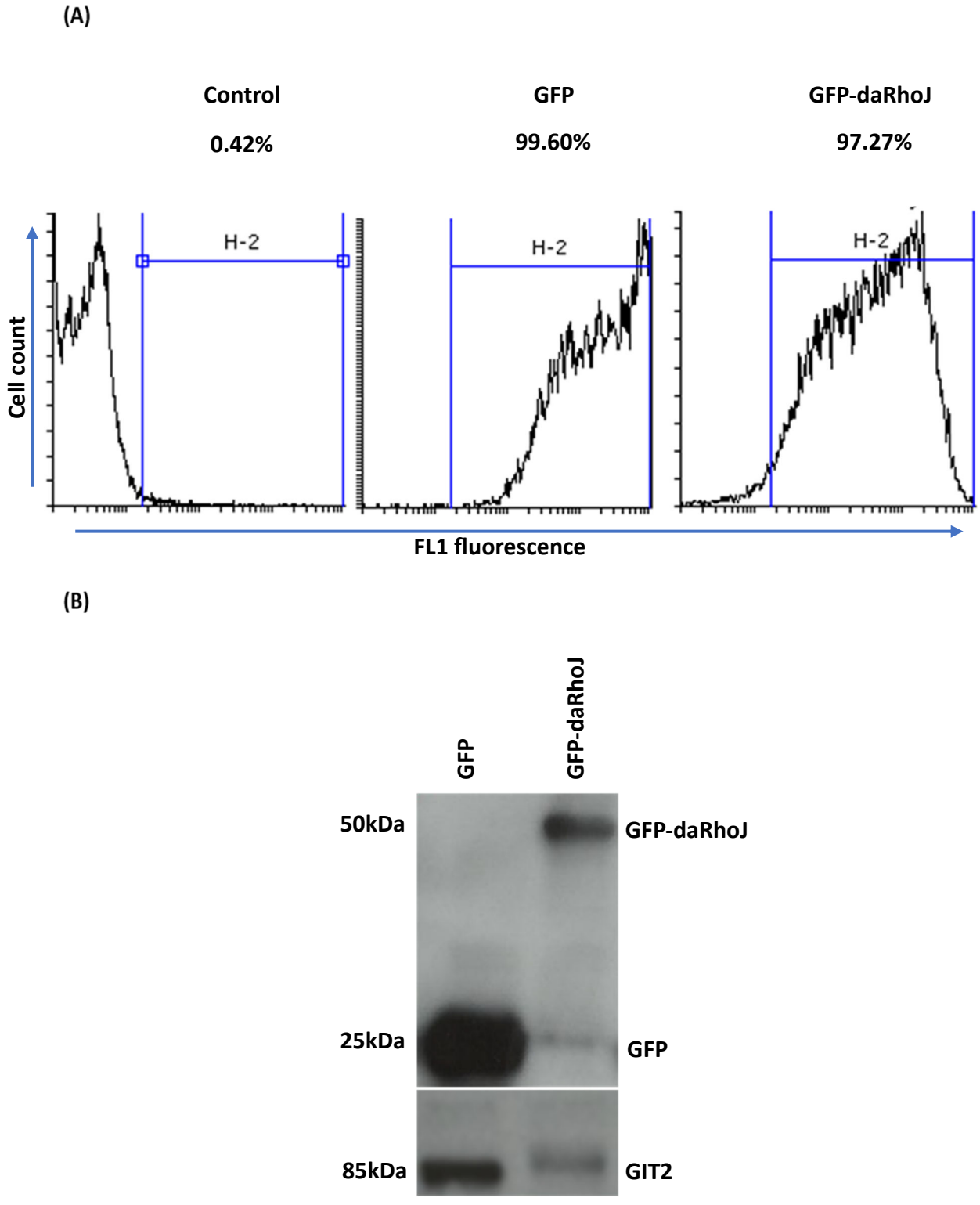

Figure 3.1. HUVECs were successfully transduced with GFP/GFP-daRhoJ and expression of daRhoJ resulted in an electrophoretic mobility shift in GIT2.
HUVECs were lentivirally transduced to express either GFP (transduction control) or GFP-daRhoJ. (A) Cells were harvested 5 days after the transduction and analysed by flow cytometry. Live cells were gated using forward and side scatter and histograms displayed showing FL1. Gating was undertaken using un-transduced cells as a control and the percentages of GFP positive cells are indicated on the figure. (B) Lysates were prepared, subjected to SDS-PAGE, and immunoblotted with GFP and GIT2 specific antibodies. This is a representative of three experiments.

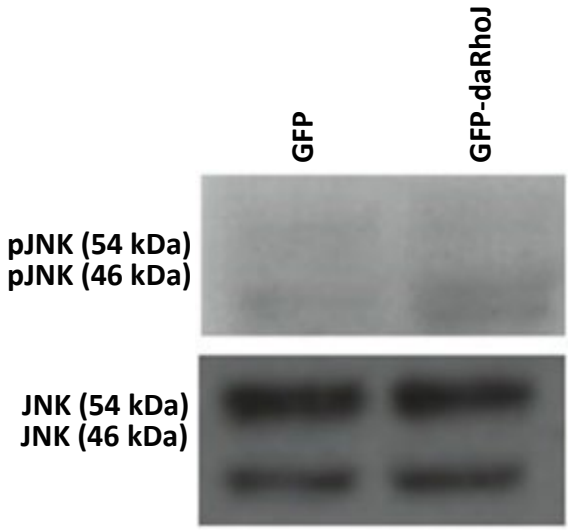

Figure 3.2. Expression of daRhoJ minimally affected JNK MAP kinase phosphorylation in HUVECs.

HUVECs were transduced with lentivirus to express either GFP or GFP-daRhoJ. When the cells were confluent, cell lysates were prepared and western blotted for phospho-JNK (pJNK), stripped and re-probed for total proteins (JNK). This is a representative of two experiments.

3.1.3 Effect of expression of daRhoJ on ERK activation

Based on this result, a similar experiment was performed blotting for phospho- and total ERK in HUVECs expressing GFP or GFP-daRhoJ, however chemiluminescence was captured using a LICOR Odyssey and this enabled more accurate quantitation of the signal. The phospho-ERK readings were calculated as a ratio relative to total ERK. Although these data showed a modest 1.4-fold increase in phospho-ERK levels in HUVECs expressing GFP-daRhoJ compared to those expressing GFP alone, this difference was statistically insignificant *(p=0.1)* (Figure 3.3).

In order to explore ERK phosphorylation kinetics in HUVECs expressing active RhoJ, a time course experiment was performed in HUVECs transduced with either GFP or GFP-daRhoJ. Cells were starved for one hour using serum-free media with M199 then either harvested directly from culture (0 mins) or stimulated for 15 mins, 60 mins and 90 mins with cM199 medium. The later time points were particularly of interest to determine if expression of daRhoJ might result in sustained activation. Protein extracts were collected from both groups and immunoblotted to detect phospho-ERK, stripped and then re-probed to determine total ERK levels at each time point and the chemiluminescent signal quantified using the LICOR as described above. First the ratio of phospho-ERK to total ERK was calculated, and then at each time point was normalised to the value of the GFP-expressing HUVECs at 0 mins. This allowed fold activation to be assessed and to evaluate whether there were any changes in the basal level of phospho-ERK in the HUVECs expressing active RhoJ. ERK phosphorylation peaked at 15 mins after stimulation in both GFP and GFP-daRhoJ expressing HUVECs and declined thereafter (Figure 3.4).

There were some problems encountered with these experiments, the first was an observation that in samples with high signals for the phospho-ERK, there were low signals for the total ERK. Since it was expected that total ERK should not change it was considered that there may have been incomplete stripping which affected the blotting for total ERK, and in turn affected the quantitation (Figure 3.4A). The other problem was one of inconsistency, in some experiments there was an enhanced signal for phospho-ERK whereas this was not observed to the same extent in other repeats. These technical issues impacted the reproducibility of the results, and combined data analysis from 3 replicates showed that active ERK levels were slightly increased in GFP-daRhoJ compared to GFP samples assayed simultaneously. However, the increase observed at each time point was statistically insignificant *(p>0.05)* (Figure 3.4B). Overall these data are inconclusive, though there is some suggestion that daRhoJ may enhance ERK phosphorlation 15 mins after stimulation.

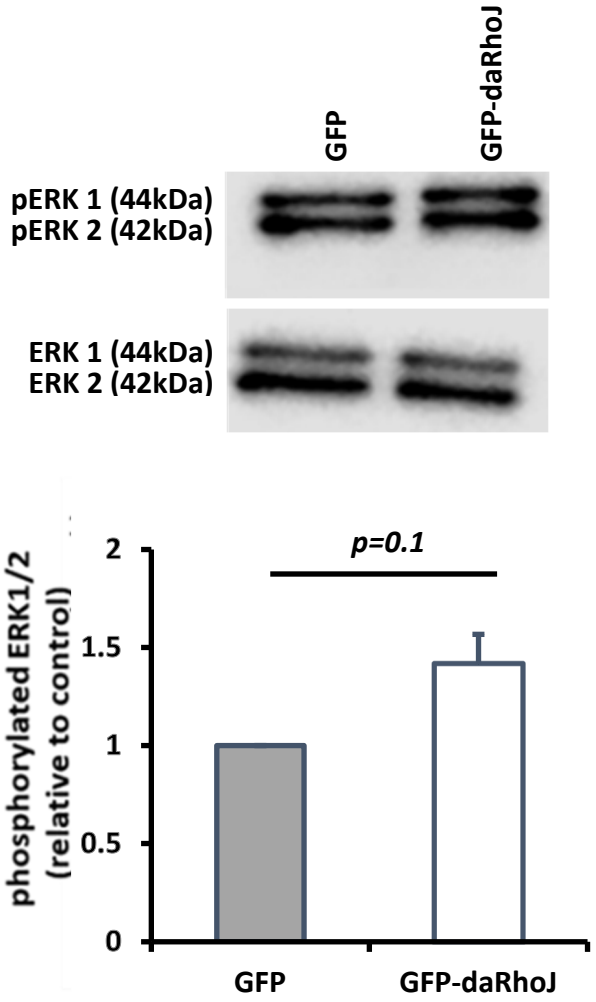

Figure 3.3. Expression of daRhoJ had a minor impact on ERK phosphorylation in HUVECs under normal culture conditions.

HUVECs were transduced with lentivirus to express GFP or GFP-daRhoJ and were cultured until confluency. Lysates were prepared subjected to SDS-PAGE and western blotted for phospho-ERK (pERK) and total ERK (ERK) levels were measured and quantified using the LICOR. To combine data, the ratio of phosphorylated-ERK1/2: total ERK1/2 was first calculated, data from different experiments (N=3) were normalised with basal GFP values set to 1, and then plotted with error bars, representing the standard error of the mean (SEM). By paired t-test there is no statistically significant difference (NS) between the two samples *(p=0.1)*.

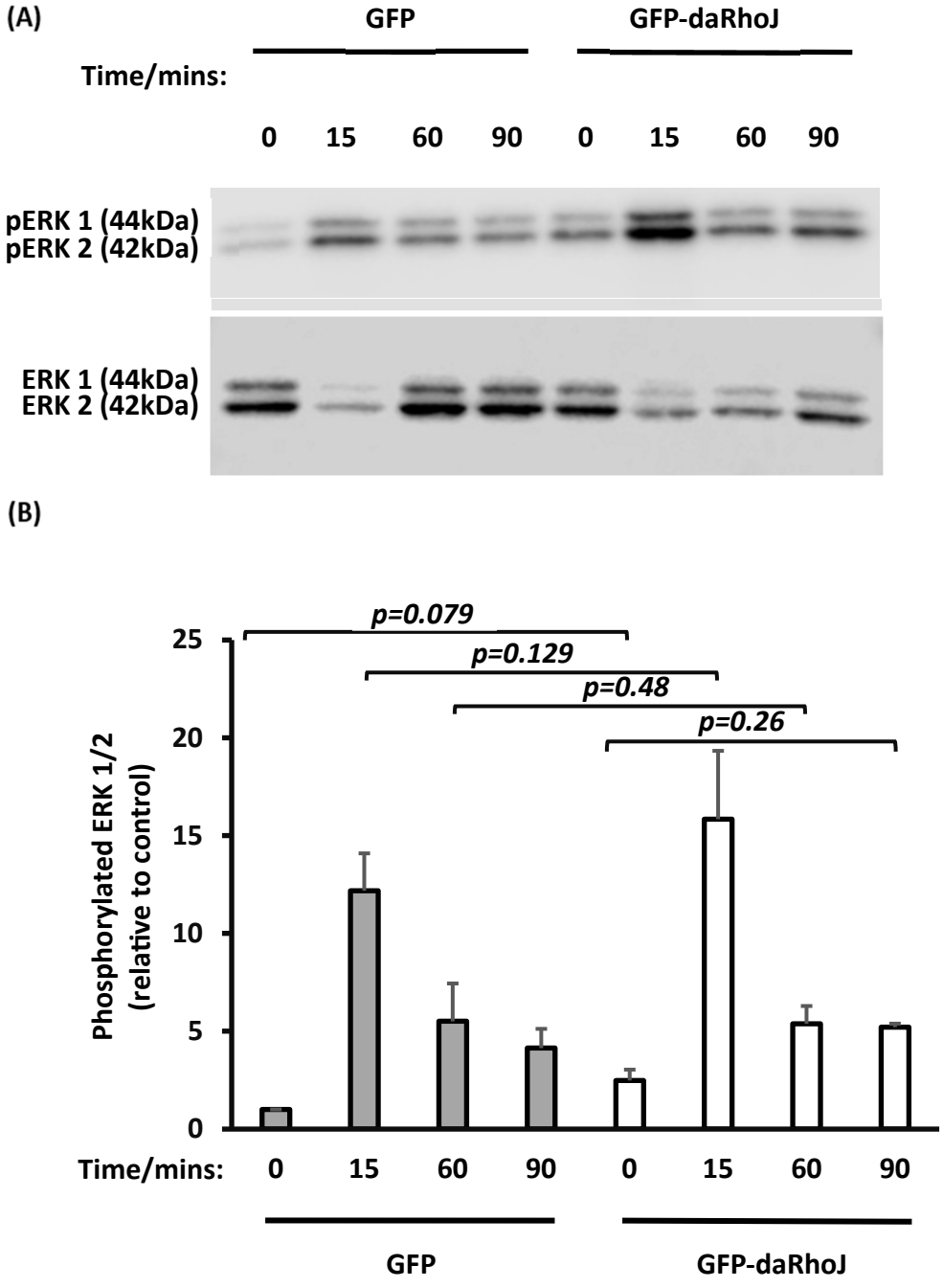

Figure 3.4. Expression of daRhoJ modulated ERK phosphorylation in HUVECs in some experiments.

(A)HUVECs were transduced with lentivirus to express either GFP or GFP-daRhoJ. Cells were starved using serum-free media with M199 for 1 hour then either harvested directly from culture (0 mins) or treated with cM199 for 15, 60, 90 mins before harvesting for preparation of cells lysates. Samples were probed for phospho-ERK and then blots were stripped and re-probed with total ERK antibodies. Phospho- and total ERK1 and 2 levels were measured and quantified using the LICOR. (B)for each experiment, the ratio of phosphorylated-ERK: total ERK was first calculated, and the estimated values were normalised with the GFP time 0 value set to 1. Data from 3 replicates (N=3) were then combined and plotted with error bars represent SEM. There are no statistically significant differences with controls assayed at the same time point by paired t-test (p>0.05).

3.1.4 RhoJ silencing resulted in reduced ERK activation

In order to determine how RhoJ knockdown affects ERK phosphorylation, the efficacy of 2 different RhoJ si-RNA duplexes was first tested to determine which to use in further experiments. For that purpose, HUVECs were either mock transfected or transfected with 20 nM of 2 different RhoJ-specific si-RNA duplexes (1 and 2) or a si-Control duplex (negative control) using lipofectamine. After 48 hours, cells lysates were collected and probed with RhoJ specific antibody and with α-Tubulin as a loading control. The blot in Figure 3.5A shows that duplex 1 was more efficient in reducing the RhoJ level than duplex 2; accordingly, duplex 1 was used in the subsequent time course experiments.

In order to detect how ERK phosphorylation is modulated in cells with reduced levels of RhoJ, HUVECs were transfected with 20 nM of either RhoJ-specific (duplex 1) or negative control (si-Control) si-RNA duplexes using lipofectamine. After 48 hours, cells were processed for a time course experiment as described above in section 3.1.3. Lysates were prepared and subjected to western blot to assess levels of phospho- and total ERK. In contrast to the time course experiments described pabove, there was no stripping of blots and lysates were directly and separately blotted for phospho- and total ERK. Successful knockdown was confirmed by western blotting for RhoJ. For the time course, a representative blot is shown in Figure 3.5B. The bands were quantified and the graph in Figure 3.5C indicates the combined data from three independent experiments. At all-time points there was a statistically significant reduction in ERK phosphorylation in RhoJ si-RNA treated cells compared to those transfected with si-Control si-RNA. In particular, there was a marked decline of ~60% in ERK activation levels in RhoJ-silenced cells incubated with cM199 media for 15 mins compared to control si-RNA samples assayed at same time point. These data indicate that silencing

of RhoJ reduced ERK activation in response to cM199 growth media, and hence RhoJ plays role in modifying ERK phosphorylation; this was further investigated.

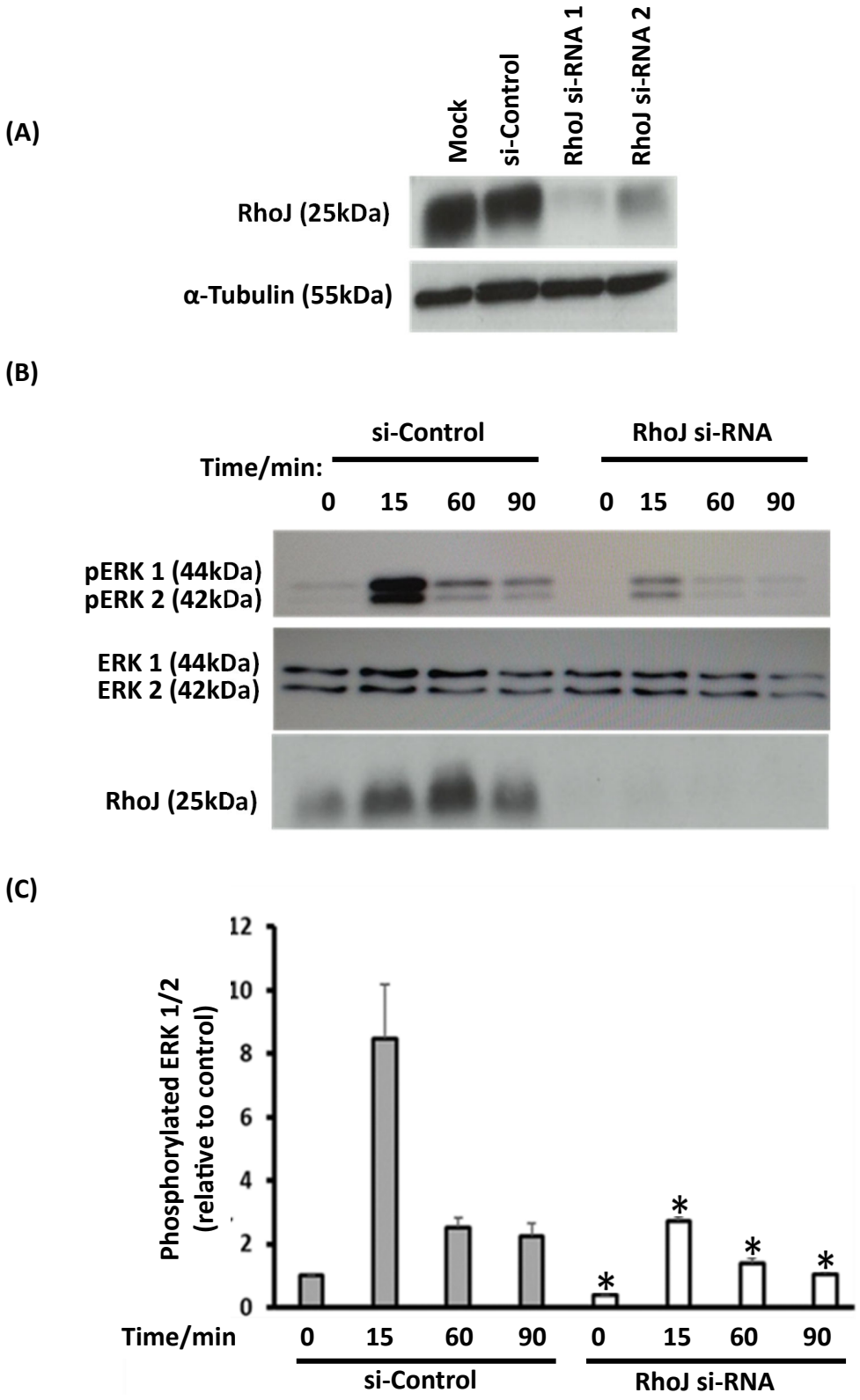

Figure 3.5. RhoJ si-RNA-mediated knockdown reduced ERK phosphorylation in HUVECs.
(A) HUVECs were either mock-transfected or transfected with 2 different RhoJ-specific si-RNA duplexes (1and 2) or a si-Control duplex (negative control). 48 hours later cells were lysed and probed with RhoJ specific antibody and α-Tubulin that was used as a loading control. (B) HUVECs were transfected with either RhoJ si-RNA (duplex 1) or negative control (si-Control) duplexes (20nM). After 48 hours cells were incubated in serum-free with M199 media for 1 hour then either assayed immediately (0 mins) or stimulated with cM199 media for 15, 60 and 90 mins. Samples were then lysed and immunoblotted for detection of RhoJ, phospho- and total ERK1/2. (C) For each experiment, the ratio of phosphorylated-ERK: total ERK1/2 was calculated, normalised to the GFP time 0 value which was set to 1, and then data from 3 independent experiments were combined. N=3, error bars represent SEM. There are statistically significant differences with controls assayed at the same time point by paired t-test (* $p \leq 0.05$).

3.1.5 RhoJ gene silencing reduced ERK activation in VEGFA, FGF2 and cM199-stimulated HUVECs

Data generated previously in our lab by Kaur, Leszczynska *et al.* (2011) showed that VEGFA and FGF2, [(prominent regulators of endothelial proliferation, survival, motility, and angiogenesis (Presta *et al.*, 2005; Olsson *et al.*, 2006)] contributed to RhoJ activation in HUVECs (Kaur *et al.*, 2011). Not only do growth factors activate RhoJ, but Fukushima *et al.* (2020) determined that RhoJ was involved it regulating ERK1 activation via RhoJ's regulation of VEGFR2 and its association with Neuropilin-1 and PlexinD1 (Fukushima *et al.*, 2020). Thus, having also shown that RhoJ regulated ERK1 activation, we wanted to determine whether this occurred in response to a variety of stimuli.

Initially unmanipulated HUVECs were treated with VEGFA and FGF2 and a time course experiment performed to determine the kinetics of ERK activity in response to these agonists. Confluent HUVECs were incubated in serum-free media with M199 for 1 hour, then either harvested directly from culture (0 mins) or stimulated with 50 ng/ml of VEGFA, 50 ng/ml FGF2 or with cM199 for 5 mins, 15 mins and 30 mins. Cells undergoing each treatment condition were harvested, lysates were prepared and western blotted for phospho- and total ERK. At 5 mins there was robust activation of ERK with VEGFA and cM199, but activation of FGF2 was weaker. ERK was robustly phosphorylated after 15 mins of stimulation by all agonists (Figure 3.6) and levels of activated ERK were reduced at 30 mins for all the agonists. Because of the strong activation of ERK observed at 15 mins by all three agonists, this time point was chosen for the next experiments investigating how RhoJ-silencing would affect ERK activation by these different stimuli.

As previously, HUVECs were transfected with 20 nM of either RhoJ-specific (duplex 1) or negative control (si-Control) si-RNA duplexes using lipofectamine. After 48 hours, cells were incubated in serum-free with M199 media for 1 hour then either immediately harvested (0 mins) or further stimulated with 50 ng/ml of VEGFA/FGF2 or with cM199 media for 15 mins. Cells were harvested, lysates were collected and immunoblotted for phospho- and total ERK. Samples were also probed with RhoJ specific antibody to confirm RhoJ knockdown (Figure 3.7A). Imaging and quantitation of the chemiluminescent signal were performed using the LICOR. The ratio of phosphorylated-ERK to total ERK was calculated for each time point of each condition and then normalised to the control sample at 0 mins. For all agonists, there was a clear and statistically significant reduction in ERK activation following RhoJ knockdown. It was clear that the different agonists activated ERK to different levels, with cM199 media being the most potent and FGF2 the weakest across the four replicate experiments (Figure 3.7B). The differing levels of ERK activation in the RhoJ silenced samples mirrored this, suggesting that levels of attenuation mediated by silencing of RhoJ occur proportionally to the level of activation. This data indicates a general role for RhoJ in regulating ERK activation via a number of different agonists, including the angiogenic regulators VEGFA and FGF2 angiogenic activators.

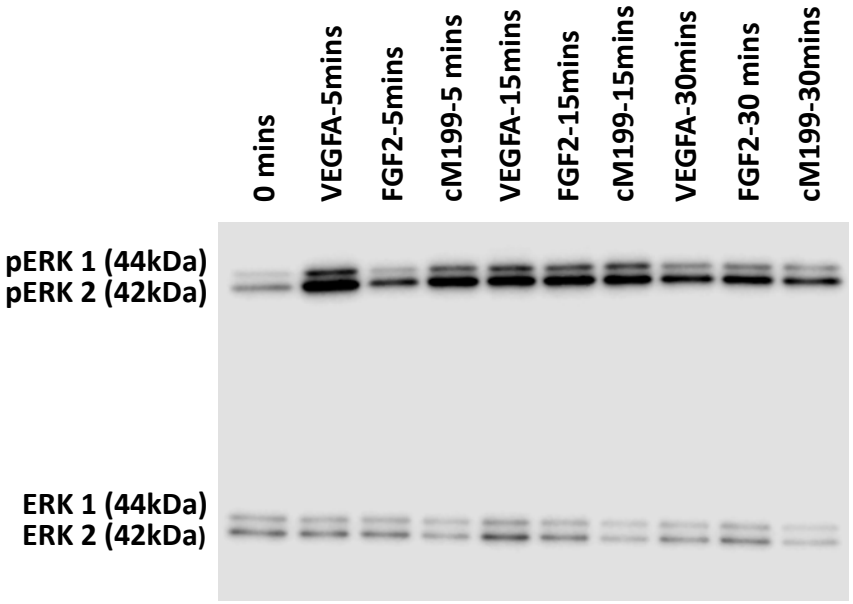

Figure 3.6. VEGFA, FGF2 and cM199 media robustly enhanced ERK activation after 15 mins of stimulation in HUVECs.

HUVECs cultured under normal conditions were starved in serum-free with M199 media for 1 hour. Cells were either directly assayed (0 mins) or stimulated with VEGFA, FGF2 or with cM199 for 5,15 and 30 mins. Cell lysates were collected and western blotted for phospho- and total ERK1/2. This was performed once.

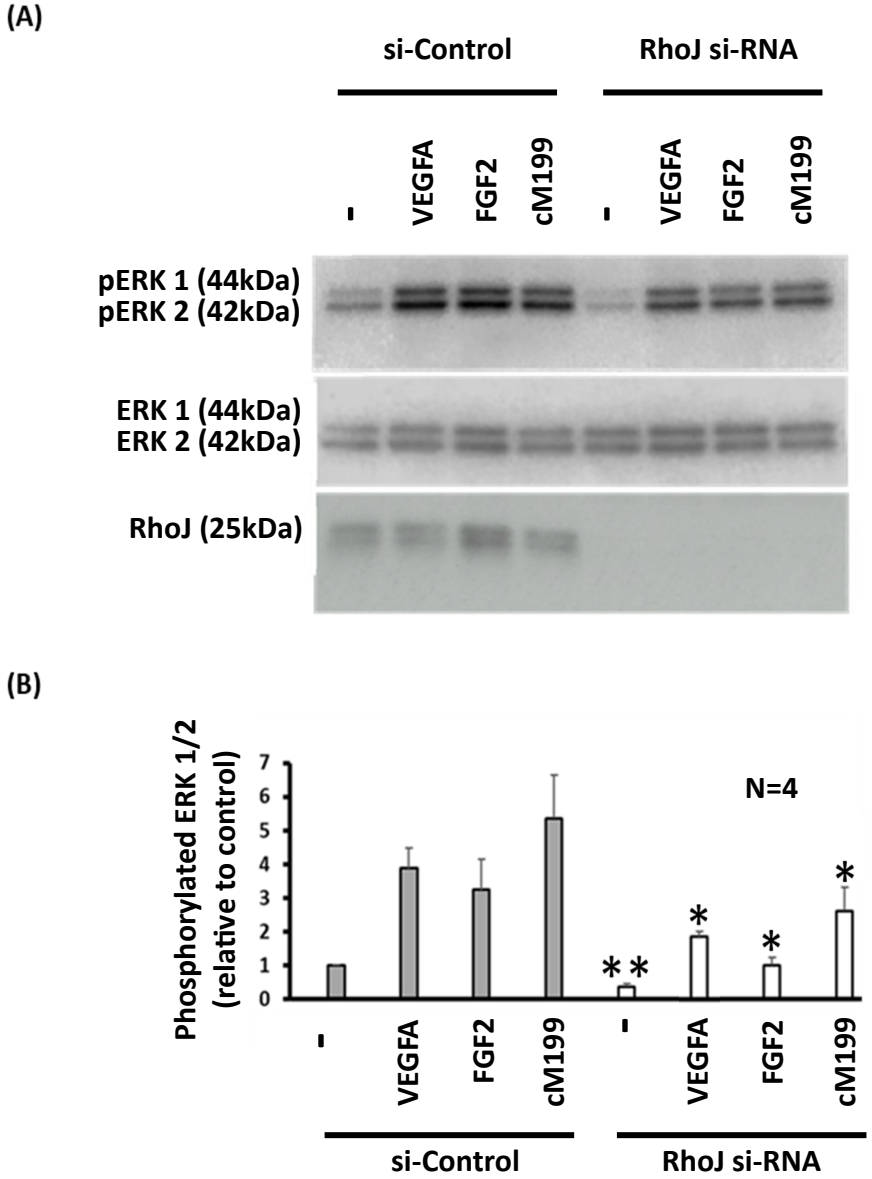

Figure 3.7. RhoJ gene silencing reduced ERK activation in VEGFA, FGF2 and cM199-stimulated HUVECs.

(A) HUVECs were transfected with either negative control (si-Control) or RhoJ si-RNA (duplex 1) duplexes (20nM). After 48 hours cells were starved in serum-free with M199 media for 1 hour then either assayed immediately at 0 mins (|) or stimulated with VEGFA, FGF2 or cM199 for 15 mins. Samples were then lysed and immunoblotted for detection of RhoJ, phospho- and total ERK1/2. (B) The ratio of phosphorylated-ERK: total ERK1/2 was calculated for each sample, normalised to the si-Control time 0 value for that experiment which was set to 1 and data from 4 (N=4) independent experiments were combined and plotted. Error bars represent SEM. Statistical differences at each time point were compared by paired t-test (* $p \leq 0.05$ and ** $p \leq 0.01$).

3.2 Discussion

Data presented in this chapter shows the role of RhoJ in regulating the activity of different MAP kinases, with a focus on ERK1/2. We demonstrated that sustained RhoJ activity modestly enhanced ERK MAP kinase phosphorylation but had a small effect on JNK MAP kinase. Conversely, RhoJ knockdown caused a statistically significant reduction of ERK phosphorylation in response to stimulation with cM199 media, VEGFA or FGF2. There were however technical difficulties which impacted the reproducibility of some experiments. Nevertheless, these findings indicate that RhoJ plays a role in modulating ERK1/2's activity downstream of VEGFA or FGF2 angiogenic signal activation in HUVECs.

This study followed up a phosphokinase screen by Wilson (2014) which showed that daRhoJ (a constitutively active form of RhoJ) enhanced the relative phosphorylation of JNK, EGFR, AMPKα2, STAT5ab, Hck, MSK1/2 and PRAS40 kinases (Wilson, 2014, pp. 182-190). We first explored whether the expression of daRhoJ would affect the activity of JNK MAP kinase in HUVECs in standard culture conditions. In contrast to the significant rise of phosphorylated-JNK levels that were detected in Wilson's study, our data did not consistently show that JNK phosphorylation was increased as a result of expression of daRhoJ in HUVECs. This discrepancy may be due to differences in culture conditions and experimental techniques such as the use of SDS-PAGE and western blotting as opposed to a dot blot array. Alternatively, this may be due to variations in gene expression and the signalling behaviour of HUVECs isolated from different cord donors (Lorant *et al.*, 1999; Wisgrill *et al.*, 2018). Interestingly, signalling via JNK and the transcription factor c-jun was found to upregulate expression of RhoJ (Wang *et al.*, 2022), thus there might be reciprocal regulation between RhoJ and JNK, with RhoJ modulating JNK activity and JNK regulating levels of RhoJ protein.

A number of studies have indicated that RhoJ may affect ERK1/2 signalling, for example RhoJ si-RNA-mediated knockdown reduced B-RAF phosphorylation in ECs (Yuan *et al.*, 2011). Based on these data and on our kinase array, which showed that EGFR was also significantly phosphorylated in the presence of daRhoJ, we decided to investigate ERK MAP kinase. At first, we evaluated phospho-ERK levels in GFP and GFP-daRhoJ-expressing HUVECs that were kept in standard culture conditions. Our data showed that ERK's phosphorylation was consistently elevated in HUVECs expressing daRhoJ, however after repeating this experiment three times, the differences observed were small and not statistically significant.

The role of RhoJ in regulation of ERK phosphorylation kinetics was then tested in cM199 deprived then stimulated HUVECs, that were either transduced to express daRhoJ or transfected with RhoJ-specific si-RNA to silence RhoJ's expression. RhoJ knockdown consistently decreased the level of ERK phosphorylation particularly after 15 mins of cM199 stimulation, and at all time points the differences observed were statistically significant. By contrast, overexpression of daRhoJ enhanced ERK's activation only in some experiments. A problem was encountered with the western blotting of ERK in the time course experiments involving expression of daRhoJ. Initially membranes were probed with antibody specific to phospho-ERK, stripped and then re-probed with antibody to measure total ERK. After a number of experiments with HUVECs transduced to express GFP or GFP-daRhoJ, it was observed that in samples with high levels of phospho-ERK the signal for total ERK was lower. Since total levels were not expected to change, it was possible that the stripping was not complete and binding of antibody to total ERK was impeded. However, in the case of the si-RNA knockdown experiments, the protocol was modified such that the lysate was independently blotted

for phospho-ERK and total ERK. The time course experiments involving daRhoJ would need to be repeated using this altered western blotted strategy to provide more reliable results.

We then further explored whether RhoJ influences ERK's activity in response to stimulation with different pro-angiogenic agonists. We first observed ERK phosphorylation dynamics in unmanipulated HUVECs; they were kept in serum-free with M199 for an hour then treated with VEGFA, FGF2 or with cM199 media for over a 30-minute time course. ERK1/2 was robustly phosphorylated by all agonists after 15 mins of stimulation. Accordingly, this induction duration was selected in the subsequent experiments to explore whether RhoJ knockdown would impact the ERK's activity induced by these different stimuli. Interestingly, ERK's phosphorylation was significantly reduced following RhoJ knockdown in response to all agonists. There were small variations in the levels of ERK activation in response to the different agonists, where cM199 media and FGF2 induced the highest and lowest levels of ERK1/2 activation, respectively, and in RhoJ-silenced cells ERK phosphorylation was proportionally reduced. Overall, these data suggest that RhoJ influences ERK's activity in response to multiple stimuli, including the pro-angiogenic growth factors VEGFA and FGF2.

Recently, Fukushima *et al*. (2020) reported a specific mechanism through which RhoJ mediated ERK's activity in response to VEGFA stimulation. Their study suggested that RhoJ regulated a complex between VEGFR2, PlexinD1 and Neuropilin-1. When VEGFA's level was relatively high, RhoJ became activated, promoted the internalisation of VEGFR2 sustaining its signalling through downstream pathways including the ERK MAP kinase pathway. In knocking down RhoJ expression the VEGR2 complex was less stable and less able to signal through ERK (Fukushima *et al.*, 2020). Our data showed that the effect of RhoJ in modulating ERK's activity was not exclusively in response to VEGFA,

reduced levels of RhoJ also limited ERK's activation induced by FGF2 or by complete media supplemented with serum and growth factors. This suggests that there might be a more general mechanism by which RhoJ regulates ERK1/2 activity downstream of multiple stimuli.

One possibility which is explored in the next chapter is that RhoJ regulates ERK1/2 via the GIT-PIX complex. Our laboratory has previously demonstrated an interaction between RhoJ and GIT1 via yeast 2-hybrid. We observed that overexpressing RhoJ caused an increased electrophoretic mobility of GIT2 suggesting that RhoJ may be able to regulate the activity of the GIT-PIX complex via post-translational modification of GIT proteins. Consistent with this was our observation that si-RNA mediated silencing of RhoJ reduced recruitment of GIT1, GIT2 and β-PIX to FAs (Wilson *et al.*, 2014). Yin *et al.* (2004) demonstrated a constitutive association between GIT1 and MEK1 and observed that ERK1/2 activation in response to EGF and Ang II in a number of non-endothelial cell types depended on levels of GIT1 (Yin *et al.*, 2004). This group went on to demonstrate that EGF stimulation promoted ERK1/2's co-localisation with GIT1 in FAs and enhanced cell migration (Yin *et al.*, 2005). They later determined that ERK1/2's CC domain was necessary for binding to GIT1 (Zhang *et al.*, 2009). Given these studies indicating a role for GIT1 in scaffolding and promoting agonist induced ERK1/2 activation and our own studies linking RhoJ with the GIT-PIX complex, one hypothesis was that RhoJ is regulating the MEK1 and ERK1/2 scaffolding function of GIT1/2. Experiments to test this hypothesis are described in the next chapter.

There are other potential mechanisms by which RhoJ may be able to more generally regulate the ERK MAP kinase pathway. One is via PAK kinase which is known to influence the activation of RAF1 (King *et al.*, 1998; Chaudhary *et al.*, 2000; Alavi *et al.*, 2003) and this is considered in the next chapter.

Recently β-Arrestin, first characterised for its role in terminating GPCR signalling, has been shown to act as a scaffold for ERK1/2-MEK1-C-RAF signalling (Kim *et al.*, 2022). Thus, it is possible that RhoJ may influence ERK1/2 activation via modulation of this function of β-Arrestin. RhoJ is also involved in protein trafficking and specifically its involvement in trafficking the transferrin receptor (de Toledo *et al.*, 2003), podocalyxin (Richards *et al.*, 2015) and $\alpha_v\beta_1$ integrin (Sundararaman *et al.*, 2020) has been demonstrated. Internalisation and recycling of RTKs are known to regulate their activation of downstream signalling pathways (Miaczynska, 2013). Gourlaouen *et al.* (2013) observed that internalisation of activated VEGFR, FGFR2 or hepatocyte growth factor receptor (HGFR) were required for inducing of ERK activity in ECs and for angiogenesis. This group also reported in an earlier study that RAB4A-mediated VEGFR2 recycling to plasma membrane (rather the internalisation process itself) in VEGFA stimulated cells sustained the endothelial mobility and tumour's neovascularisation (Reynolds *et al.*, 2009; Gourlaouen *et al.*, 2013). Thus, RhoJ might be involved in the regulation of RAB4-mediated vesicular uptake and plasma membrane trafficking of pro-angiogenic receptors, which in turn would augment ERK signalling during angiogenesis. It would be interesting to determine whether modulating the activity of RhoJ affected the intracellular trafficking of RTKs such as FGFR2.

In summary, we showed that RhoJ knockdown had impacted ERK1/2's activity downstream of the pro-angiogenic stimulators VEGFA and FGF2. There are a variety of possible molecular mechanisms by which this could occur. The role of the GIT-PIX complex and the relationship between RhoJ and PAK are explored in the next chapter.

CHAPTER 4

Investigating the role of RhoJ in regulating GIT2 phosphorylation and interaction between GIT1/2 and MEK1 and ERK1/2 in ECs

4.1 Introduction

Previous data generated in our laboratory demonstrated that the expression of daRhoJ (an active mutant form of RhoJ) caused reduced GIT2 electrophoretic mobility, and this was likely due to post-translational modifications. Wilson *et al.* (2014) showed that upwards shift of GIT2's electrophoretic mobility observed with daRhoJ expression was not due to tyrosine phosphorylation mediated by Src and focal adhesion kinase (FAK) (Wilson *et al.*, 2014). Some preliminary data generated by our laboratory suggested that multiple serine and threonine residues in GIT2 protein were phosphorylated in daRhoJ-expressing HUVECs but not in HUVECs expressing GFP. Since studies have indicated that RhoJ is involved in the activation of PAK serine/threonine kinases (Yuan *et al.*, 2011; Wang *et al.*, 2022), one aim of this chapter was to test our hypothesis that RhoJ activates PAK resulting in it phosphorylating threonine and serine residues of GIT. To interrogate this, we determined how pan and selective small molecule PAK inhibitors affected the daRhoJ-induced electrophoretic shift of GIT2.

As discussed in the previous chapter, GIT1 was shown to scaffold MEK1 and promoted signalling of MEK1-ERK1/2 in non-endothelial cells stimulated with RTK and G protein coupled receptor (GPCR) agonists (Yin *et al.*, 2004). Subsequent studies demonstrated that GIT1 specifically interacted with ERK2, and this enhanced ERK1/2's localisation to FAs (Yin *et al.*, 2005; Zhang *et al.*, 2009). Prior data generated in our lab showed that RhoJ interacted with GIT1 in a yeast 2-hybrid assay, co-immunoprecipitated with GIT1/2-β-PIX in HUVECs and promoted the localisation of GIT-PIX complex to FAs (Wilson *et al.*, 2014). This led to the hypothesis that RhoJ modulates ERK1/2 activation via modulation of the GIT-PIX complex. Thus, a second aim of the experiments described in this chapter

was to determine if modulating RhoJ activity affected the association of MEK1 and ERK1/2 with GIT1/2 by co-IP and ERK1/2's localisation to FAs using IF.

4.2 The PAK inhibitor PF-3758309 prevented GIT2 mobility shift in daRhoJ-transduced HUVECs

Data generated in this study, and previously reported in our lab, showed that GIT2 electrophoretic mobility was shifted upwards in GFP-daRhoJ-expressing HUVECs. To follow this up and to examine a potential role for PAK kinases in mediating this phosphorylation, small molecule inhibitors were used to abrogate PAK kinase functions in HUVECs. HUVECs were transduced with lentivirus to express either GFP (control) or GFP-daRhoJ. After 24 hours, cells were either DMSO-treated (vehicle control) or treated with PF-3758309 (2, 4 and 10 µM) or with 20 µM IPA-3 PAK inhibitors for another 24 hours. PF-3758309 is a competitive ATP inhibitor targeting all PAKs, while IPA-3 is an allosteric inhibitor with specificity for PAK1 (Deacon *et al.*, 2008; Viaud and Peterson, 2009; Murray *et al.*, 2010). After the drug treatment, cellular lysates were prepared, subjected to SDS-PAGE and western blotting using a GIT2 specific antibody to investigate the electrophoretic mobility of GIT2 and the anti-GFP antibody to confirm expression of the transduced proteins. The expected higher shift of GIT2 electromobility observed in DMSO-treated cells expressing daRhoJ, was abrogated following PF-3758309 treatment, but not after IPA-3 treatment. This effect was found to occur with both 4 and 10 µM PF-3758309 as shown in Figure 4.1 and also with 2 and 4 µM in 3 biological repeats. A high concentration of 20 µM IPA-3 inhibitor treatment also failed to cause alteration of the shifted GIT2 electrophoretic mobility in daRhoJ-transduced HUVECs (Figure 4.1).

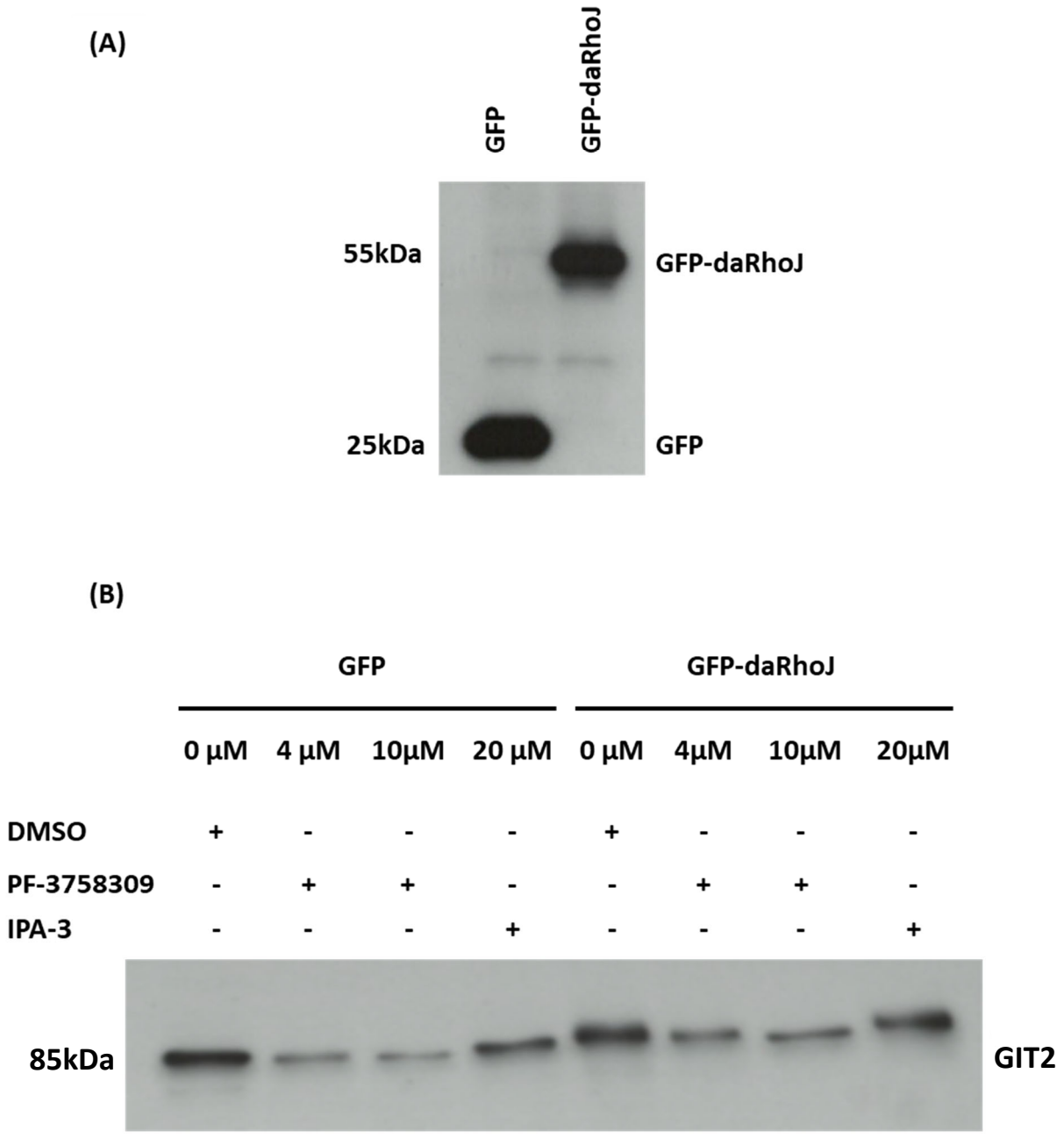

Figure 4.1. PAK inhibitors prevented the GIT2 mobility shift in daRhoJ-transduced HUVECs. (A) HUVECs were transduced with lentivirus to express either GFP (control) or GFP-daRhoJ. Protein extracts were immunoblotted for GFP. (B) Transduced cells were either DMSO treated or treated with different concentrations of PF-3758309 or with 20 µM IPA-3 PAK inhibitors for 24 hours. Cellular lysates from all treatment conditions in both cell groups were prepared and western blotted for GIT2. Similar results were obtained from 2 more biological repeats on cells treated with PF-3758309 or with 20 µM IPA-3 PAK inhibitors.

4.3 Investigating whether RhoJ regulates interactions between the GIT-PIX complex and the ERK MAP kinase signalling pathway

Data presented in this thesis indicated that RhoJ regulates ERK activation downstream of multiple growth factor receptors, however the mechanism by which this was acting was not known. Previously, Yin *et al.* (2004) published data which suggested that GIT1 interacts with and provides a scaffold for MEK1 for ERK activation in vascular smooth-muscle cells and human embryonic kidney 293 cells-stimulated with AngII and EGF (Yin *et al.*, 2004). Previous data generated in our lab also showed that daRhoJ was co-immunoprecipitated with GIT1 and GIT2 in HUVECs and interacted with GIT1 in a yeast 2-hybrid assay (Wilson *et al.*, 2014). Given RhoJ's interaction with the GIT-PIX complex, it is possible that RhoJ may affect the ability of GIT1/2 to interact with this MAP kinase signalling proteins, and this is what was investigated in the next series of experiments. The experimental approach taken initially was similar to that used by Yin *et al.* (2004) where co-IP of GIT1 or GIT2 with MEK1 and ERK1/2 was used. Once robust co-IP of these proteins was demonstrated then levels of RhoJ were manipulated to determine if this would affect the interaction.

4.3.1 Selection of HUVECs as the cell type to use for the biochemical investigation into RhoJ's regulation of the interaction of GIT1/2 with the MAP kinase signalling proteins

Given the large amounts of cell lysate that would be required for such a biochemical approach, initial experiments were performed to determine whether an immortalised EC line might be suitable for these experiments. One such cell line is the human brain microvascular endothelial cell (hBMEC) line (Stins *et al.*, 2001) and since this was available in our laboratory, this was tested for expression of key proteins relevant to this investigation. Cell lysates were prepared from confluent hBMECs and HUVECs and protein levels in the lysates of both cell types were then quantified; equal amounts of

protein were loaded on to an SDS-PAGE gel, transferred and western blotted for MEK1, phospho-ERK, total ERK1/2, GIT1, GIT2 and RhoJ (Figure 4.2). Levels of GIT1 were similar in both cell types and higher levels of total ERK1/2, phospho-ERK1/2 and MEK1 were observed in HUVECs compared with hBMEC. Most notable, however, was a lack of RhoJ and GIT2 expression in hBMEC, the lack of RhoJ in particular made this an unsuitable cell line to use to investigate how RhoJ regulates the interaction of the GIT-PIX complex with the MAP kinase signalling pathway. On that basis, HUVECs were used for further biochemical investigations.

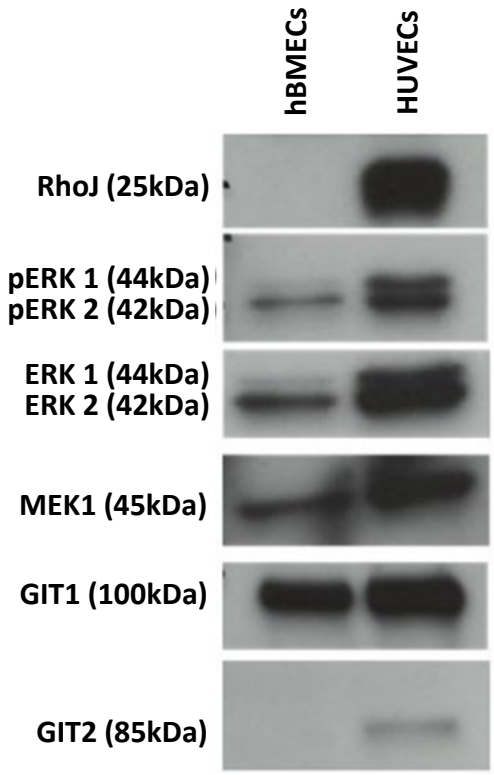

Figure 4.2. hBMECs do not express RhoJ or GIT2.
HUVECs and hBMECs were cultured until confluency and cell lysates were prepared and protein concentration were quantified. 10 µg of protein extract was subjected to SDS-PAGE and western blotted for RhoJ, phospho-ERK, total ERK, MEK1, GIT1 and 2. This experiment was performed once.

4.3.2 MEK1 interacts with GIT1 and GIT2 in HUVECs

Before assessing how RhoJ may affect an interaction between GIT1/2 and proteins of the MAP kinase cascade, it was first key to confirm whether MEK1 interacted with GIT1 and GIT2 in ECs. In order to do this, 10 confluent plates of HUVECs cultured under regular conditions were harvested and lysates prepared. A small amount of lysate was used to confirm the presence of the proteins of interest in the protein extracts. The remaining lysate was incubated with protein A Sepharose beads and either anti-MEK1 monoclonal antibody or mouse Immunoglobulin (Ig) G as a control, as described in section 2.11. Samples were run on SDS-PAGE and then immunoblotted with MEK1, GIT1 and GIT2 specific antibodies (Figure 4.3). Data representative of two experiments confirmed that MEK1 co-precipitated with GIT1 and GIT2 in HUVECs, with bands evident for GIT1 and GIT2 in the MEK1 IP lane, but not in the control. Due to GIT1 being more abundant in HUVECs lysate and some difficulties in consistently demonstrating interaction between MEK1 and GIT2, only the interaction between GIT1 and MEK1 was probed in the next experiments.

4.3.3 The effect of RhoJ knockdown in the interaction between GIT1 and MEK1

To investigate the role of RhoJ in mediating this interaction, this co-IP approach was taken in HUVECs which had been transfected with si-RNA duplexes to silence RhoJ. HUVECs were transfected with either si-Control or RhoJ- specific si-RNA duplexes and after 48 hours lysates were prepared. As before, a small amount of lysate was retained for confirming expression in the WCL and the remainder was divided between two IPs containing either control mouse IgG or anti-MEK1 antibody and protein A Sepharose beads. After a 1-hour incubation at 4 ^{0}C with rotation, the beads were washed, and sample buffer was added. These were then subjected to SDS-PAGE and western blotting

with GIT1 and MEK1 specific antibodies to examine the co-precipitation (Figure 4.4A) and western blotting WCLs with anti-RhoJ antibodies confirmed RhoJ knockdown (Figure 4.4B).

Unlike the co-IP experiment using untreated HUVECs, there was no interaction between MEK1 and GIT1 detected in either the control or RhoJ si-RNA-treated HUVECs. There was an expectation that as with the unmanipulated HUVECs, GIT1 should have co-precipitated the control si-RNA treated HUVECs and it is not clear why this did not occur. A likely explanation is that despite using similar numbers of plates, introducing the si-RNA transfection protocol into the method resulted in insufficiently concentrated lysate to observe this interaction. In order to pursue this further, it was decided to instead investigate the interaction between GIT1 and ERK1/2 and determine whether this interaction was more readily detectable.

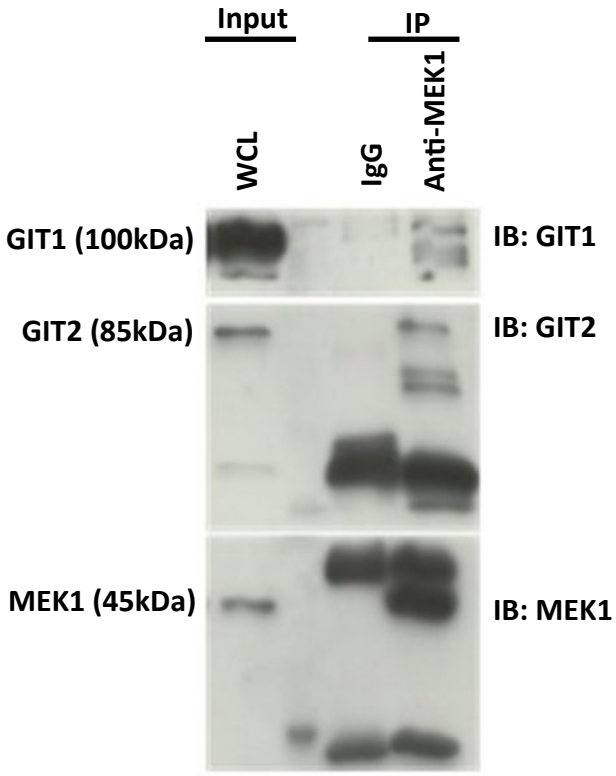

Figure 4.3. MEK1 interacted with GIT1 and GIT2 in HUVECs.
HUVECs were grown under standard culture conditions until confluency then harvested. Lysates were collected, added to prewashed protein A Sepharose beads along with anti-MEK1 antibody or mouse IgG and rotated for 1 hour at 4 ^{0}C. The beads were washed, and the captured immune complexes were denatured in 2X SDS sample buffer. Interacting partners (GIT1/2) of MEK1 were determined by western blotting using specific antibodies. This is a representative of 2 biological repeats.

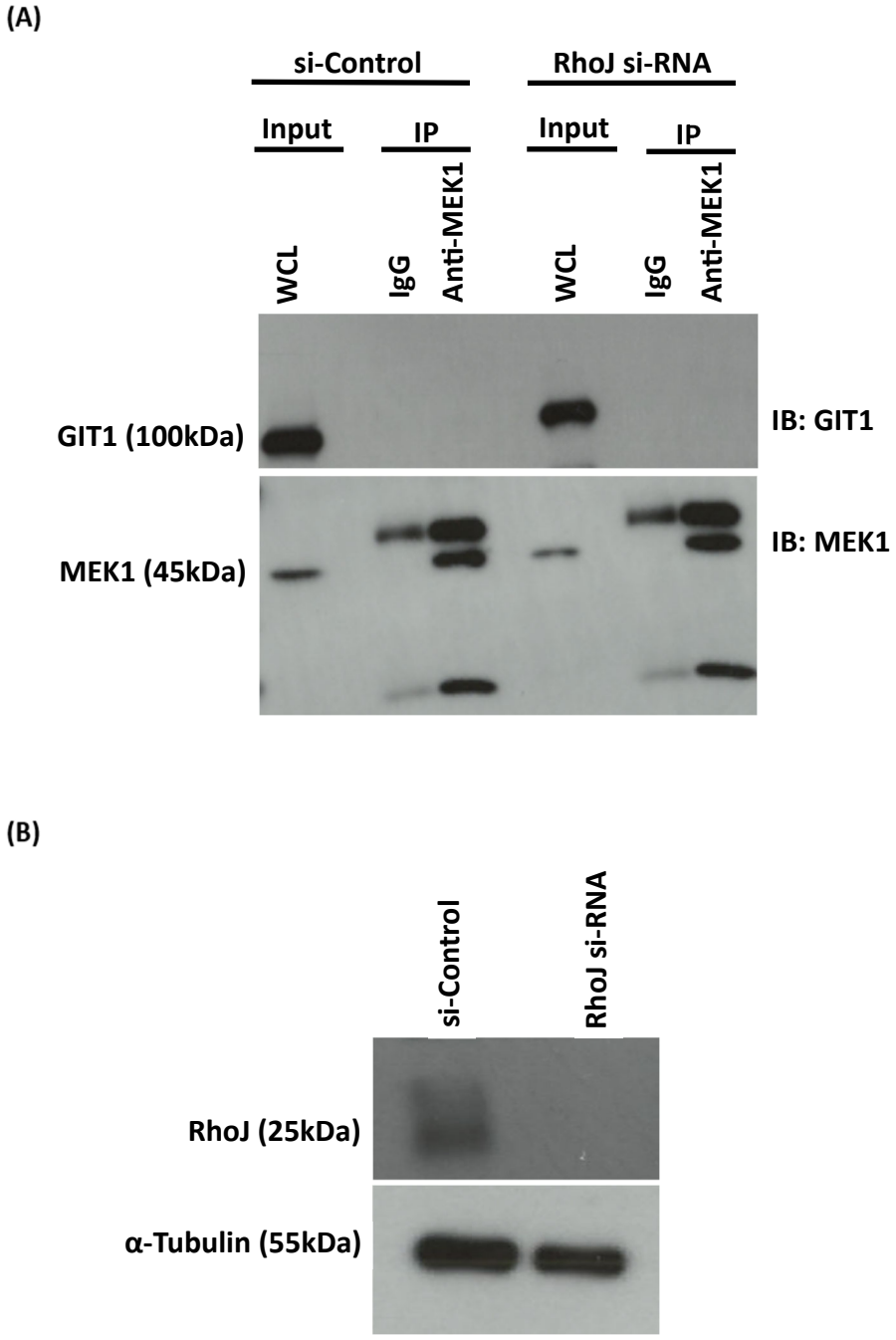

Figure 4.4. The MEK1-GIT1 interaction was not detected in HUVECs following transfection with control or RhoJ-specific si-RNA duplexes.

(A) HUVECs were transfected with 20 nM of either RhoJ-specific si-RNA or si-Control (negative control) duplexes. After 48 hours, cellular lysates were collected, incubated with prewashed protein A Seaphrose beads together with MEK1 specific antibody or mouse IgG and rotated at 4 ^{0}C for 1 hour. Beads were washed and the captured protein complexes were eluted into 2X SDS sample buffer. (B) WCL from si-Control and RhoJ si-RNA-treated cells were western blotted with RhoJ specific antibodies to confirm RhoJ knockdown, as a loading control, lysates were blotted with α-Tubulin specific antibodies. This was performed once.

4.3.4 ERK1/2 could not be detected in cytoskeletal extracts

Given the difficulties in detecting interactions between the GIT proteins with MEK1, it was considered that the interaction between GIT1 and ERK1/2 may be more readily detected from the enriched CSF of cells rather than in whole cell extract (Yin *et al.*, 2005). To test this, both HEK293T cells and HUVECs were grown until confluent at which point, they were harvested, pelleted, and homogenised in hypotonic buffer. The homogenate was then centrifuged at low speed to pellet and remove the nuclei; the resulting supernatant was next centrifuged at a high speed to sediment the cytoskeletal and the cell membrane proteins. For final purification of the CSF, samples were incubated in a buffer with a low concentration of sucrose for an hour and then centrifuged. The pellets containing the cytoskeletal proteins were then dissolved into RIPA lysis buffer, some was reserved for the input sample and the remainder incubated with Sepharose beads and either rabbit IgG or anti-ERK1/2 antisera. These IPs were incubated at 4 ^{0}C with mixing for an hour and then the beads were washed, and bound proteins eluted into sample buffer. These samples were subjected to SDS-PAGE and western blotting for GIT1 for ERK1/2 and the blots were presented in Figure 4.5. These data show that both ERK1/2 and GIT1 were detectable in the CSF, however the ERK1/2 was not successfully precipitated by the anti-ERK antisera, and this made it impossible to evaluate co-precipitation of GIT1 with ERK1/2.

It is not clear why the IP should have failed, but it may be due to poor solubility of the CSF such that there was insufficient soluble ERK1/2 available to bind the antisera. Another problem evident in this blot is the background signal produced by the rabbit IgG, both the GIT1 western blotting antibody and the ERK1/2 IP antibody were generated in rabbits. This resulted in the secondary antibody detecting the control rabbit Ig, and it did so more readily than with the anti-ERK1/2

antibody despite equal amounts of each of the antibody being used. Because of the failure to immunoprecipitate ERK1/2 from the CSF, it was instead decided to repeat the experiment using WCL.

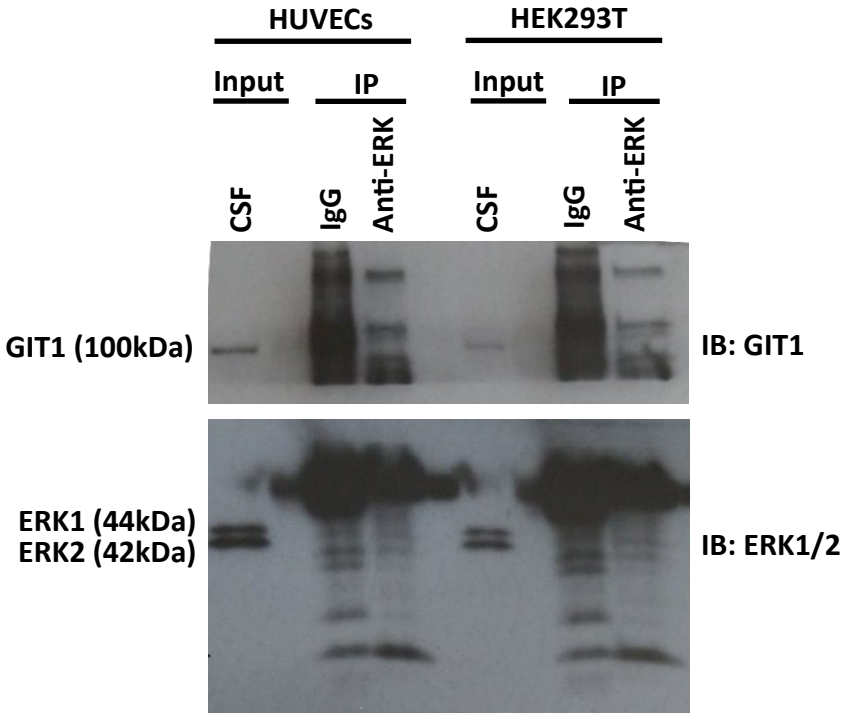

Figure 4.5. ERK1/2 protein was not precipitated from the CSF of HUVECs or HEK293T cells. HEK293T cells and HUVECs were homogenised and then subjected to cell fractionation. The cytoskeletal pellets were resuspended in the buffer and a volume was added to SDS 2X sample buffer to serve as input sample (HUVECs and HEK293T's CSF). The remaining amounts were incubated with prewashed protein A Seapharose beads and with anti-ERK or rabbit IgG for 1 hour at 4 ^{0}C with rotation. Bound protein complexes were eluted in SDS 2X sample buffer and immunoblotted for GIT1 and ERK1/2 specific antibodies. This experiment was performed once for HUVECs and twice for HEK293T cells.

4.3.5 Investigating the effect of RhoJ knockdown on the interactions between GIT1 and ERK1/2

To determine if ERK1/2 could be successfully immunoprecipitated from WCL, confluent HUVECs were lysed in RIPA buffer, a small amount of lysate was set aside for the input and the remaining lysate divided between two tubes, one containing protein A Sepharose and control rabbit Ig, and the other containing protein A Sepharose and anti-ERK antibody. After incubation for an hour at 4 ^{0}C with agitation, the beads were washed, and the bound proteins were eluted in sample buffer. Samples were then run on SDS-PAGE gels and western blotted for ERK1/2 and GIT1. Unlike the IP from cytoskeletal extract, ERK was successfully immunoprecipitated from the WCL (Figure 4.6). There remained some difficulties with high background in the control Ig IP lanes, however a band was present in the anti-ERK1/2 lane that was not evident in the control lane which was a size consistent with it being GIT1.

To pursue this further and determine the effect of RhoJ knockdown on this interaction, the co-IP experiment described above was repeated in HUVECs which had been transfected either with 20 nM control si-RNA or si-RNA duplexes specific for RhoJ. Twelve plates of HUVECs were used per condition. After 48 hours, cell lysates were prepared and IPs set up as described above, samples were subjected to SDS-PAGE and western blotting with antibodies specific to ERK1/2 and GIT1 (Figure 4.7A). Samples were also probed for RhoJ and α-Tubulin specific antibodies to confirm knockdown of RhoJ, with α-Tubulin blotting being used as a loading control (Figure 4.7B). There were problems with background signal particularly in the control Ig IP lanes, but also in the anti-ERK1/2 lanes which hampered identification of any GIT1 specific signal. Unfortunately, due to constraints of time it was not possible to pursue this further and consideration of how this methodology could be improved will be included in the discussion.

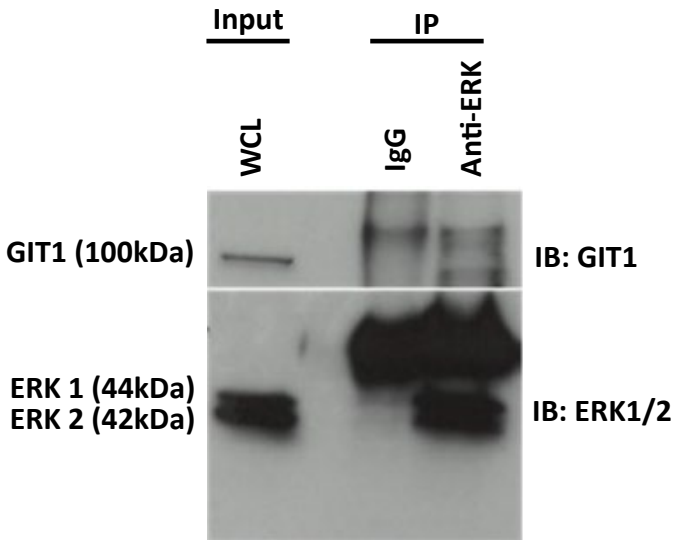

Figure 4.6. GIT1 was co-immunoprecipitated with ERK1/2 in HUVECs after cell lysis in RIPA buffer.

HUVECs were normally cultured in cM199 medium then harvested at confluency. Cell lysates were prepared with a portion reserved for the WCL which was added to 2X SDS PAGE buffer (input). The remaining lysate was incubated with prewashed protein A Seapharose beads, anti-ERK1/2 or rabbit IgG and agitated on a rotator for 1 hour at 4 ^{0}C. Samples were denatured in SDS 2X sample buffer, subjected to gel electrophoresis and probed with GIT1 and ERK1/2 specific antibodies. This was performed once.

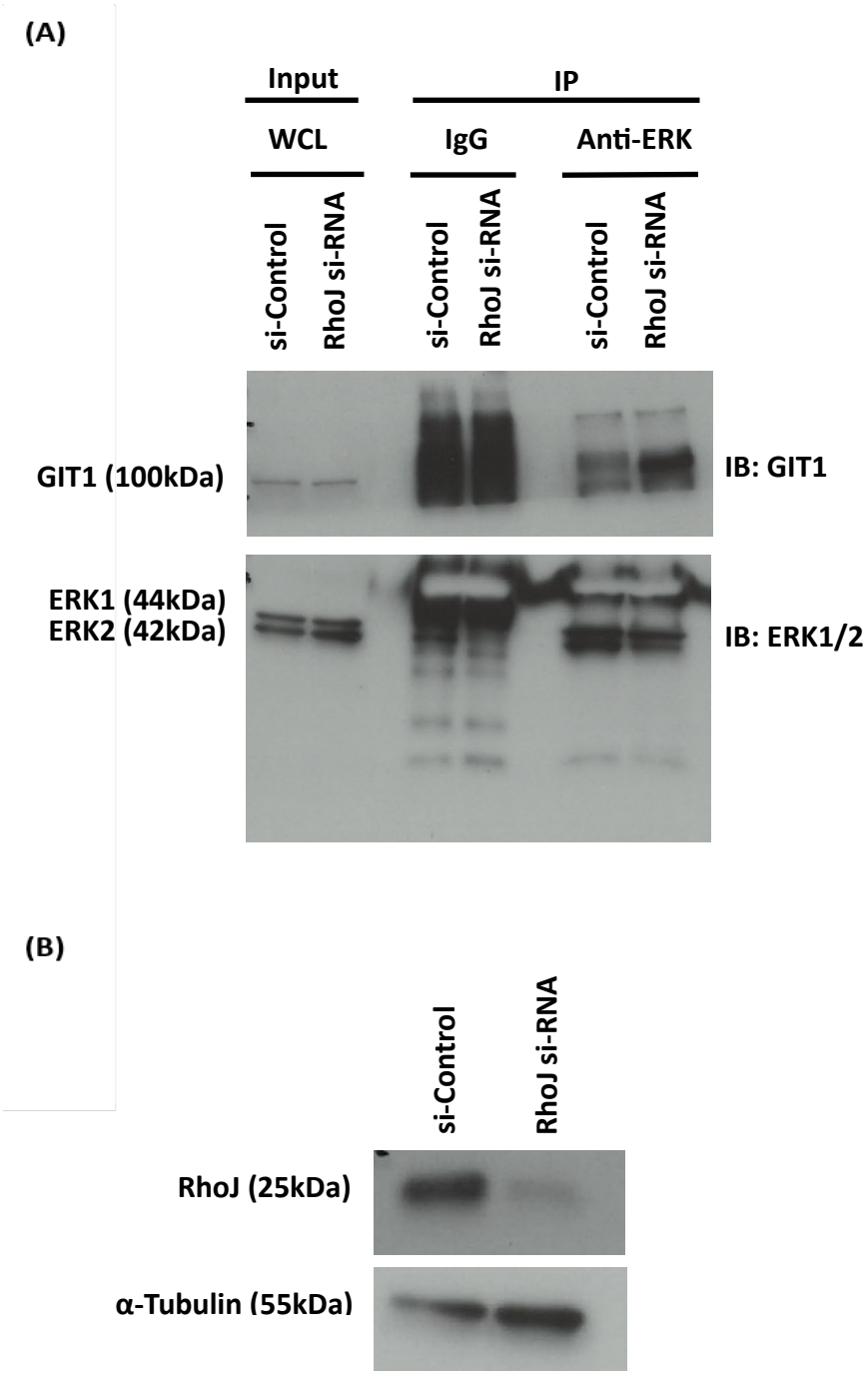

Figure 4.7. Co-IP of GIT1 with ERK1/2 in control and RhoJ si-RNA-treated HUVECs.
(A) HUVECs were transfected with RhoJ-specific si-RNA or a si-Control (negative control) duplexes (20 nM). After 48 hours lysates were collected, and IP set up with either anti-ERK1/2 or rabbit IgG (control) and were incubated for 1 hour at 4 ^{0}C with rotation. Western blotting was carried out on the WCL and immunoprecipitated samples using GIT1 and ERK1/2 specific antibodies. (B) RhoJ knockdown in WCL samples was confirmed by western blot using RhoJ specific antibody and α-Tubulin was used as a loading control. This is a representative of 2 biological replicates.

4.4 Minimal localisation of ERK1/2 to FAs in HUVECs

Previously, it had been demonstrated that GIT1 interacted specifically with ERK2 in fibronectin-seeded HeLa cells, and this in turn had enhanced the recruitment and phosphorylation of ERK at FAs (Yin *et al.*, 2005; Zhang *et al.*, 2009). In addition, our laboratory had demonstrated that expression of active RhoJ promoted the recruitment of GIT-PIX complex to FAs (Wilson *et al.*, 2014), and so the aim of this experiment was to determine if RhoJ had any impact on the localisation of ERK1/2 to FAs. Before addressing this question, it was first important to establish if ERK localised to FAs in HUVECs and set up an imaging protocol which would enable co-localisation to be examined.

HUVECs were plated on gelatin-coated coverslips at a sub-confluent cell density. This was because previously we demonstrated that RhoJ activity affected FA numbers in sub-confluent HUVECs. Cells were then paraformaldehyde fixed, permeabilised and incubated with antibodies specific for ERK1/2 and vinculin, the latter was used as a marker for FAs. After washing, the coverslips were incubated with secondary antibodies each conjugated to different Alexafluors. Prior to mounting, coverslips were incubated with DAPI to enable clear visualisation of nuclei. The stained cells were then imaged using epifluorescence microscopy (Figures 4.8A and B). The images acquired show strong localisation of ERK to the nucleus with some diffuse peri-nuclear staining. The vinculin staining clearly identified FAs which were readily detectable in the lamellipodia. There was, however, little co-localisation of ERK1/2 with FAs in these samples, in the expanded sections it is evident that faint staining or ERK is observed in the lamellipodia, but it is not concentrated at the site of FAs. There is a small degree of co-localisation at the leading edge of the cell, observable in in the expanded section of Figure 4.8A.

Overall, the lack of evident ERK localisation at FAs meant that it was not going to be feasible to determine if RhoJ activity affected this and so this line of investigation was not pursued.

(A)

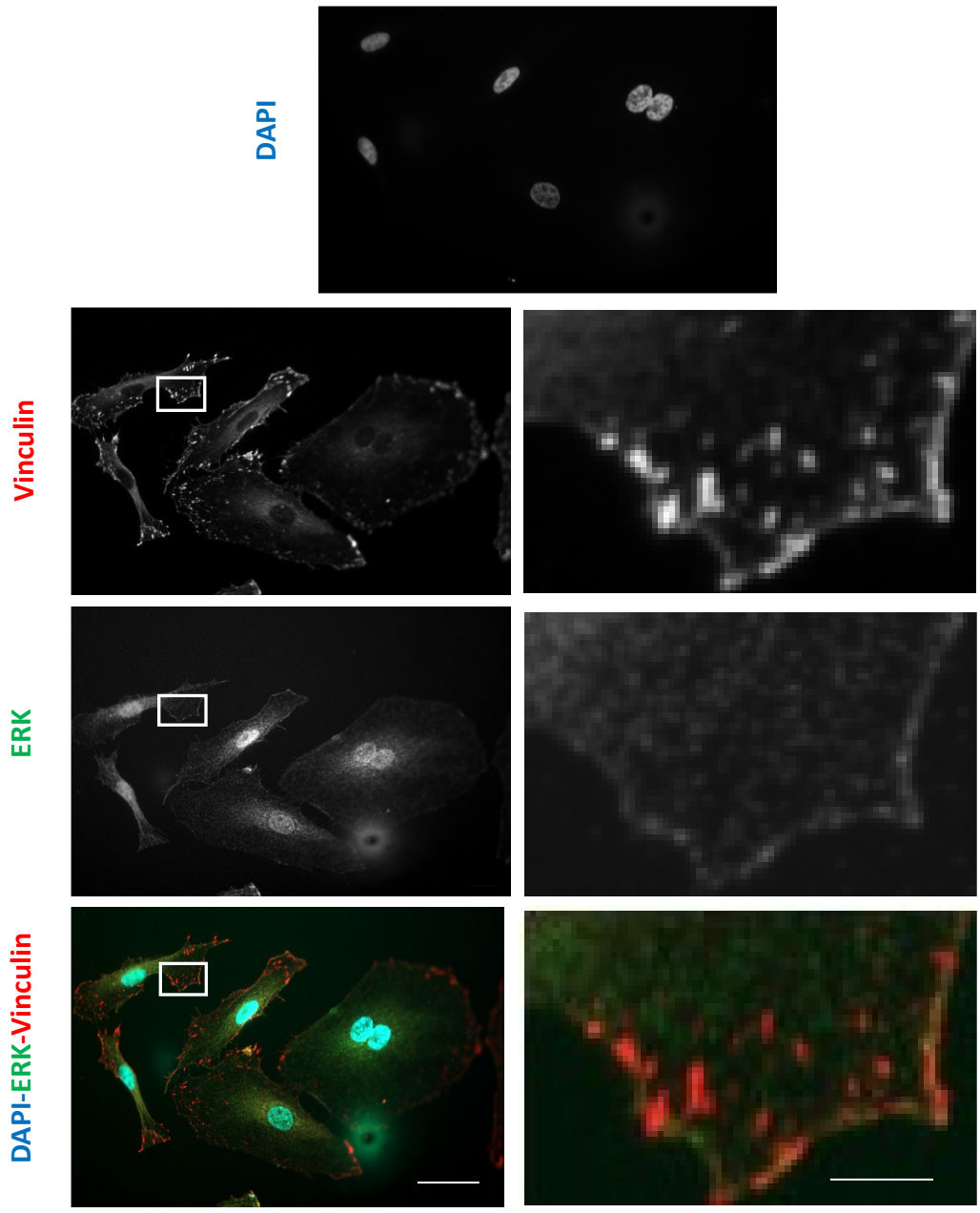

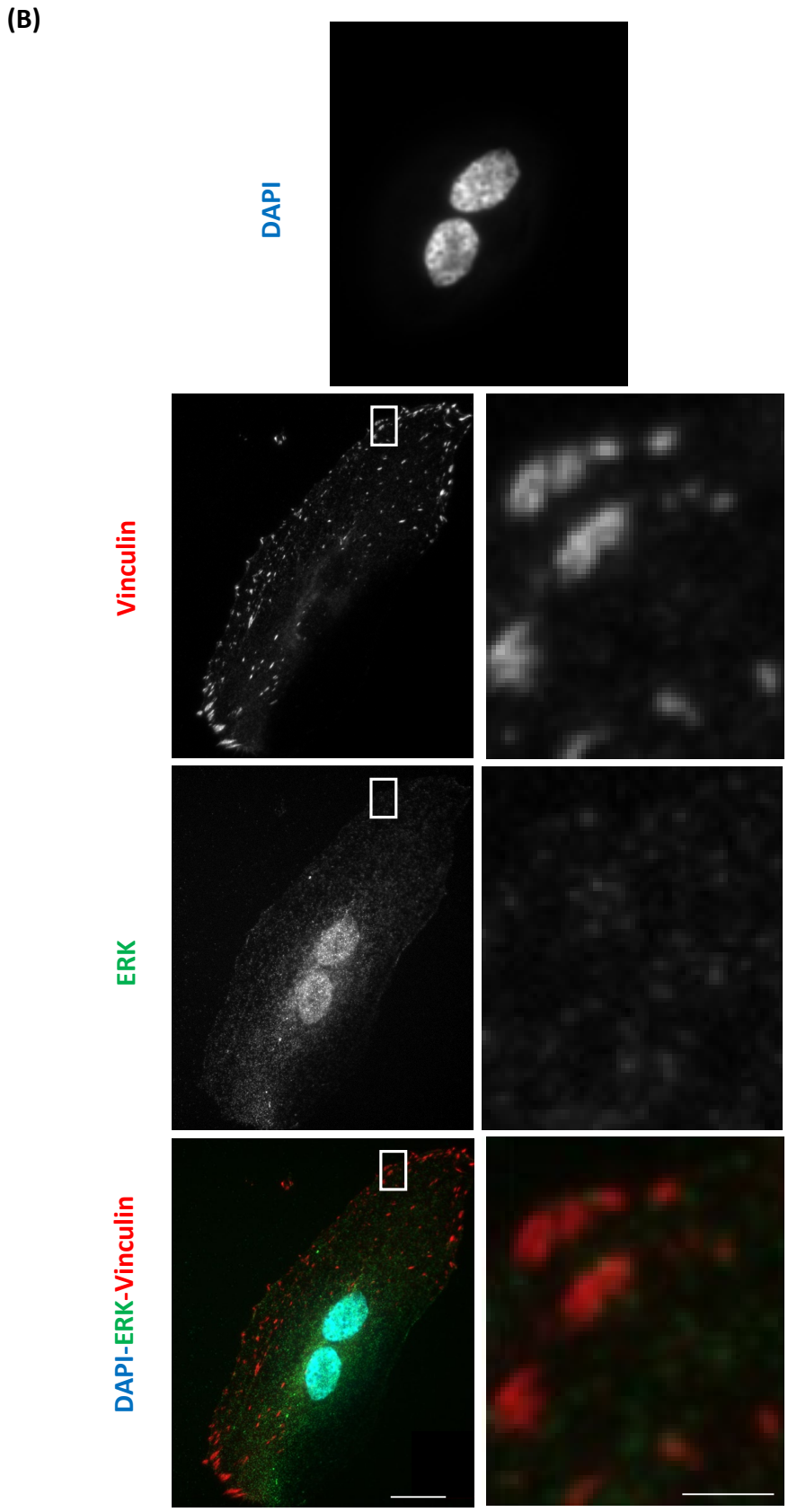

Figure 4.8. No evident localisation of ERK1/2 to FAs in HUVECs.
HUVECs were cultured on gelatin coated coverslips. After 48 hours, cells were paraformaldehyde-fixed, stained with vinculin and ERK1/2 specific antibodies and imaged by epifluorescence microscopy at 40X (A) and at 100X (B). Coverslips were incubated for 10 mins with DAPI for nuclear visualisation. Scale bar: 20, 10 µm for Figure A and B, respectively.

4.5 Discussion

Data presented in this chapter show that PAK is potentially the RhoJ activated kinase involved in causing the reduced electrophoretic mobility of GIT2 in ECs expressing an active mutant of RhoJ (daRhoJ). We showed that blocking PAK activity using the PF-3758309 pan-PAK inhibitor successfully prevented the upwards mobility shift of GIT2 in HUVECs expressing daRhoJ. By contrast, the selective Group I PAK inhibitor IPA-3 did not alter the electrophoretic mobility of GIT2. We have also demonstrated that MEK1 associated with GIT1 and GIT2 and ERK1/2 associated with GIT1 in unmanipulated HUVECs. However, it was not possible to demonstrate that RhoJ knockdown affected any of these interactions. In addition, we did not find that ERK1/2 localised to FAs in ECs.

Both in this study and in previous work published by our laboratory, it has been demonstrated that the expression of daRhoJ decelerated GIT2's electrophoretic migration. This was likely to be due to a post-translational modification and our hypothesis was that this was phosphorylation. Src and FAK kinases have both been reported to phosphorylate tyrosine residues on GIT necessary for FA localisation (Brown *et al.*, 2005). However, we had previously demonstrated that Src and FAK inhibition did not affect the daRhoJ-mediated electromobility shift (Wilson *et al.*, 2014). Multiple phospho-serine and threonine sites have been identified in GIT1 (Webb *et al.*, 2006) and preliminary mass spectrometry data generated by our laboratory also indicated that serine and threonine residues on GIT2 were differentially phosphorylated in daRhoJ-expressing HUVECs. As with RhoJ, PAK kinases were also shown to interact with the GIT-PIX complex (Nayal *et al.*, 2006) and PAK kinases may be activated by RhoJ, because like CDC42, in its active form RhoJ interacts with CRIB-domain containing proteins such as PAK (Vignal *et al.*, 2000; Leszczynska *et al.*, 2011). Hence it is possible that RhoJ-activated PAK is phosphorylating GIT2. To practically test this, PF-3758309 (ATP-

competitive, pan PAK inhibitor) and IPA-3 (allosteric Group I) small molecule inhibitors were used to block PAK's activity in HUVECs expressing daRhoJ. Our data showed that PF-3758309, but not IPA-3, effectively inhibited GIT2 mobility shift in a dose dependent fashion. Since an experiment to test the activity of the IPA-3 compound was active was not included, we cannot rule out the possibility that the lack of effect of IPA-3 was due to a problem with this compound's activity. However, these data suggest that the Group II PAK kinases (PAK4/5/6) are mediating the phosphorylation. The Human Protein Atlas database indicates that at the transcriptomic level PAK4 is the most abundantly expressed Group II PAKs in ECs and is expressed at 25 times the amount of PAK5 or PAK6 (www.proteinatlas.org). The differential effect of the PAK inhibitors and the endothelial abundance of PAK4, would suggest that PAK4 is most likely to be the candidate kinase phosphorylating GIT2, and this could be explored by determining the effect of si-RNA knockdown of this PAK on GIT2 phosphorylation. It would also be important to definitively demonstrate that the post-translational modifications of GIT2 are indeed phosphorylation, this could be done using IP and western blotting with phospho-serine and phospho-threonine specific antibodies or using mass spectrometry.

Previously our group has demonstrated a role for RhoJ in promoting FA disassembly and it is highly likely that PAK is involved in this process. Multiple studies have demonstrated that enhancement of PAK's association with the GIT-PIX complex at FAs augments FA turnover, cell protrusion and movement (Zhao *et al.*, 2000; West *et al.*, 2001; Manabe *et al.*, 2002; Nayal *et al.*, 2006). A proline-rich region in PAK interacts with β-PIX's SH3 domain (Manser *et al.*, 1998), and both β-PIX and active GTP-bound RhoJ interact with the SHD of GIT1 (Schlenker and Rittinger, 2009; Wilson *et al.*, 2014). Thus, it is possible that the GIT-PIX complex is providing a scaffold required for RhoJ-mediated activation of PAK. IF microscopy could be used to investigate co-localisation of PAK with RhoJ and

the GIT-PIX complex in ECs, and it would be interesting to determine whether this is affected by modulating the activity of RhoJ. We have already demonstrated that RhoJ si-RNA knockdown reduces the level of GIT1/2 and β-PIX localisation to FAs (Wilson *et al.*, 2014) and this may also be the case for PAK proteins.

The majority of experiments in this chapter were then aimed to address our hypothesis that RhoJ was regulating ERK1/2 activity via the GIT-PIX complex, since interactions between MEK1 and ERK1/2 and GIT1 had been previously reported (Yin *et al.*, 2004; Yin *et al.*, 2005). Two approaches were taken similar to what had been done in this original study, the first was a biochemical approach to determine if modulating RhoJ activity had any influence on co-precipitation of GIT1/2 with MEK1 or ERK1/2 and the second was to use microscopy to investigate the localization of ERK1/2 to FAs. Consistent with previous reports, it was possible to co-precipitate GIT1 with ERK1/2 and both GIT1 and GIT2 with MEK1 from the WCL of unmanipulated HUVECs. However, the co-precipitated signal of GIT1 or GIT2 was always weak even when using large amounts of lysate, and long exposure times were required to reveal any signal. The large numbers of HUVECs required to demonstrate an interaction made the introduction of si-RNA knockdown into the protocol challenging, and these experiments might have been improved by better establishing cell numbers and lysate concentrations needed for reliable co-precipitation.

Another challenge was the availability of suitable antibodies for IP. There were no antibodies available which successfully immunoprecipitated endogenous GIT1 or GIT2, and so instead MEK1 or ERK1/2 were precipitated. With the ERK1/2 IP, the fact that GIT1 western blotting antibodies were from the same species as the IP antibody gave rise to difficulties with background signal. This was

particularly problematic with the control Ig which both obscured the region of the blot where the weak signal from the GIT1 blotting was expected and introduced a series of background bands which hampered interpretation. With more time and resources, it might have been possible to identify more suitable antibodies for these experiments. Some other approaches were attempted such as trying to identify suitable faster growing ECs lines expressing RhoJ or the purification cytoskeletal proteins to enrich for the relevant proteins, however they did not overcome the difficulties faced.

As noted above work in this chapter also investigated the localisation of ERK1/2 to FAs with an aim to identify how this might be affected by RhoJ activity. Previously, Yin *et al. (*2005) and Zhang *et al.* (2009) demonstrated a co-localisation of phospho-ERK1/2 and GIT1 in HeLa cells (Yin *et al.*, 2005; Zhang *et al.*, 2009). Initially we checked for the co-localisation of ERK1/2 with the FA protein vinculin in sparsely cultured HUVECs by IF. We had previously shown that it was in sub-confluent migratory HUVECs where RhoJ activity affected FA numbers and disassembly time (Wilson *et al.*, 2014). In contrast what had been previously observed, we saw no co-localization of vinculin with ERK1/2 in sparsely plated HUVECs, with ERK1/2 being predominantly localised to the nucleus and peri-nuclear region of cells. There was some faint signal of ERK1/2 in lamellipodia, but it did not overlap with the strong vinculin staining. These data indicate that little ERK1/2 are localised to FAs in HUVECs under the conditions investigated and so there is little evidence to support the notion that RhoJ may be regulating the localisation and hence activity of ERK1/2 to FAs. This observation is consistent with the very low level of ERK1/2 and MEK1 co-precipitation with GIT proteins and because of the lack of ERK1/2 staining in FAs, the effect of RhoJ knockdown or expression of daRhoJ on ERK1/2 localisation was not pursued.

There are a number of possible reasons to which might explain the discrepancies between our data and that of Yin *et al.* (2005) and Zhang *et al.* (2009). We used primary vein ECs, while their studies involved EGF pre-treated immortalised HeLa cell line, and there may have been differences in the expression levels of GIT1 in these two cell types. Another difference was that Yin *et al.* (2005) and Zhang *et al.* (2009) seeded cells on fibronectin in some experiments which affected cell spreading and ERK activation at FAs, whereas our HUVECs were cultured on collagen. Hence it might be useful to consider investigating whether fibronectin versus collagen affects ERK localisation to FAs in HUVECs. Another key difference between the two studies is that Yin *et al.* (2005) showed that phopho-ERK1/2 was localised to FAs (co-localised with either paxillin or vinculin) after acute stimulation with EGF, in contrast we were investigating steady-state localisation of ERK in HUVECs in cM199 media. It would be interesting to determine if acute stimulation of HUVECs with either VEGFA or FGF2 transiently affects ERK1/2 localisation.

Our observation that levels of ERK1/2 at FAs are low suggests that RhoJ is not likely to be regulating MEK1 or ERK1/2 via the GIT-PIX complex. An alternative possibility is that RhoJ is activating the ERK MAP kinase pathway via PAK, indeed several studies have demonstrated that PAK can affect MAP kinase activity via enhancing RAF phosphorylation. For example, PAK3 was shown to mediate site-specific RAF1 phosphorylation (S338) required for RAS-RAF signal activation, and this effect was augmented by activated CDC42 and Rac (King *et al.*, 1998). A second study showed that FGF2 activated PAK1 which in turn resulted in RAF1 phosphorylation and functionally this prevented EC death (Alavi *et al.*, 2003). Previously Koh *et al.* (2008) demonstrated that CDC42 promoted endothelial tubulogenesis via the activation of PAK2, PAK4, PKCϵ, Src, Yes, B-RAF, C-RAF and ERK1/2 (Koh *et al.*, 2008). These researchers went on to show that si-RNA-mediated knockdown of RhoJ

resulted in reduced Rac1 and CDC42 activation as well as diminished levels of phospho-PAK2, phospho-PAK4 and phospho-B-RAF (Yuan *et al.*, 2011). It is not clear from these studies if RhoJ was acting directly via PAK2 and/or PAK4 to modulate RAF activation or whether this might be via CDC42 or Rac1. These data are, however, consistent with our observations that reduced RhoJ activity impairs ERK1/2 activation. It would be interesting to determine how daRhoJ affects RAF phosphorylation and to investigate how inhibiting PAK with either inhibitors or si-RNA knockdown might affect this.

Data presented in this chapter has suggested that PAK4 is the RhoJ activated kinase involved in the daRhoJ-mediated increase GIT2 phosphorylation, which causes the retarded electrophoretic mobility of GIT2. Although GIT1 co-precipitated with MEK1 and ERK1/2, there was no conclusive evidence that RhoJ knockdown influenced any of these interactions. Although some technical issues hampered these experiments, a lack of ERK1/2 localisation at FAs likely provided an explanation for the challenges that were encountered while investigating these interactions in IP experiments. In the future it would be important to delineate the molecular pathway connecting RhoJ with the ERK MAP kinase pathway.

CHAPTER 5

General discussion

This project has clearly demonstrated a link between the activity of RhoJ and the activity of MAP kinases, and in particular ERK1/2. Silencing of RhoJ using si-RNA duplexes diminished the activation of ERK1/2 to a range of stimuli; though RhoJ's modulation of ERK1/2 in response to VEGFA had been previously reported (Fukushima *et al.*, 2020), our observations that this also occurred in response to FGF2, and complete medium are novel. The mechanism of action, and in particular a link to the GIT-PIX complex, was interrogated. Though we confirmed reports that MEK1 and ERK1/2 interact with the GIT-PIX complex, we were not able to establish whether this was affected by RhoJ. We also found that localisation of ERK1/2 to FAs that had been reported in other cell types was not observed in ECs under our culture conditions. Finally, we did demonstrate that the electromobility shift of GIT2 induced by an active mutant of RhoJ was sensitive to PAK inhibition. Given the sensitivity to the different inhibitors used and endothelial expression patterns of Group II PAKs, this was likely mediated by PAK4. Other techniques such as si-RNA-mediated knockdown of the different PAK kinases would enable further delineation of this pathway and identification of which PAK is involved.

The identification of PAK as a potential downstream mediator of RhoJ provides a potential mechanistic link between RhoJ and its role in promoting FA disassembly which has been previously reported by our laboratory (Wilson *et al.*, 2014). A number of studies have indicated a role for the GIT-PIX complex in regulating FA turnover (Feng *et al.*, 2010; Zhao *et al.*, 2000; Kuo *et al.*, 2011; Nayal *et al.*, 2006) and its localisation to FA depends on interactions between GIT and paxillin (Di Cesare *et al.*, 2000; Turner *et al.*, 1999; Zhao *et al.*, 2000). Zhao *et al.* (2000) proposed a model whereby CDC42 mediates activation and recruitment of PAK and PIX which in turn promotes the association of GIT1 with FAs. This then promotes the dissociation of paxillin from FAs because of interaction of the C-terminal region of GIT1 with Paxillin's LD4 motif (Zhao *et al.*, 2000). A subsequent study

demonstrated that phosphorylation of GIT1 at serine 709 played a critical role in its interaction with paxillin and effects on cell protrusion, and PAK was demonstrated to phosphorylate this residue using *in vitro* kinase assays (Webb *et al.*, 2006). PAK is also able to modulate actomyosin contractility via phosphorylating and inhibiting myosin light chain kinase (MLCK) (Zhao *et al.*, 2000); we have previously observed reduced contractility in ECs expressing daRhoJ (Kaur *et al.*, 2011) and so this activity of RhoJ may also be mediated by PAK. Accordingly, we propose that active GTP-bound RhoJ, like CDC42, is able to bind the CRIB of PAK and activate its kinase activity. Active GTP-bound RhoJ interacts with GIT1/2 and together with PIX and PAK is recruited to FAs. This movement of GIT1/2 to FAs results in its interaction with paxillin which facilitates the dissociation of paxillin from FAs and their disassembly. This dissociation of paxillin is also promoted by the phosphorylation of GIT1/2 by PAK which in turn is activated by RhoJ. It is possible that β-PIX is also involved in this process by acting as the GEF for RhoJ, as it does for CDC42 (Feng *et al.*, 2006). Whether β-PIX can act in this way would require the use of nucleotide exchange assays and the production of recombinant RhoJ and β-PIX and could be subject of future studies.

In this study we showed that RhoJ positively regulated ERK1/2 activation downstream of VEGFA, cM199 and FGF2. The fact that this occurred downstream of a variety of stimuli suggested that any mechanism was not likely to depend on complex regulation of receptor internalisation, but rather would utilise more direct interaction between RhoJ and MAP kinase signalling. Given RhoJ's interaction with GIT1/2 and a reported scaffolding function of GIT proteins for MEK1 and ERK1/2 (Yin *et al.*, 2004; Yin *et al.*, 2005; Zhang *et al.*, 2009), our original hypothesis was that RhoJ was regulating the interaction between GIT proteins and MEK1 and/or ERK1/2. Our experiments did not rule out this possibility, but we found very low levels co-precipitation of GIT1/2 with MEK1 or ERK1/2

and a failure to localise ERK1/2 to FAs prompted other mechanisms to be considered. An alternative mechanism could involve PAK which has been shown to modulate ERK MAP kinase signalling via both kinase-dependant and kinase-independent mechanisms. PAK can phosphorylate RAF1 at S338 and MEK1 at S298, in both cases promoting their activity (King *et al.*, 1998; Chaudhary *et al.*, 2000; Slack-Davis *et al.*, 2003). Overexpression a kinase dead form of PAK was also able to potentiate ERK MAP kinase signalling possibly through scaffolding interactions between the ERK MAP kinase signalling components (Radu *et al.*, 2014). We demonstrated that pharmacological inhibition of PAK abrogated the decreased electrophoretic mobility of GIT2, and it would be interesting to determine what effect it might have had on the activation levels of the components of the MAP kinase signalling cascade in cells expressing an active mutant of RhoJ. An involvement of PAK in endothelial RhoJ biology was identified by Yuan et al. who demonstrated si-RNA knockdown of RhoJ resulted in reduced levels of phospho-PAK2, phospho-PAK4 and phospho-B-RAF (Yuan *et al.*, 2011). Depletion of RhoJ also reduced the levels of GTP-bound Rac1 and CDC42. Moreover, their study also suggested that RhoJ may act on PAK via these other related Rho GTPases, which delineates the complex interplay between these different Rho GTPases and hence more investigation will be required to determine precisely how they act to regulate PAK. In our model we have proposed a direct link between RhoJ, PAK and RAF (Figure 5.1), but it may be that RhoJ acts on PAK via modulation of other Rho GTPases. For example, RhoJ associates with the GIT-PIX complex, and β-PIX is a GEF for CDC42, thus RhoJ may influence CDC42 activation via its association with β-PIX.

In conclusion, while there is considerable work still to be done to fully elucidate its various functions, this work adds to our understanding of the multifaceted role of RhoJ in EC biology and gives a greater

insight into mechanisms by which it can modulate processes such as cell motility which is fundamental in angiogenesis.

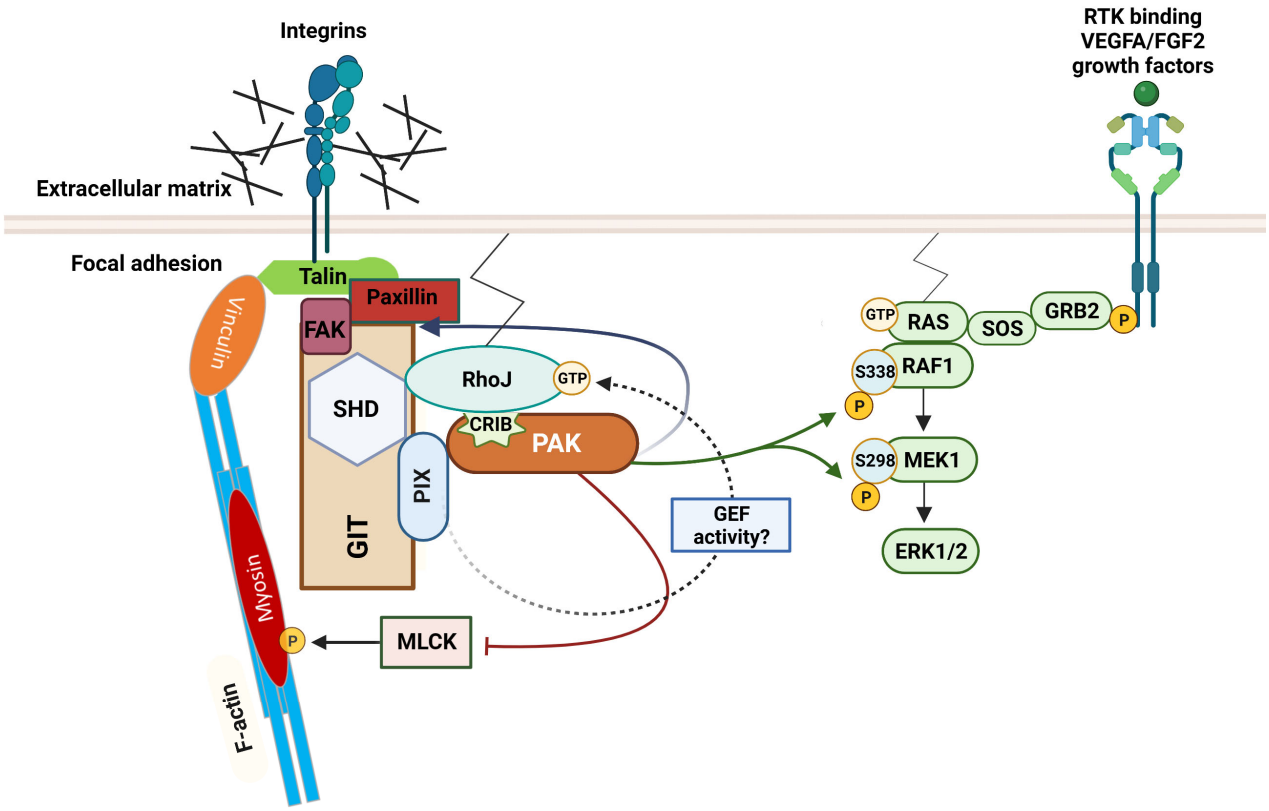

Figure 5.1. A model illustrating RhoJ-PAK regulation of FA disassembly and MAP kinase activation.
Active GTP-bound RhoJ binds the CRIB of PAK causing its activation. In addition, active RhoJ also binds the SHD of GIT proteins while PAK associates with PIX's SH3 domain. This causes the recruitment of GIT to FAs, allowing its interaction with paxillin. RhoJ's activation of PAK results in PAK phosphorylating GIT (blue curved arrow), facilitating the dissociation of paxillin and FA disassembly. Activated PAK also inhibits MLCK-mediated myosin II phosphorylation (red curved line) reducing actomyosin contractility. RhoJ's GTP loading and activation could be mediated by PIX's GEF activity (black dashed curved arrow). Active PAK phosphorylates S338 and S298 on RAF1 and MEK1, respectively (green arrows). This potentiates signalling through the ERK1/2 MAP kinase pathway in response to pro-angiogenic receptor stimulation.

References

Abe, T., Kato, M., Miki, H., Takenawa, T., and Endo, T. (2003). Small GTPase Tc10 and its homologue RhoT induce N-WASP-mediated long process formation and neurite outgrowth. *Journal of cell science, 116*(1), 155-168.

Abo, A., Qu, J., Cammarano, M. S., Dan, C., Fritsch, A., Baud, V., Belisle, B., and Minden, A. (1998). PAK4, a novel effector for Cdc42Hs, is implicated in the reorganization of the actin cytoskeleton and in the formation of filopodia. *The EMBO journal, 17*(22), 6527-6540.

Ackermann, K. L., Florke, R. R., Reyes, S. S., Tader, B. R., and Hamann, M. J. (2016). TCL/RhoJ Plasma Membrane Localization and Nucleotide Exchange Is Coordinately Regulated by Amino Acids within the N Terminus and a Distal Loop Region. *The Journal of biological chemistry, 291*(45), 23604-23617.

Adams, R. H., and Alitalo, K. (2007). Molecular regulation of angiogenesis and lymphangiogenesis. *Nature reviews Molecular cell biology, 8*(6), 464-478.

Aicart-Ramos, C., Valero, R. A., and Rodriguez-Crespo, I. (2011). Protein palmitoylation and subcellular trafficking. *Biochimica et Biophysica Acta (BBA)-Biomembranes, 1808*(12), 2981-2994.

Alavi, A., Hood, J. D., Frausto, R., Stupack, D. G., and Cheresh, D. A. (2003). Role of Raf in vascular protection from distinct apoptotic stimuli. *Science, 301*(5629), 94-96.

Alitalo, K., Tammela, T., and Petrova, T. V. (2005). Lymphangiogenesis in development and human disease. *Nature, 438*(7070), 946-953.

Angelos, M. G., Abrahante, J. E., Blum, R. H., and Kaufman, D. S. (2018). Single cell resolution of human hematoendothelial cells defines transcriptional signatures of hemogenic endothelium. *Stem Cells, 36*(2), 206-217.

Arts, J. J., Mahlandt, E. K., Schimmel, L., Grönloh, M. L., Van der Niet, S., Klein, B. J., Fernandez-Borja, M., van Geemen, D., Huveneers, S., and van Rijssel, J. (2021). Endothelial Focal Adhesions Are Functional Obstacles for Leukocytes During Basolateral Crawling. *Frontiers in Immunology, 12*, 667213.

Aspenström, P., Fransson, Å., and Saras, J. (2004). Rho GTPases have diverse effects on the organization of the actin filament system. *Biochemical Journal, 377*(2), 327-337.

Auerbach, S. S., Thomas, R., Shah, R., Xu, H., Vallant, M. K., Nyska, A., and Dunnick, J. K. (2010). Comparative phenotypic assessment of cardiac pathology, physiology, and gene expression in C3H/HeJ, C57BL/6J, and B6C3F1/J mice. *Toxicol Pathol, 38*(6), 923-942.

Bagrodia, S., Taylor, S. J., Jordon, K. A., Van Aelst, L., and Cerione, R. A. (1998). A novel regulator of p21-activated kinases. *Journal of Biological Chemistry, 273*(37), 23633-23636.

Bai, Y., Wei, C., Zhong, Y., Zhang, Y., Long, J., Huang, S., Xie, F., Tian, Y., Wang, X., and Zhao, H. (2020). Development and Validation of a Prognostic Nomogram for Gastric Cancer Based on DNA Methylation-Driven Differentially Expressed Genes. *Int J Biol Sci, 16*(7), 1153-1165.

Barkefors, I., Le Jan, S., Jakobsson, L., Hejll, E., Carlson, G., Johansson, H., Jarvius, J., Park, J. W., Jeon, N. L., and Kreuger, J. (2008). Endothelial cell migration in stable gradients of vascular endothelial growth factor A and fibroblast growth factor 2: effects on chemotaxis and chemokinesis. *Journal of Biological Chemistry, 283*(20), 13905-13912.

Beck Jr, L., and D'Amore, P. A. (1997). Vascular development: cellular and molecular regulation. *The FASEB journal, 11*(5), 365-373.

Bellon, A., Luchino, J., Haigh, K., Rougon, G., Haigh, J., Chauvet, S., and Mann, F. (2010). VEGFR2 (KDR/Flk1) signaling mediates axon growth in response to semaphorin 3E in the developing brain. *Neuron, 66*(2), 205-219.

Billottet, C., Rottiers, P., Tatin, F., Varon, C., Reuzeau, E., Maître, J.-L., Saltel, F., Moreau, V., and Génot, E. (2008). Regulatory signals for endothelial podosome formation. *European journal of cell biology, 87*(8-9), 543-554.

Blanco, R., and Gerhardt, H. (2013). VEGF and Notch in tip and stalk cell selection. *Cold Spring Harbor perspectives in medicine, 3*(1), a006569.

Breier, G., and Risau, W. (1996). The role of vascular endothelial growth factor in blood vessel formation. *Trends in cell biology, 6*(12), 454-456.

Brown, M. C., Cary, L. A., Jamieson, J. S., Cooper, J. A., and Turner, C. E. (2005). Src and FAK kinases cooperate to phosphorylate paxillin kinase linker, stimulate its focal adhesion localization, and regulate cell spreading and protrusiveness. *Molecular biology of the cell, 16*(9), 4316-4328.

Bryan, B., and D'amore, P. (2007). What tangled webs they weave: Rho-GTPase control of angiogenesis. *Cellular and molecular life sciences, 64*, 2053-2065.

Buchwald, G., Hostinova, E., Rudolph, M. G., Kraemer, A., Sickmann, A., Meyer, H. E., Scheffzek, K., and Wittinghofer, A. (2001). Conformational switch and role of phosphorylation in PAK activation. *Molecular and cellular biology, 21*(15), 5179-5189.

Burridge, K., and Wennerberg, K. (2004). Rho and Rac take center stage. *Cell, 116*(2), 167-179.

Buscà, R., Pouysségur, J., and Lenormand, P. (2016). ERK1 and ERK2 map kinases: specific roles or functional redundancy? *Frontiers in cell and developmental biology, 4*, 53.

Caduff, J., Fischer, L., and Burri, P. H. (1986). Scanning electron microscope study of the developing microvasculature in the postnatal rat lung. *The Anatomical Record, 216*(2), 154-164.

Carmeliet, P. (2003). Angiogenesis in health and disease. *Nature medicine, 9*(6), 653-660.

Carmeliet, P., Ferreira, V., Breier, G., Pollefeyt, S., Kieckens, L., Gertsenstein, M., Fahrig, M., Vandenhoeck, A., Harpal, K., and Eberhardt, C. (1996). Abnormal blood vessel development and lethality in embryos lacking a single VEGF allele. *Nature, 380*(6573), 435-439.

Cernohorska, M., Sulimenko, V., Hajkova, Z., Sulimenko, T., Sladkova, V., Vinopal, S., Draberova, E., and Draber, P. (2017). Corrigendum to "GIT1/betaPIX signaling proteins and PAK1 kinase regulate microtubule nucleation" [Biochim. Biophys. Acta 1863/6PA (2016) 1282-1297. *Biochimica et biophysica acta.Molecular cell research, 1864*(4), 747.

Chang, L., and Karin, M. (2001). Mammalian MAP kinase signalling cascades. *Nature, 410*(6824), 37-40.

Chang, T. Y., Tsai, W. C., Huang, T. S., Su, S. H., Chang, C. Y., Ma, H. Y., Wu, C. H., Yang, C. Y., Lin, C. H., Huang, P. H., Cheng, C. C., Cheng, S. M., and Wang, H. W. (2017). Dysregulation of endothelial colony-forming cell function by a negative feedback loop of circulating miR-146a and -146b in cardiovascular disease patients. *PloS one, 12*(7), e0181562.

Chaudhary, A., King, W., Mattaliano, M., Frost, J., Diaz, B., Morrison, D., Cobb, M., Marshall, M., and Brugge, J. (2000). Phosphatidylinositol 3-kinase regulates Raf1 through Pak phosphorylation of serine 338. *Current Biology, 10*(9), 551-554.

Chen, B., Yuan, Y., Sun, L., Chen, J., Yang, M., Yin, Y., and Xu, Y. (2020). MKL1 Mediates TGF-β Induced RhoJ Transcription to Promote Breast Cancer Cell Migration and Invasion. *Front Cell Dev Biol, 8*, 832.

Cherfils, J., and Chardin, P. (1999). GEFs: structural basis for their activation of small GTP-binding proteins. *Trends in biochemical sciences, 24*(8), 306-311.

Cherfils, J., and Zeghouf, M. (2013). Regulation of small gtpases by gefs, gaps, and gdis. *Physiological reviews, 93*(1), 269-309.

Chiang, S.-H., Hou, J. C., Hwang, J., Pessin, J. E., and Saltiel, A. R. (2002). Cloning and Functional Characterization of Related TC10 Isoforms, a Subfamily of Rho Proteins Involved in Insulin-stimulated Glucose Transport∗. *Journal of Biological Chemistry, 277*(15), 13067-13073.

Cines, D. B., Pollak, E. S., Buck, C. A., Loscalzo, J., Zimmerman, G. A., McEver, R. P., Pober, J. S., Wick, T. M., Konkle, B. A., and Schwartz, B. S. (1998). Endothelial cells in physiology and in the pathophysiology of vascular disorders. *Blood, The Journal of the American Society of Hematology, 91*(10), 3527-3561.

Color-Aparicio, V. M., Cervantes-Villagrana, R. D., Garcia-Jimenez, I., Beltran-Navarro, Y. M., Castillo-Kauil, A., Escobar-Islas, E., Reyes-Cruz, G., and Vazquez-Prado, J. (2020). Endothelial cell sprouting driven by RhoJ directly activated by a membrane-anchored Intersectin 1 (ITSN1) RhoGEF module. *Biochemical and biophysical research communications, 524*(1), 109-116.

Crawford, T. N., Alfaro III, D. V., Kerrison, J. B., and Jablon, E. P. (2009). Diabetic retinopathy and angiogenesis. *Current diabetes reviews, 5*(1), 8-13.

de Toledo, M., Senic-Matuglia, F., Salamero, J., Uze, G., Comunale, F., Fort, P., and Blangy, A. (2003). The GTP/GDP cycling of rho GTPase TCL is an essential regulator of the early endocytic pathway. *Molecular biology of the cell, 14*(12), 4846-4856.

Deacon, S. W., Beeser, A., Fukui, J. A., Rennefahrt, U. E., Myers, C., Chernoff, J., and Peterson, J. R. (2008). An isoform-selective, small-molecule inhibitor targets the autoregulatory mechanism of p21-activated kinase. *Chemistry & biology, 15*(4), 322-331.

Di Cesare, A., Paris, S., Albertinazzi, C., Dariozzi, S., Andersen, J., Mann, M., Longhi, R., and de Curtis, I. (2000). p95-APP1 links membrane transport to Rac-mediated reorganization of actin. *Nature cell biology, 2*(8), 521-530.

Distler, J., Hirth, A., Kurowska-Stolarska, M., and Gay, R. (2003). Angiogenic and angiostatic factors in the molecular control of angiogenesis. *The Quarterly Journal of Nuclear Medicine and Molecular Imaging, 47*(3), 149.

Dong, J.-f., Moake, J. L., Nolasco, L., Bernardo, A., Arceneaux, W., Shrimpton, C. N., Schade, A. J., McIntire, L. V., Fujikawa, K., and López, J. A. (2002). ADAMTS-13 rapidly cleaves newly secreted ultralarge von Willebrand factor multimers on the endothelial surface under flowing conditions. *Blood, The Journal of the American Society of Hematology, 100*(12), 4033-4039.

Donners, M. M. P. C., and Biessen, E. A. L. (2019). SCRIBbling the role of endothelial polarity in atherosclerosis. *Cardiovascular research, 115*(14), 1937-1939.

Duzen, I. V., Yavuz, F., Vuruskan, E., Saracoglu, E., Poyraz, F., Cekici, Y., Alici, H., Goksuluk, H., Candemir, B., Sucu, M., and Demiryurek, A. T. (2019). Investigation of leukocyte RHO/ROCK gene expressions in patients with non-valvular atrial fibrillation. *Experimental and therapeutic medicine, 18*(4), 2777-2782.

Eelen, G., Dubois, C., Cantelmo, A. R., Goveia, J., Brüning, U., DeRan, M., Jarugumilli, G., van Rijssel, J., Saladino, G., and Comitani, F. (2018). Role of glutamine synthetase in angiogenesis beyond glutamine synthesis. *Nature, 561*(7721), 63-69.

Elsherif, L., Ozler, M., Zayed, M. A., Shen, J. H., Chernoff, J., Faber, J. E., and Parise, L. V. (2014). Potential Compensation among Group I PAK Members in Hindlimb Ischemia and Wound Healing. *PloS one, 9*(11).

Eswaran, J., Soundararajan, M., Kumar, R., and Knapp, S. (2008). UnPAKing the class differences among p21-activated kinases. *Trends in biochemical sciences, 33*(8), 394-403.

Feng, Q., Baird, D., Peng, X., Wang, J., Ly, T., Guan, J. L., and Cerione, R. A. (2006). Cool-1 functions as an essential regulatory node for EGF receptor- and Src-mediated cell growth. *Nature cell biology, 8*(9), 945-956.

Feng, Q., Baird, D., Yoo, S., Antonyak, M., and Cerione, R. A. (2010). Phosphorylation of the cool-1/beta-Pix protein serves as a regulatory signal for the migration and invasive activity of Src-transformed cells. *The Journal of biological chemistry, 285*(24), 18806-18816.

Ferrara, N., Gerber, H.-P., and LeCouter, J. (2003). The biology of VEGF and its receptors. *Nature medicine, 9*(6), 669-676.

Flamme, I., Frölich, T., and Risau, W. (1997). Molecular mechanisms of vasculogenesis and embryonic angiogenesis. *Journal of cellular physiology, 173*(2), 206-210.

Foster, R., Hu, K.-Q., Lu, Y., Nolan, K. M., Thissen, J., and Settleman, J. (1996). Identification of a novel human Rho protein with unusual properties: GTPase deficiency and in vivo farnesylation. *Molecular and cellular biology, 16*(6), 2689-2699.

Frank, S. R., and Hansen, S. H. (2008). *The PIX–GIT complex: AG protein signaling cassette in control of cell shape.* Paper presented at the Seminars in cell & developmental biology.

Fukushima, Y., Nishiyama, K., Kataoka, H., Fruttiger, M., Fukuhara, S., Nishida, K., Mochizuki, N., Kurihara, H., Nishikawa, S. I., and Uemura, A. (2020). RhoJ integrates attractive and repulsive cues in directional migration of endothelial cells. *The EMBO journal, 39*(12), e102930.

Fukushima, Y., Okada, M., Kataoka, H., Hirashima, M., Yoshida, Y., Mann, F., Gomi, F., Nishida, K., Nishikawa, S.-I., and Uemura, A. (2011). Sema3E-PlexinD1 signaling selectively suppresses disoriented angiogenesis in ischemic retinopathy in mice. *The Journal of clinical investigation, 121*(5), 1974-1985.

Goldstein, N. B., Steel, A., Barbulescu, C. C., Koster, M. I., Wright, M. J., Jones, K. L., Gao, B., Ward, B., Woessner, B., Trottier, Z., Pakieser, J., Hu, J., Lambert, K. A., Shellman, Y. G., Fujita, M.,

Robinson, W. A., Roop, D. R., Norris, D. A., and Birlea, S. A. (2021). Melanocyte Precursors in the Hair Follicle Bulge of Repigmented Vitiligo Skin Are Controlled by RHO-GTPase, KCTD10, and CTNNB1 Signaling. *Journal of Investigative Dermatology, 141*(3), 638-647.e613.

Gonlugur, U., and Efeoglu, T. (2004). Vascular adhesion and transendothelial migration of eosinophil leukocytes. *Cell and tissue research, 318*, 473-482.

Gopal, S. K., Greening, D. W., Hanssen, E. G., Zhu, H.-J., Simpson, R. J., and Mathias, R. A. (2016). Oncogenic epithelial cell-derived exosomes containing Rac1 and PAK2 induce angiogenesis in recipient endothelial cells. *Oncotarget, 7*(15), 19709-19722.

Gourlaouen, M., Welti, J. C., Vasudev, N. S., and Reynolds, A. R. (2013). Essential role for endocytosis in the growth factor-stimulated activation of ERK1/2 in endothelial cells. *Journal of Biological Chemistry, 288*(11), 7467-7480.

Grise, F., Bidaud, A., and Moreau, V. (2009). Rho GTPases in hepatocellular carcinoma. *Biochimica et Biophysica Acta (BBA) - Reviews on Cancer, 1795*(2), 137-151.

Ha, B. H., Davis, M. J., Chen, C., Lou, H. J., Gao, J., Zhang, R., Krauthammer, M., Halaban, R., Schlessinger, J., and Turk, B. E. (2012). Type II p21-activated kinases (PAKs) are regulated by an autoinhibitory pseudosubstrate. *Proceedings of the National Academy of Sciences, 109*(40), 16107-16112.

Ha, B. H., Morse, E. M., Turk, B. E., and Boggon, T. J. (2015). Signaling, regulation, and specificity of the type II p21-activated kinases. *Journal of Biological Chemistry, 290*(21), 12975-12983.

Hao, X. D., Le, C. S., Zhang, H. M., Shang, D. S., Tong, L. S., and Gao, F. (2019). Thrombin disrupts vascular endothelial-cadherin and leads to hydrocephalus via protease-activated receptors-1 pathway. *CNS Neurosci Ther, 25*(10), 1142-1150.

Heasman, S. J., and Ridley, A. J. (2008). Mammalian Rho GTPases: new insights into their functions from in vivo studies. *Nature reviews Molecular cell biology, 9*(9), 690-701.

Hillen, F., and Griffioen, A. W. (2007). Tumour vascularization: sprouting angiogenesis and beyond. *Cancer and Metastasis Reviews, 26*(3), 489-502.

Ho, H., Aruri, J., Kapadia, R., Mehr, H., White, M. A., and Ganesan, A. K. (2012). RhoJ regulates melanoma chemoresistance by suppressing pathways that sense DNA damage. *Cancer research, 72*(21), 5516-5528.

Ho, H., Soto Hopkin, A., Kapadia, R., Vasudeva, P., Schilling, J., and Ganesan, A. K. (2013). RhoJ modulates melanoma invasion by altering actin cytoskeletal dynamics. *Pigment Cell Melanoma Res, 26*(2), 218-225.

Hoefen, R. J., and Berk, B. C. (2006). The multifunctional GIT family of proteins. *Journal of cell science, 119*(8), 1469-1475.

Hofmann, C., Shepelev, M., and Chernoff, J. (2004). The genetics of Pak. *Journal of cell science, 117*(19), 4343-4354.

Jack, E. R., Jack, E. R., Madine, J., Lian, L.-y., and Middleton, D. A. (2008). Membrane interactions of peptides representing the polybasic regions of three Rho GTPases are sensitive to the distribution of arginine and lysine residues. *Molecular membrane biology, 25*(1), 14-22.

Jaffe, A. B., and Hall, A. (2005). Rho GTPases: biochemistry and biology. *Annual review of cell and developmental biology, 21*(1), 247-269.

Jagadeeshan, S., Sagayaraj, R. V., Paneerselvan, N., Ghouse, S. S., and Malathi, R. (2017). Toxicity and anti-angiogenicity evaluation of Pak1 inhibitor IPA-3 using zebrafish embryo model. *Cell Biol Toxicol, 33*(1), 41-56.

Jones, C. A., Nishiya, N., London, N. R., Zhu, W., Sorensen, L. K., Chan, A. C., Lim, C. J., Chen, H., Zhang, Q., and Schultz, P. G. (2009). Slit2–Robo4 signalling promotes vascular stability by blocking Arf6 activity. *Nature cell biology, 11*(11), 1325-1331.

Kalluri, R. (2003). Basement membranes: structure, assembly and role in tumour angiogenesis. *Nature Reviews Cancer, 3*(6), 422-433.

K Karlsson, M., Zhang, C., Méar, L., Zhong, W., Digre, A., Katona, B., Sjöstedt, E., Butler, L., Odeberg, J., and Dusart, P. (2021). A single–cell type transcriptomics map of human tissues. Science advances, 7(31), eabh2169.

https://www.proteinatlas.org/ENSG00000130669-PAK4/single+cell+type Single cell type - PAK4 - The Human Protein Atlas

https://www.proteinatlas.org/ENSG00000101349-PAK5/single+cell+ty Single cell type - PAK5 - The Human Protein Atlas

https://www.proteinatlas.org/ENSG00000137843-PAK6/single+cell+typeSingle cell type - PAK6 - The Human Protein Atlasaramysheva, A. (2008). Mechanisms of angiogenesis. *Biochemistry (Moscow), 73*(7), 751-762.

Kaur, S., Leszczynska, K., Abraham, S., Scarcia, M., Hiltbrunner, S., Marshall, C. J., Mavria, G., Bicknell, R., and Heath, V. L. (2011). RhoJ/TCL regulates endothelial motility and tube formation and modulates actomyosin contractility and focal adhesion numbers. *Arteriosclerosis, Thrombosis, and Vascular Biology, 31*(3), 657-664.

Kim, C., Yang, H., Fukushima, Y., Saw, P. E., Lee, J., Park, J.-S., Park, I., Jung, J., Kataoka, H., and Lee, D. (2014a). Vascular RhoJ is an effective and selective target for tumor angiogenesis and vascular disruption. *Cancer cell, 25*(1), 102-117.

Kim, C., Yang, H., Park, I., Chon, H. J., Kim, J. H., Kwon, W. S., Lee, W. S., Kim, T. S., and Rha, S. Y. (2016). Rho GTPase RhoJ is Associated with Gastric Cancer Progression and Metastasis. *J Cancer, 7*(11), 1550-1556.

Kim, J. J., Khalid, O., Namazi, A., Tu, T. G., Elie, O., Lee, C., and Kim, Y. (2014b). Discovery of consensus gene signature and intermodular connectivity defining self-renewal of human embryonic stem cells. *Stem Cells, 32*(6), 1468-1479.

Kim, K., Han, Y., Duan, L., and Chung, K. Y. (2022). Scaffolding of mitogen-activated protein kinase signaling by β-arrestins. *International Journal of Molecular Sciences, 23*(2), 1000.

King, A. J., Sun, H., Diaz, B., Barnard, D., Miao, W., Bagrodia, S., and Marshall, M. S. (1998). The protein kinase Pak3 positively regulates Raf-1 activity through phosphorylation of serine 338. *Nature, 396*(6707), 180-183.

King, C. C., Gardiner, E. M., Zenke, F. T., Bohl, B. P., Newton, A. C., Hemmings, B. A., and Bokoch, G. M. (2000). p21-activated kinase (PAK1) is phosphorylated and activated by 3-phosphoinositide-dependent kinase-1 (PDK1). *Journal of Biological Chemistry, 275*(52), 41201-41209.

Klapper, L. N., Kirschbaum, M. H., Sela, M., and Yarden, Y. (2000). Biochemical and clinical implications of the ErbB/HER signaling network of growth factor receptors. *Adv Cancer Res, 77*, 25-79.

Koh, W., Mahan, R. D., and Davis, G. E. (2008). Cdc42- and Rac1-mediated endothelial lumen formation requires Pak2, Pak4 and Par3, and PKC-dependent signaling. *Journal of cell science, 121*(Pt 7), 989-1001.

Kumar, R., Sanawar, R., Li, X., and Li, F. (2017). Structure, biochemistry, and biology of PAK kinases. *Gene, 605*, 20-31.

Kuo, J. C., Han, X., Hsiao, C. T., Yates, J. R., and Waterman, C. M. (2011). Analysis of the myosin-II-responsive focal adhesion proteome reveals a role for beta-Pix in negative regulation of focal adhesion maturation. *Nature cell biology, 13*(4), 383-393.

Kusuhara, S., Fukushima, Y., Fukuhara, S., Jakt, L. M., Okada, M., Shimizu, Y., Hata, M., Nishida, K., Negi, A., and Hirashima, M. (2012). Arhgef15 promotes retinal angiogenesis by mediating VEGF-induced Cdc42 activation and potentiating RhoJ inactivation in endothelial cells.

Lamalice, L., Le Boeuf, F., and Huot, J. (2007). Endothelial cell migration during angiogenesis. *Circulation research, 100*(6), 782-794.

Lavoie, H., Gagnon, J., and Therrien, M. (2020). ERK signalling: a master regulator of cell behaviour, life and fate. *Nature reviews Molecular cell biology, 21*(10), 607-632.

Lebkowski, J. S., Clancy, S., and Calos, M. P. (1985). Simian virus 40 replication in adenovirus-transformed human cells antagonizes gene expression. *Nature, 317*(6033), 169-171.

Lee, A. R., Gan, Y., Xie, N., Ramnarine, V. R., Lovnicki, J. M., and Dong, X. (2019). Alternative RNA splicing of the GIT 1 gene is associated with neuroendocrine prostate cancer. *Cancer Science, 110*(1), 245-255.

Lei, M., Lu, W., Meng, W., Parrini, M.-C., Eck, M. J., Mayer, B. J., and Harrison, S. C. (2000). Structure of PAK1 in an autoinhibited conformation reveals a multistage activation switch. *Cell, 102*(3), 387-397.

Leszczynska, K., Kaur, S., Wilson, E., Bicknell, R., and Heath, V. L. (2011). The role of RhoJ in endothelial cell biology and angiogenesis. *Biochemical Society transactions, 39*(6), 1606-1611.

Liang, P. H., Ko, T. P., and Wang, A. H. J. (2002). Structure, mechanism and function of prenyltransferases. *European Journal of Biochemistry, 269*(14), 3339-3354.

Liu, J., Fraser, S. D., Faloon, P. W., Rollins, E. L., Vom Berg, J., Starovic-Subota, O., Laliberte, A. L., Chen, J.-N., Serluca, F. C., and Childs, S. J. (2007). A βPix–Pak2a signaling pathway regulates cerebral vascular stability in zebrafish. *Proceedings of the National Academy of Sciences, 104*(35), 13990-13995.

Liu, J., Zeng, L., Kennedy, R. M., Gruenig, N. M., and Childs, S. J. (2012). βPix plays a dual role in cerebral vascular stability and angiogenesis, and interacts with integrin αvβ8. *Developmental biology, 363*(1), 95-105.

Liu, L., Chen, J., Sun, L., and Xu, Y. (2018). RhoJ promotes hypoxia induced endothelial-to-mesenchymal transition by activating WDR5 expression. *J Cell Biochem, 119*(4), 3384-3393.

Liu, S., Premont, R. T., Park, K.-H., and Rockey, D. C. (2022). β-PIX cooperates with GIT1 to regulate eNOS in sinusoidal endothelial cells. *American Journal of Physiology-Gastrointestinal and Liver Physiology*.

Liu, S., Premont, R. T., and Rockey, D. C. (2014). Endothelial nitric-oxide synthase (eNOS) is activated through G-protein-coupled receptor kinase-interacting protein 1 (GIT1) tyrosine phosphorylation and Src protein. *Journal of Biological Chemistry, 289*(26), 18163-18174.

Lorant, D. E., Li, W., Tabatabaei, N., Garver, M. K., and Albertine, K. H. (1999). P-selectin expression by endothelial cells is decreased in neonatal rats and human premature infants. *Blood, The Journal of the American Society of Hematology, 94*(2), 600-609.

Madaule, P., and Axel, R. (1985). A novel ras-related gene family. *Cell, 41*(1), 31-40.

Manabe, R., Kovalenko, M., Webb, D. J., and Horwitz, A. R. (2002). GIT1 functions in a motile, multi-molecular signaling complex that regulates protrusive activity and cell migration. *Journal of cell science, 115*(Pt 7), 1497-1510.

Manser, E., Loo, T. H., Koh, C. G., Zhao, Z. S., Chen, X. Q., Tan, L., Tan, I., Leung, T., and Lim, L. (1998). PAK kinases are directly coupled to the PIX family of nucleotide exchange factors. *Molecular cell, 1*(2), 183-192.

Martin, G. A., Bollag, G., McCormick, F., and Abo, A. (1995). A novel serine kinase activated by rac1/CDC42Hs-dependent autophosphorylation is related to PAK65 and STE20. *The EMBO journal, 14*(9), 1970-1978.

Masiero, M., Simões, F. C., Han, H. D., Snell, C., Peterkin, T., Bridges, E., Mangala, L. S., Wu, S. Y.-Y., Pradeep, S., and Li, D. (2013). A core human primary tumor angiogenesis signature identifies the endothelial orphan receptor ELTD1 as a key regulator of angiogenesis. *Cancer cell, 24*(2), 229-241.

Mavria, G., Vercoulen, Y., Yeo, M., Paterson, H., Karasarides, M., Marais, R., Bird, D., and Marshall, C. J. (2006). ERK-MAPK signaling opposes Rho-kinase to promote endothelial cell survival and sprouting during angiogenesis. *Cancer cell, 9*(1), 33-44.

Menard, R. E., and Mattingly, R. R. (2004). Gβγ subunits stimulate p21-activated kinase 1 (PAK1) through activation of PI3-kinase and Akt but act independently of Rac1/Cdc42. *FEBS letters, 556*(1-3), 187-192.

Mentzer, S. J., and Konerding, M. A. (2014). Intussusceptive angiogenesis: expansion and remodeling of microvascular networks. *Angiogenesis, 17*, 499-509.

Miaczynska, M. (2013). Effects of membrane trafficking on signaling by receptor tyrosine kinases. *Cold Spring Harbor perspectives in biology, 5*(11), a009035.

Mills, J., Hricik, T., Siddiqi, S., and Matushansky, I. (2011). Chromatin structure predicts epigenetic therapy responsiveness in sarcoma. *Molecular cancer therapeutics, 10*(2), 313-324.

Molina-Navarro, M. M., Trivino, J. C., Martinez-Dolz, L., Lago, F., Gonzalez-Juanatey, J. R., Portoles, M., and Rivera, M. (2014). Functional networks of nucleocytoplasmic transport-related

genes differentiate ischemic and dilated cardiomyopathies. A new therapeutic opportunity. *PloS one, 9*(8), e104709.

Monypenny, J., Zicha, D., Higashida, C., Oceguera-Yanez, F., Narumiya, S., and Watanabe, N. (2009). Cdc42 and Rac family GTPases regulate mode and speed but not direction of primary fibroblast migration during platelet-derived growth factor-dependent chemotaxis. *Molecular and cellular biology, 29*(10), 2730-2747.

Murray, B. W., Guo, C., Piraino, J., Westwick, J. K., Zhang, C., Lamerdin, J., Dagostino, E., Knighton, D., Loi, C.-M., and Zager, M. (2010). Small-molecule p21-activated kinase inhibitor PF-3758309 is a potent inhibitor of oncogenic signaling and tumor growth. *Proceedings of the National Academy of Sciences, 107*(20), 9446-9451.

Nayal, A., Webb, D. J., Brown, C. M., Schaefer, E. M., Vicente-Manzanares, M., and Horwitz, A. R. (2006). Paxillin phosphorylation at Ser273 localizes a GIT1-PIX-PAK complex and regulates adhesion and protrusion dynamics. *The Journal of cell biology, 173*(4), 587-589.

Neufeld, G., and Kessler, O. (2006). Pro-angiogenic cytokines and their role in tumor angiogenesis. *Cancer and Metastasis Reviews, 25*(3), 373-385.

Nishizuka, M., Arimoto, E., Tsuchiya, T., Nishihara, T., and Imagawa, M. (2003). Crucial role of TCL/TC10βL, a subfamily of Rho GTPase, in adipocyte differentiation. *Journal of Biological Chemistry, 278*(17), 15279-15284.

Nozaki, M., and Nishizuka, M. (2021). Repression of RhoJ expression promotes TGF-β-mediated EMT in human non-small-cell lung cancer A549cells. *Biochemical and biophysical research communications, 566*, 94-100.

Oakley, C. E., and Oakley, B. R. (1989). Identification of gamma-tubulin, a new member of the tubulin superfamily encoded by mipA gene of Aspergillus nidulans. *Nature, 338*(6217), 662-664.

Ohara, O., Nagase, T., Ishikawa, K.-i., Nakajima, D., Ohira, M., Seki, N., and Nomura, N. (1997). Construction and characterization of human brain cDNA libraries suitable for analysis of cDNA clones encoding relatively large proteins. *DNA Research, 4*(1), 53-59.

Olsson, A.-K., Dimberg, A., Kreuger, J., and Claesson-Welsh, L. (2006). VEGF receptor signalling - in control of vascular function. *Nature Reviews. Molecular Cell Biology, 7*(5), 359-371.

Paduch, M., Jeleń, F., and Otlewski, J. (2001). Structure of small G proteins and their regulators. *Acta Biochimica Polonica, 48*(4), 829-850.

Pandya, N. M., Dhalla, N. S., and Santani, D. D. (2006). Angiogenesis—a new target for future therapy. *Vascular pharmacology, 44*(5), 265-274.

Pang, J., Hoefen, R., Pryhuber, G. S., Wang, J., Yin, G., White, R. J., Xu, X., O'Dell, M. R., Mohan, A., and Michaloski, H. (2009). G-protein–coupled receptor kinase interacting protein-1 is required for pulmonary vascular development. *Circulation, 119*(11), 1524-1532.

Papetti, M., and Herman, I. M. (2002). Mechanisms of normal and tumor-derived angiogenesis. *American Journal of Physiology-Cell Physiology, 282*(5), C947-C970.

Pearson, G., Robinson, F., Beers Gibson, T., Xu, B.-e., Karandikar, M., Berman, K., and Cobb, M. H. (2001). Mitogen-activated protein (MAP) kinase pathways: regulation and physiological functions. *Endocrine reviews, 22*(2), 153-183.

Premont, R. T., Claing, A., Vitale, N., Perry, S. J., and Lefkowitz, R. J. (2000). The GIT family of ADP-ribosylation factor GTPase-activating proteins: functional diversity of GIT2 through alternative splicing. *Journal of Biological Chemistry, 275*(29), 22373-22380.

Premont, R. T., Perry, S. J., Schmalzigaug, R., Roseman, J. T., Xing, Y., and Claing, A. (2004). The GIT/PIX complex: an oligomeric assembly of GIT family ARF GTPase-activating proteins and PIX family Rac1/Cdc42 guanine nucleotide exchange factors. *Cellular signalling, 16*(9), 1001-1011.

Presta, M., Dell'Era, P., Mitola, S., Moroni, E., Ronca, R., and Rusnati, M. (2005). Fibroblast growth factor/fibroblast growth factor receptor system in angiogenesis. *Cytokine & growth factor reviews, 16*(2), 159-178.

Qu, J., Li, X., Novitch, B. G., Zheng, Y., Kohn, M., Xie, J.-M., Kozinn, S., Bronson, R., Beg, A. A., and Minden, A. (2003). PAK4 kinase is essential for embryonic viability and for proper neuronal development. *Molecular and cellular biology, 23*(20), 7122-7133.

Radu, M., Lyle, K., Hoeflich, K. P., Villamar-Cruz, O., Koeppen, H., and Chernoff, J. (2015). p21-activated kinase 2 regulates endothelial development and function through the Bmk1/Erk5 pathway. *Molecular and cellular biology, 35*(23), 3990-4005.

Radu, M., Semenova, G., Kosoff, R., and Chernoff, J. (2014). PAK signalling during the development and progression of cancer. *Nature Reviews Cancer, 14*(1), 13-25.

Reynolds, A. R., Hart, I. R., Watson, A. R., Welti, J. C., Silva, R. G., Robinson, S. D., Da Violante, G., Gourlaouen, M., Salih, M., and Jones, M. C. (2009). Stimulation of tumor growth and angiogenesis by low concentrations of RGD-mimetic integrin inhibitors. *Nature medicine, 15*(4), 392-400.

Richards, M., Hetheridge, C., and Mellor, H. (2015). The Formin FMNL3 Controls Early Apical Specification in Endothelial Cells by Regulating the Polarized Trafficking of Podocalyxin. *Current biology : CB, 25*(17), 2325-2331.

Risau, W. (1997). Mechanisms of angiogenesis. *Nature, 386*(6626), 671-674.

Risau, W., and Flamme, I. (1995). Vasculogenesis. *Annual review of cell and developmental biology, 11*(1), 73-91.

Roberts, P. J., Mitin, N., Keller, P. J., Chenette, E. J., Madigan, J. P., Currin, R. O., Cox, A. D., Wilson, O., Kirschmeier, P., and Der, C. J. (2008). Rho Family GTPase modification and dependence on CAAX motif-signaled posttranslational modification. *Journal of Biological Chemistry, 283*(37), 25150-25163.

Roy, H., Bhardwaj, S., and Ylä-Herttuala, S. (2006). Biology of vascular endothelial growth factors. *FEBS letters, 580*(12), 2879-2887.

Rüegg, C., Dormond, O., and Mariotti, A. (2004). Endothelial cell integrins and COX-2: mediators and therapeutic targets of tumor angiogenesis. *Biochimica et Biophysica Acta (BBA)-Reviews on Cancer, 1654*(1), 51-67.

Ruiz, R., Jahid, S., Harris, M., Marzese, D. M., Espitia, F., Vasudeva, P., Chen, C. F., de Feraudy, S., Wu, J., Gillen, D. L., Krasieva, T. B., Tromberg, B. J., Pavan, W. J., Hoon, D. S., and Ganesan, A. K. (2017). The RhoJ-BAD signaling network: An Achilles' heel for BRAF mutant melanomas. *PLoS genetics, 13*(7), e1006913.

Schlenker, O., and Rittinger, K. (2009). Structures of dimeric GIT1 and trimeric β-PIX and implications for GIT–PIX complex assembly. *Journal of molecular biology, 386*(2), 280-289.

Schmalzigaug, R., Phee, H., Davidson, C. E., Weiss, A., and Premont, R. T. (2007). Differential expression of the ARF GAP genes GIT1 and GIT2 in mouse tissues. *Journal of Histochemistry & Cytochemistry, 55*(10), 1039-1048.

Schmidt, A., and Hall, A. (2002). Guanine nucleotide exchange factors for Rho GTPases: turning on the switch. *Genes & development, 16*(13), 1587-1609.

Schott, R. J., and Morrow, L. A. (1993). Growth factors and angiogenesis. *Cardiovascular research, 27*(7), 1155-1161.

Schürmann, C., Dienst, F. L., Pálfi, K., Vasconez, A. E., Oo, J. A., Wang, S., Buchmann, G. K., Offermanns, S., van de Sluis, B., Leisegang, M. S., Günther, S., Humbert, P. O., Lee, E., Zhu, J., Weigert, A., Mathoor, P., Wittig, I., Kruse, C., and Brandes, R. P. (2019). The polarity protein Scrib limits atherosclerosis development in mice. *Cardiovascular research, 115*(14), 1963-1974.

Semenova, G., and Chernoff, J. (2017). Targeting PAK1. *Biochem Soc Trans, 45*(1), 79-88.

Shao, Y.-G., Ning, K., and Li, F. (2016). Group II p21-activated kinases as therapeutic targets in gastrointestinal cancer. *World journal of gastroenterology, 22*(3), 1224.

Shikata, Y., Birukov, K. G., and Garcia, J. G. N. (2003). S1P induces FA remodeling in human pulmonary endothelial cells: role of Rac, GIT1, FAK, and paxillin. *Journal of Applied Physiology, 94*(3), 1193-1203.

Shin, M., Beane, T. J., Quillien, A., Male, I., Zhu, L. J., and Lawson, N. D. (2016). Vegfa signals through ERK to promote angiogenesis, but not artery differentiation. *Development (Cambridge, England), 143*(20), 3796-3805.

Shweiki, D., Itin, A., Soffer, D., and Keshet, E. (1992). Vascular endothelial growth factor induced by hypoxia may mediate hypoxia-initiated angiogenesis. *Nature, 359*(6398), 843-845.

Singh, B. N., Sierra-Pagan, J. E., Gong, W., Das, S., Theisen, J. W. M., Skie, E., Garry, M. G., and Garry, D. J. (2020). ETV2 (Ets Variant Transcription Factor 2)-Rhoj Cascade Regulates Endothelial Progenitor Cell Migration During Embryogenesis. *Arteriosclerosis, Thrombosis, and Vascular Biology*, ATVBAHA120314488.

Slack-Davis, J. K., Eblen, S. T., Zecevic, M., Boerner, S. A., Tarcsafalvi, A., Diaz, H. B., Marshall, M. S., Weber, M. J., Parsons, J. T., and Catling, A. D. (2003). PAK1 phosphorylation of MEK1 regulates fibronectin-stimulated MAPK activation. *The Journal of cell biology, 162*(2), 281-291.

Song, M., and Finley, S. D. (2018). Mechanistic insight into activation of MAPK signaling by pro-angiogenic factors. *BMC systems biology, 12*, 1-17.

Sorrell, F. J., Kilian, L. M., and Elkins, J. M. (2019). Solution structures and biophysical analysis of full-length group A PAKs reveal they are monomeric and auto-inhibited in cis. *Biochemical Journal, 476*(7), 1037-1051.

Srinivasan, R., Zabuawala, T., Huang, H., Zhang, J., Gulati, P., Fernandez, S., Karlo, J. C., Landreth, G. E., Leone, G., and Ostrowski, M. C. (2009). Erk1 and Erk2 regulate endothelial cell proliferation and migration during mouse embryonic angiogenesis. *PloS one, 4*(12), e8283.

Staton, C., Kumar, I., Reed, M., and Brown, N. (2007). Neuropilins in physiological and pathological angiogenesis. *The Journal of Pathology: A Journal of the Pathological Society of Great Britain and Ireland, 212*(3), 237-248.

Stins, M. F., Badger, J., and Kim, K. S. (2001). Bacterial invasion and transcytosis in transfected human brain microvascular endothelial cells. *Microbial pathogenesis, 30*(1), 19-28.

Stockton, R., Reutershan, J., Scott, D., Sanders, J., Ley, K., and Schwartz, M. A. (2007). Induction of vascular permeability: βPIX and GIT1 scaffold the activation of extracellular signal-regulated kinase by PAK. *Molecular biology of the cell, 18*(6), 2346-2355.

Strochlic, T. I., Viaud, J., Rennefahrt, U. E., Anastassiadis, T., and Peterson, J. R. (2010). Phosphoinositides are essential coactivators for p21-activated kinase 1. *Molecular cell, 40*(3), 493-500.

Sundararaman, A., Fukushima, Y., Norman, J. C., Uemura, A., and Mellor, H. (2020). RhoJ Regulates alpha5beta1 Integrin Trafficking to Control Fibronectin Remodeling during Angiogenesis. *Current biology : CB, 30*(11), 2146-2155.e2145.

Takase, H., Matsumoto, K., Yamadera, R., Kubota, Y., Otsu, A., Suzuki, R., Ishitobi, H., Mochizuki, H., Kojima, T., Takano, S., Uchida, K., Takahashi, S., and Ema, M. (2012). Genome-wide identification of endothelial cell-enriched genes in the mouse embryo. *Blood, 120*(4), 914-923.

Tanimura, S., and Takeda, K. (2017). ERK signalling as a regulator of cell motility. *The Journal of Biochemistry*.

Turner, C. E., Brown, M. C., Perrotta, J. A., Riedy, M., Nikolopoulos, S. N., McDonald, A. R., Bagrodia, S., Thomas, S., and Leventhal, P. S. (1999). Paxillin LD4 motif binds PAK and PIX through a novel 95-kD ankyrin repeat, ARF–GAP protein: a role in cytoskeletal remodeling. *The Journal of cell biology, 145*(4), 851-863.

van Nieuw Amerongen, G. P., Natarajan, K., Yin, G., Hoefen, R. J., Osawa, M., Haendeler, J., Ridley, A., Fujiwara, K., Van Hinsbergh, V. W., and Berk, B. C. (2004). GIT1 mediates thrombin signaling in endothelial cells: role in turnover of RhoA-type focal adhesions. *Circulation research, 94*(8), 1041-1049.

Viaud, J., and Peterson, J. R. (2009). An allosteric kinase inhibitor binds the p21-activated kinase autoregulatory domain covalentlyAllosteric Kinase Inhibition. *Molecular cancer therapeutics, 8*(9), 2559-2565.

Vignal, E., De Toledo, M., Comunale, F., Ladopoulou, A., Gauthier-Rouviere, C., Blangy, A., and Fort, P. (2000). Characterization of TCL, a new GTPase of the rho family related to TC10 andCcdc42. *The Journal of biological chemistry, 275*(46), 36457-36464.

Walls, J. R., Coultas, L., Rossant, J., and Henkelman, R. M. (2008). Three-dimensional analysis of vascular development in the mouse embryo. *PloS one, 3*(8), e2853.

Walter, B. N., Huang, Z., Jakobi, R., Tuazon, P. T., Alnemri, E. S., Litwack, G., and Traugh, J. A. (1998). Cleavage and activation of p21-activated protein kinase γ-PAK by CPP32 (caspase 3): effects of autophosphorylation on activity. *Journal of Biological Chemistry, 273*(44), 28733-28739.

Wang, H., Schaefer, T., Konantz, M., Braun, M., Varga, Z., Paczulla, A. M., Reich, S., Jacob, F., Perner, S., Moch, H., Fehm, T. N., Kanz, L., Schulze-Osthoff, K., and Lengerke, C. (2017). Prominent Oncogenic Roles of EVI1 in Breast Carcinoma. *Cancer research, 77*(8), 2148-2160.

Wang, J., Wu, J.-W., and Wang, Z.-X. (2011). Mechanistic studies of the autoactivation of PAK2: a two-step model of cis initiation followed by trans amplification. *Journal of Biological Chemistry, 286*(4), 2689-2695.

Wang, M., Jiang, X., Yang, Y., Chen, H., Zhang, C., Xu, H., Qi, B., Yao, C., and Xia, H. (2020). Rhoj Is a Novel Target for Progression and Invasion of Glioblastoma by Impairing Cytoskeleton Dynamics. *Neurotherapeutics : the journal of the American Society for Experimental NeuroTherapeutics*.

Wang, M., Zhang, C., Zheng, Q., Ma, Z., Qi, M., Di, G., Ling, S., Xu, H., Qi, B., Yao, C., Xia, H., and Jiang, X. (2022). RhoJ facilitates angiogenesis in glioblastoma via JNK/VEGFR2 mediated activation of PAK and ERK signaling pathways. *Int J Biol Sci, 18*(3), 942-955.

Webb, D. J., Kovalenko, M., Whitmore, L., and Horwitz, A. F. (2006). Phosphorylation of serine 709 in GIT1 regulates protrusive activity in cells. *Biochemical and biophysical research communications, 346*(4), 1284-1288.

West, K. A., Zhang, H., Brown, M. C., Nikolopoulos, S. N., Riedy, M. C., Horwitz, A. F., and Turner, C. E. (2001). The LD4 motif of paxillin regulates cell spreading and motility through an interaction with paxillin kinase linker (PKL). *The Journal of cell biology, 154*(1), 161-176.

Wilson, E. (2014). Characterising the molecular function of the Rho GTPase RhoJ in endothelial cells. http://etheses.bham.ac.uk/5363/

Wilson, E., Leszczynska, K., Poulter, N. S., Edelmann, F., Salisbury, V. A., Noy, P. J., Bacon, A., Rappoport, J. Z., Heath, J. K., Bicknell, R., and Heath, V. L. (2014). RhoJ interacts with the GIT-PIX complex and regulates focal adhesion disassembly. *Journal of cell science, 127*(Pt 14), 3039-3051.

Wisgrill, L., Muck, M., Wessely, I., Berger, A., Spittler, A., Förster-Waldl, E., and Sadeghi, K. (2018). Endothelial cells of extremely premature infants display impaired immune response after proinflammatory stimulation. *Pediatric Research, 83*(1), 128-134.

Won, S.-Y., Park, J.-J., Shin, E.-Y., and Kim, E.-G. (2019). PAK4 signaling in health and disease: defining the PAK4–CREB axis. *Experimental & Molecular Medicine, 51*(2), 1-9.

Yan, J., Manaenko, A., Chen, S., Klebe, D., Ma, Q., Caner, B., Fujii, M., Zhou, C., and Zhang, J. H. (2013). Role of SCH79797 in maintaining vascular integrity in rat model of subarachnoid hemorrhage. *Stroke, 44*(5), 1410-1417.

Yao, D., Li, C., Rajoka, M. S. R., He, Z., Huang, J., Wang, J., and Zhang, J. (2020). P21-Activated Kinase 1: Emerging biological functions and potential therapeutic targets in Cancer. *Theranostics, 10*(21), 9741.

Yin, G., Haendeler, J., Yan, C., and Berk, B. C. (2004). GIT1 functions as a scaffold for MEK1-extracellular signal-regulated kinase 1 and 2 activation by angiotensin II and epidermal growth factor. *Molecular and cellular biology, 24*(2), 875-885.

Yin, G., Zheng, Q., Yan, C., and Berk, B. C. (2005). GIT1 is a scaffold for ERK1/2 activation in focal adhesions. *The Journal of biological chemistry, 280*(30), 27705-27712.

Yuan, L., Sacharidou, A., Stratman, A. N., Le Bras, A., Zwiers, P. J., Spokes, K., Bhasin, M., Shih, S. C., Nagy, J. A., Molema, G., Aird, W. C., Davis, G. E., and Oettgen, P. (2011). RhoJ is an endothelial cell-restricted Rho GTPase that mediates vascular morphogenesis and is regulated by the transcription factor ERG. *Blood, 118*(4), 1145-1153.

Zhang, N., Cai, W., Yin, G., Nagel, D. J., and Berk, B. C. (2009). GIT1 is a novel MEK1-ERK1/2 scaffold that localizes to focal adhesions. *Cell biology international, 34*(1), 41-47.

Zhang, S., Yin, Y., Li, C., Zhao, Y., Wang, Q., and Zhang, X. (2020). PAK4 suppresses TNF-induced release of endothelial microparticles in HUVECs cells. *Aging (Albany NY), 12*(13), 12740.

Zhao, Z.-s., and Manser, E. (2012). PAK family kinases: Physiological roles and regulation. *Cellular logistics, 2*(2), 59-68.

Zhao, Z.-s., Manser, E., Loo, T.-H., and Lim, L. (2000). Coupling of PAK-interacting exchange factor PIX to GIT1 promotes focal complex disassembly. *Molecular and cellular biology, 20*(17), 6354-6363.

Zhou, W., Li, X., and Premont, R. T. (2016). Expanding functions of GIT Arf GTPase-activating proteins, PIX Rho guanine nucleotide exchange factors and GIT–PIX complexes. *Journal of cell science, 129*(10), 1963-1974.